DISCOVERY AND DEVELOPMENT OF PREDICTIVE BIOMARKERS FOR THE PERSONALIZATION OF PEMETREXED THERAPY IN NON-SMALL CELL LUNG CANCER

APPROVED BY SUPERVISORY COMMITTEE

_____
Rolf Brekken, Ph.D.

_____
Melanie Cobb, Ph.D.

_____
Philip Thorpe, Ph.D.

_____
Helen Yin, Ph.D.

_____
John Minna, M.D.

Special Acknowledgements

I would like to express gratitude to my fourth grade science teacher, Mrs. Herring, who opened my eyes to science and medicine and challenged me to always do my best.

I would like to thank my graduate school mentor, John Minna, M.D, for his extraordinary guidance, incredible support, investment in me, and our shared devotion to science and medicine.

I would like to express immeasurable appreciation to my clinical mentors, David Gerber, M.D, and Joan Schiller, M.D. for their unbelievable assistance, expertise and direction.

Finally, I would like to express the most heartfelt gratefulness to my husband, my parents, my family and my friends for their unconditional love, encouragement and support throughout my life. I could not have accomplished any of my dreams without you.

Dedication

In loving memory of my father, Larry Tim Watson.

DISCOVERY AND DEVELOPMENT OF PREDICTIVE BIOMARKERS FOR THE PERSONALIZATION OF PEMETREXED THERAPY IN NON-SMALL CELL LUNG CANCER

by

MISTY DAWN SHIELDS

DISSERTATION

Presented to the Faculty of the Graduate School of Biomedical Sciences

The University of Texas Southwestern Medical Center at Dallas

In Partial Fulfillment of the Requirements

For the Degree of

DOCTOR OF PHILOSOPHY

The University of Texas Southwestern Medical Center at Dallas

Dallas, Texas

December, 2011

DISCOVERY AND DEVELOPMENT OF PREDICTIVE BIOMARKERS FOR THE PERSONALIZATION OF PEMETREXED THERAPY IN NON-SMALL CELL LUNG CANCER

MISTY DAWN SHIELDS

The University of Texas Southwestern Medical Center at Dallas, 2011

John Minna, M.D.

Lung cancer is a major health problem, and is the leading cause of cancer-related deaths. This research proposal was designed to personalize and improve overall response rates to the FDA-approved chemotherapeutic pemetrexed. To do so, clinically-applicable response phenotypes of a large panel of lung cancer lines needed to be defined to identify gene expression profiles driving response to pemetrexed treatment. To mimic clinical exposure and duration *in vitro*, published pharmacokinetics of patients treated with pemetrexed were extrapolated to develop the dose schedule used in this study. Although two drug response assays were simultaneously performed, liquid colony formation assay

most closely mimicked clinical indications for the treatment of patients with pemetrexed, and was non-toxic to normal human bronchial epithelial cells. There were three distinct pemetrexed response phenotypes across this cell line panel: sensitive, intermediate and resistant. Interestingly, large cell carcinomas and a subset of adenocarcinomas are sensitive to pemetrexed treatment. Upon oncogenotype analysis, I found that mutations in *EGFR* correlated significantly with pemetrexed resistance, and this was confirmed by mRNA expression profiling and reverse phase protein arrays. Furthermore, I determined that mutations in *KRAS* were significantly more frequent in sensitive lines, and EML4/ALK adenocarcinomas conferred sensitivity to pemetrexed, consistent with recent clinical findings. In order to test whether the *in vitro* pemetrexed response phenotypes could be recapitulated *in vivo*, doses from 26.6 mg/kg up to 1000 mg/kg pemetrexed *qwx3* were administered to and well tolerated by *NOD/SCID* mice. Treatment of established lung cancer xenografts with doses of pemetrexed 500 mg/kg or higher *qwx3* were consistent with *in vitro* findings. To elucidate mechanisms of response, intratumoral mRNA levels of *TYMS* and pemetrexed-related genes did not have any significant correlation with response. However, microarray expression profiling, RNA-Seq and western blot analysis independently highlighted FTCD overexpression can be found only in pemetrexed-sensitive lung cancer lines. Stable knockdown of *FTCD* in a FTCD-overexpressed lung cancer line resulted in specific and abrupt cell death. I further describe the ongoing analysis of retrospective clinical datasets. Our plans for prospective FTCD biomarker enrollment in future pemetrexed clinical trials highlight the translational potential and progression of this dissertation proposal.

TABLE OF CONTENTS

FIGURES AND TABLES

Chapter One: Pemetrexed Personalized Medicine: Introduction and Thesis Objectives

Chapter Two: Pemetrexed Personalized Medicine: *In Vitro* Screen Determination

Chapter Five: Chapter Five: Pemetrexed Personalized Medicine: FTCD and Pemetrexed-Related Gene Expression Across Cell Line Panel

Chapter Six: Pemetrexed Personalized Medicine: Retrospective Clinical Analysis of Pemetrexed Treated Patients, Proposed Plans and Translational Potential

Appendix: Gemcitabine Cisplatin Combination: *In Vitro* Response Phenotypes, *In Vivo* Toxicity Study, and Mouse Hospital Trials

ABBREVIATIONS

PEM: Pemetrexed, Alimta, LY231514, MTA

CIS: Cisplatin, CDDP

CARB: Carboplatin

GEM: Gemcitabine, Gemzar

PAC: Paclitaxel, Taxol

CF: Colony Formation

MTS: 3-(4,5-dimethylthiazol-2-yl)-5-(3-carboxymethoxyphenyl)-2-(4-sulfophenyl)-2H-tetrazolium salt

PMS: Phenazine Methosulfate, Electron Coupling Reagent for MTS Assay

IC50: Inhibitory Concentration of 50 Percent

IC100: Inhibitory Concentration of 100 Percent

NSCLC: Non-Small Cell Lung Cancer

TNM: Tumor Node Metastasis, Classification of Malignant Tumors

AC: Adenocarcinoma

LC: Large Cell Carcinoma

SQ: Squamous Cell Carcinoma

HBEC: Human Bronchial Epithelial Cell

HCC: Hamon Cancer Center

R5: RPMI 1640 Media with L-Glutamine Supplemented with 5% Fetal Bovine Serum

R10: RPMI 1640 Media with L-Glutamine Supplemented with 10% Fetal Bovine Serum

KSFM: Keratinocyte Serum Free Media Supplemented with Epidermal Growth Factor 1-53 and Bovine Pituitary Extract

ECOG: Eastern Cooperative Oncology Group

TX: Treatment

CT: Computed Tomography

PET: Positron Emission Tomography

q3w: Every three weeks

qwx3: Once weekly, for three weeks

THF: Tetrahydrofolate

MTX: Methotrexate

FTCD: Formiminotransferase Cyclodeaminase

EGFR: Epithelial Growth Factor Receptor

EML4: Echinoderm Microtubule Associated Protein Like 4

ALK: Anaplastic Lymphoma Receptor Tyrosine Kinase

TP53: Tumor Suppressor Protein 53, p53

KRAS: v-Ki-ras2 Kirsten rat sarcoma viral oncogene homolog

TYMS: Thymidylate Synthase/Synthetase

DHFR: Dihydrofolate Reductase

GARFT/GART: Glycinamide Ribonucleotide Formyl Transferase

FPGS: Folylpolyglutamate Synthase/Synthetase

RFC1: Reduced Folate Carrier 1

ATIC: AICARFT, 5-Aminoimidazole-4-Carboxamide Ribonucleotide Formyltransferase

FR-α: Folate Receptor Alpha

HSP90: Heat Shock Protein 90

RL53: TP53 Knockdown (p53RNAi), Constitutive Mutant K-RAS^{V12}

KT: Ectopic Expression of CDK4 and hTERT

glu5: Pentaglutamation

MTD: Maximum Tolerated Dose

Cpmax: Maximum Plasma Concentration

ORR: Overall Response Rate

OS: Overall Survival

PFS: Progression Free Survival

TTP: Time to Progression

qRT-PCR: Quantitative Real Time Polymerase Chain Reaction

WB: Western Blot

TXN: Transfection

KD: Knockdown

O/E: Overexpression

CTL: Control

WT: Wild-type

shRNA: Short Hairpin RNA

NOD/SCID: Non-Obese Diabetic/Severely Compromised Immunodeficient

i.p.: Intraperitoneal

i.v.: Intravenous

subQ: Subcutaneous

HTG: High Throughput Genomics

qNPA: Quantitative nuclease protection assay

PEMETREXED PERSONALIZED MEDICINE:

INTRODUCTION AND THESIS OBJECTIVES

ABSTRACT

In this chapter, I describe the current clinical indications for the FDA-approved chemotherapeutic pemetrexed, and the significant survival benefits observed in a subset of lung cancer patients after treatment with this drug. The exploration of this dissertation project was sparked from available legacy MTS response data on pemetrexed from the Minna laboratory on a large panel of lung cancer cell lines. Specifically, pemetrexed is a potent inhibitor of three folate-dependent enzymes TYMS, DHFR and GARFT, and its inhibitory activity is increased upon specific pentaglutamation by FPGS. Currently, mechanisms of pemetrexed response have been weakly associated with mRNA levels of the enzyme TYMS. This is suggestive that other mechanisms of response may be playing a key clinical role. In order to determine non-canonical mechanisms driving clinical response to pemetrexed, I outline the development of the doses and schedule chosen for our clinically applicable liquid colony formation model that was derived from published Phase I pharmacokinetics. Important background information is introduced on the key identified biomarker from this research, FTCD. Lastly, I define the thesis objectives of this dissertation proposal and the translational potential of this research project in lung cancer.

INTRODUCTION

Lung cancer is a major health problem. The estimated number of new cases and deaths from lung cancer in the United States in 2009 are 219,440 and 159,390, respectively (SEER Cancer Statistics Review, 2010). Lung cancer affects both men and women, and is the estimated to be the cause of more cancer-related deaths than breast, prostate, ovarian and colon cancers combined in 2011 (American Cancer Society Surveillance Research, 2011). Major improvements in these statistics through translational research are required if significant progress is to be made in lung cancer therapy.

Pemetrexed (Alimta®, LY231514) is a multi-targeted anti-folate chemotherapy that is well tolerated in lung cancer patients with advanced stage disease. The FDA approved pemetrexed for NSCLC first-line combination therapy with cisplatin (Vogelzang et al., 2003), and as a single agent for second-line or maintenance therapy (Hanna et al., 2004). Moreover, pemetrexed was recently introduced into multiple Phase II clinical trials as a single-agent first-line NSCLC therapeutic (Ricciardi et al., 2009). Pemetrexed can be given to elderly patients (Gridelli et al., 2007) because there are minimal adverse events with supplementation of 1 mg oral folic acid daily and 1 mg intramuscular vitamin B12 injections before therapy induction every three cycles, and higher doses (up to 925 mg/m^2) can be achieved in heavily pre-treated cancer patients (Hanauske et al., 2007). Interestingly, pemetrexed is not indicated for lung cancer patients with squamous cell carcinoma histology, as a result of two multi-center, double-

blind, randomized clinical trials by Eli Lilly (Figures 1 and 2). The precise mechanism of resistance of squamous cell lung cancer to pemetrexed is unknown (Kubota et al., 2009), although average *TYMS* mRNA was shown to be two-fold higher across a panel of SQ NSCLCs compared to other lung cancers (Ceppi et al., 2006).

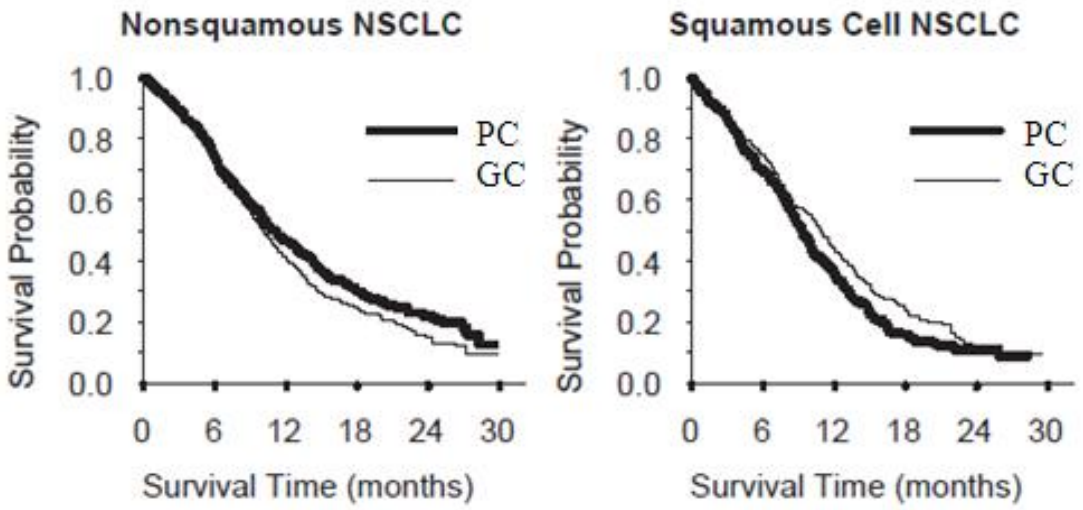

Figure 1. NSCLC Patients with Nonsquamous Histotypes Have Improved Overall Survival with Pemetrexed/Cisplatin Combination Chemotherapy. 1,725 chemonaïve patients were randomized to either pemetrexed/cisplatin (n=862, PC) or gemcitabine/cisplatin (n=863, GC) for first-line combination therapy. Adapted from FDA Approval of Pemetrexed, 2009.

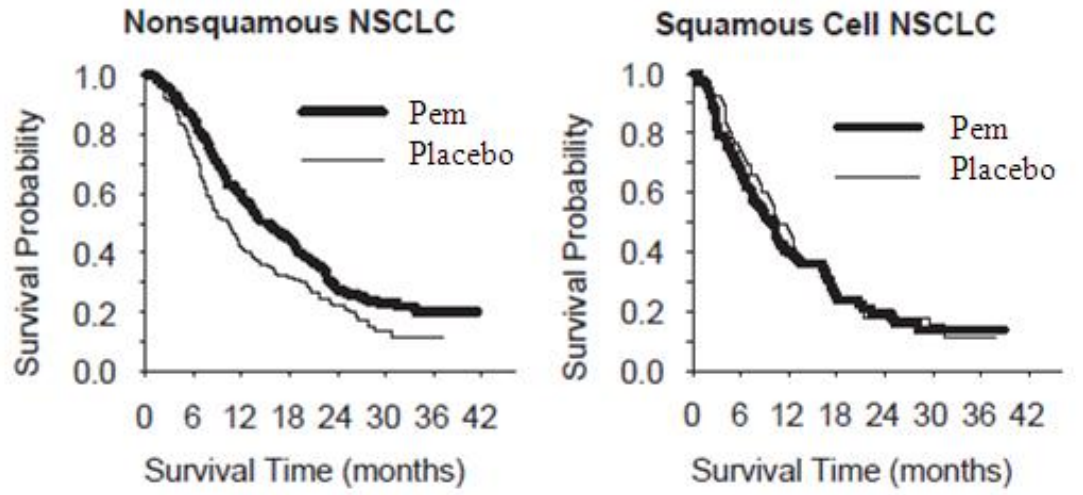

Figure 2. NSCLC Patients with Nonsquamous Histotypes Have Improved Overall Survival with Pemetrexed Maintenance Chemotherapy. Placebo-controlled

maintenance pemetrexed clinical trial performed with 663 patients with stage IIIb/IV NSCLC (who did not progress after four cycles of platinum-based chemotherapy). Patients were randomized 2:1 to either pemetrexed (n=441) or placebo (n=222) for maintenance therapy, until progression. Adapted from FDA Approval of Pemetrexed, 2009.

Anti-folate chemotherapeutics have been administered as cancer treatment regimens for over 50 years. Classical anti-folate therapeutics including methotrexate specifically target the enzyme dihydrofolate reductase (DHFR), depleting the cancer cell of intermediate tetrahydrofolates (THF). The loss of THF cofactors indirectly inhibits the mechanism of action of other folate-dependent enzymes such as thymidylate synthase (TYMS) and glycinamide ribonucleotide formyl transferase (GARFT). Pemetrexed differs from previous anti-folates as pemetrexed directly targets three folate-dependent enzymes: DHFR, TYMS and GARFT (Figure 3) (Shih et al., 1997). Inhibition of folate metabolism with pemetrexed subsequently results in the termination of RNA and DNA synthesis.

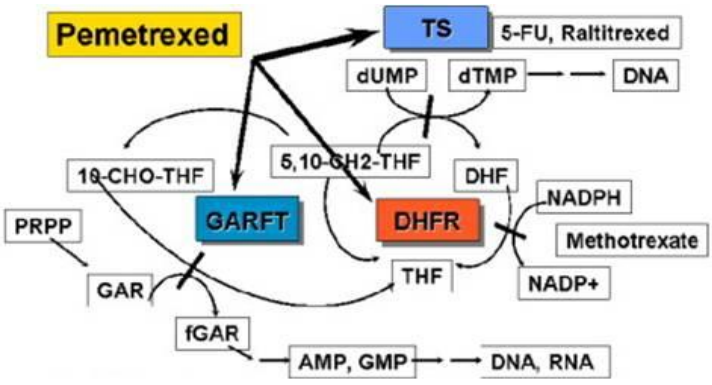

Figure 3. Pemetrexed Inhibits Three Folate-Dependent Enzymes: TYMS, DHFR, and GARFT. Model of pathway adapted from Hanauske, et al., 2001.

Pemetrexed inhibits these enzymes with great specificity as a result of pentaglutamation (glu5) of pemetrexed by folylpolyglutamate synthase (FPGS) (Shih et

al., 1997). It is thought that pentaglutamation is much greater in tumor than in normal tissues (Shih et al., 1997). In addition to specificity enhancement, pentaglutamation of pemetrexed results in longer drug retention in cancer cells (Shih et al., 1997).

				Fold Decrease in K_i with Pentaglutamation		
Compound	**TYMS**	**DHFR**	**GARFT**	**TYMS**	**DHFR**	**GARFT**
Pemetrexed	109 ± 9.0	7 ±1.9	9,300 ± 690	100	0	175
Pemetrexed glu5	1.3 ± 0.3	7.2 ± 0.4	65 ± 16			
Methotrexate	13,000	0.004	80,000	276	0	32
Methotrexate glu5	47	0.004	2,500			
Raltitrexed	6 ± 0.9	45 ± 3.0	424,000	4	1	3
Raltitrexed glu5	1.4 ± 0.1	30 ± 3.0	132,000			

Figure 4. K_i Values of Three Folate-Dependent Enzymes (TYMS, DHFR, and GARFT) Before and After Pentaglutamation of Anti-Folates. Comparison of the inhibition constants, of respective parent compounds versus pentaglutamated daughter compounds, to TYMS, DHFR, and GARFT. K_i values were plotted as inhibition concentrations (nM).

Pemetrexed is a polar charged chemical compound that requires a transporter for the drug to enter cells. Pemetrexed is shuttled into the cell by reduced folate carrier (RFC1) (Jackman and Calvert, 1995) and folate receptor alpha (FR-α) (Westerhof et al., 1995). Interestingly, pemetrexed has a relatively small volume of biodistribution (78% drug is excreted unchanged after 24 hours), due to rapid clearance (Rinaldi et al., 1999). Furthermore, pemetrexed is administered intravenously to patients, where preclinical bioavailability pilot experiments results in generally poor absorption of drug from the gastrointestinal tract (Hanauske et al., 2001).

As there is a large subset of NSCLC patients that fail to respond to pemetrexed chemotherapy, research groups have been working to determine the intrinsic mechanisms

driving resistance. As of late, the general dogma has been pemetrexed resistance is associated with higher mRNA levels of the enzyme TYMS (also, the target for 5-FU and raltitrexed) (Ceppi et al., 2006). TYMS is not the only target of pemetrexed, and secondary sites of pemetrexed inhibition can exhibit anti-tumor effects independent of TYMS levels, upon the addition of thymidine to rescue TYMS-specific cytotoxicity (Schultz et al., 1999). The combination of exogenous hypoxanthine and thymidine are required for complete rescue of pemetrexed-related cytotoxicity (Smith et al., 2001). Furthermore, tumor lines MCFTDX and H630RIO, which overexpress TYMS are resistant to the TYMS inhibitors 5-FU and raltitrexed, but are 261- and 1,289-fold more sensitive to pemetrexed than raltitrexed, suggesting *TYMS* levels are not solely predictive of pemetrexed response (Hanauske et al., 2001). Therefore, these results necessitate for a comprehensive genome-wide research study on a large panel of NSCLC to determine mechanisms driving pemetrexed response.

Phase II clinical trials for pemetrexed first-line single-agent therapy exhibited overall response rates of 4-23%, and pemetrexed therapy is very expensive (Ricciardi et al., 2009). Given pemetrexed's relatively low toxicity, it has become common in the oncology community to treat patients with pemetrexed until progression, either as a monotherapy maintenance option or as a continuation of pemetrexed alone from the initial first line combination with platinum (Camidge et al., 2011). However, only a subset (~25%) of NSCLC patients benefit from pemetrexed therapy while most do not. Thus, it would be useful to develop tumor biomarkers to predict which patients would benefit ("personalized medicine").

Previous NSCLC Pemetrexed Response Phenotypes Identified by Minna Lab Members

This project was established as a result of intriguing, legacy data using a mass culture MTS assay produced by other members of the John Minna laboratory (Michael Peyton, Ph.D, Sunny Zachariah, Stephanie Weber, Yao Ma, MK Hyland and Rachel Greer, UT Southwestern) (Figure 5). Their research identified two populations of NSCLC pemetrexed response phenotypes suggesting there were potentially pemetrexed-sensitive and –resistant NSCLC lines. These legacy data suggested study of a much larger panel of lung cancer lines, the use of other assays, and the need for mechanistic studies.

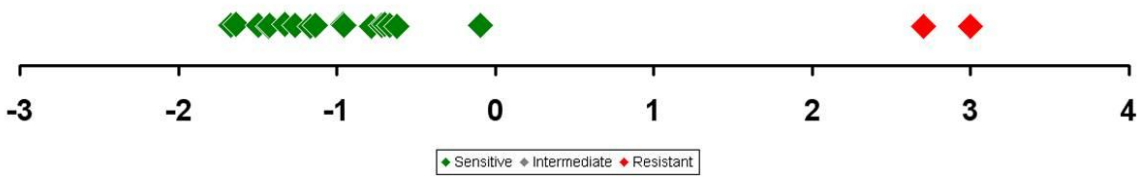

Figure 5. Pemetrexed Legacy MTS Data from Minna Laboratory Members. Previous MTS IC50 data for pemetrexed across lung cancer panel, plotted as $\log_2$ values. Each dot represents one cell line. Using a normal mixture model, NSCLC lines were classified as green, sensitive; grey, intermediate; red, resistant.

Determination of *In Vitro* Pemetrexed Dose Schedule

I first wanted to identify pemetrexed doses to be tested in preclinical models that were similar to those found in the clinic. From Phase I clinical trial pharmacokinetics, I identified the maximum achievable plasma concentration (Cpmax, µg/mL) at the maximum tolerated dose (MTD) of 600 mg/m^2 (Figure 6) (Rinaldi et al., 1999). The equivalent achievable tissue culture concentration of pemetrexed was extrapolated to be

229 µM. Therefore, 240 µM (143.39 µg/mL) was the highest dose tested to ensure the upper range of response at the MTD was determined.

Clinical Dose Received	Max Plasma Concentration Cp_{max} (µg/mL)	Equivalent Dose for Tissue Culture (µM)
350 mg/m²	91.4	152.9
525 mg/m²	121.2	202.5
600 mg/m² (MTD)	137	229.3

Figure 6. Determination of Pemetrexed Dose for Preclinical Studies Based on Phase I Clinical Trial Pharmacokinetics. The achievable molarity was determined by the division of the Cpmax by the molecular weight of the drug. Adapted from Rinaldi, et al. 1999.

To determine the schedule of pemetrexed treatment for tissue culture experiments, I observed the time-to-1,000-fold drug clearance at the MTD of pemetrexed. Phase I clinical trial pharmacokinetics suggest that pemetrexed is greater than 99.9% cleared within a 24 hour period (Figure 7) (Britten et al., 1999). The pharmacokinetic behavior of pemetrexed treated patients achieves steady state clearance levels consistent from cycle one of treatment to cycle four.

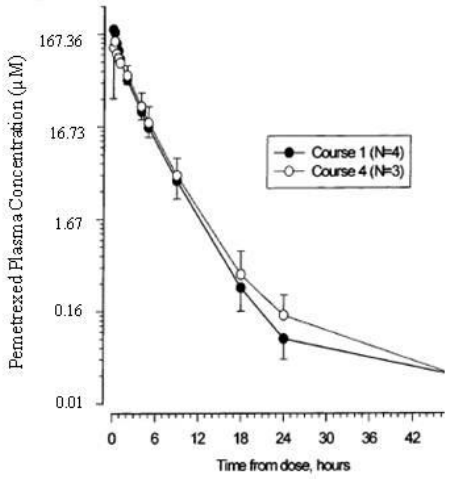

Figure 7. Pemetrexed Schedule Determination Based on Phase I Clinical Trial Pharmacokinetics. The time of treatment in culture was determined by the time to

1,000-fold drug clearance in patients treated with pemetrexed from the Phase I clinical trial. Pemetrexed plasma concentrations are plotted in log scale. Adapted from Rinaldi, et al. 1999.

Formiminotransferase cyclodeaminase (FTCD, 21q22.3) is a cytosolic bifunctional homooctameric enzyme with transferase and deaminase active domains, where both functions are involved in folate metabolism (Bashour and Bloom, 1998). Specifically, FTCD catalyzes two consecutive steps in the modification of tetrahydrofolate to 5,10-methenyl tetrahydrofolate. Ironically, FTCD was initially identified in-house at UT Southwestern Medical Center (Dallas, TX) as a 58 KDa Golgi apparatus-specific protein (Bashour and Bloom, 1998). FTCD was readily detected in rat liver but not in other rat organs (Figure 8), unless under much higher protein loading or long exposure conditions (Bashour and Bloom, 1998).

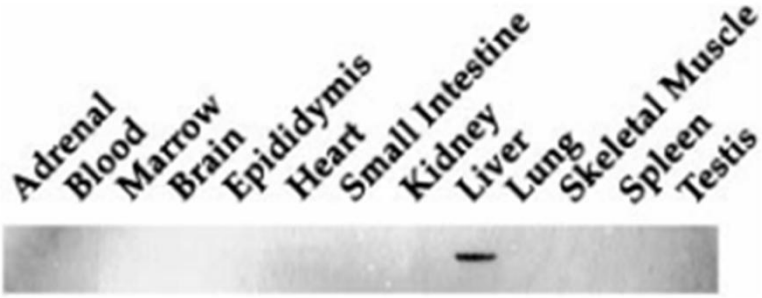

Figure 8. FTCD is Exclusively Expressed in Rat Liver, and Not in Other Tissues. Rat tissue was extracted, lysed and immunoblotted for FTCD (58 KDa). Adapted from Bashour and Bloom, 1998.

Furthermore, later studies elucidated that FTCD was differentially expressed in normal liver tissue and not in hepatocellular carcinoma (Figure 9), thus developing a novel immunohistochemical marker for identification of hepatocellular carcinomas (Seimiya et al., 2008).

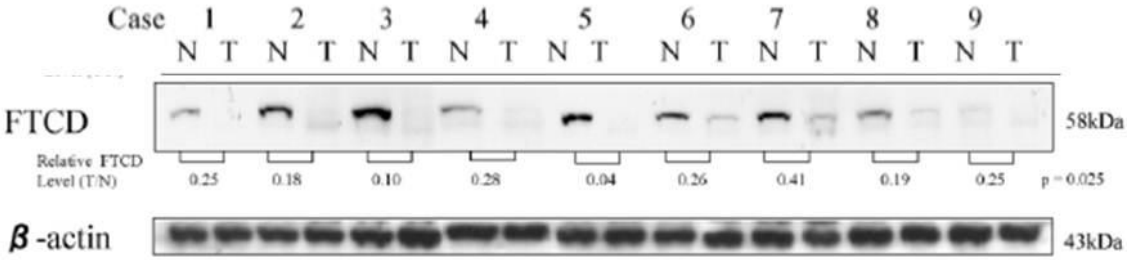

Figure 9. FTCD is Exclusively Expressed in Normal Liver Tissue in Patients, Not in Hepatocellular Carcinoma. Immunoblotting of protein extracts from resected hepatocellular tumor (T) and adjacent non-tumor (N) normal tissue for FTCD (58 KDa and β-actin (43 KDa). T/N ratios were calculated and plotted beneath FTCD immunoblot. Adapted from Seimiya et al., 2008.

Interestingly, FTCD has been shown to interact with and stabilize mesenchymal-associated vimentin intermediate filaments at the Golgi Apparatus in COS-7 cells (Gao and Sztul, 2001).

To date, expression of FTCD has not been identified in lung cancer. More importantly, FTCD has not been implicated in anti-folate chemotherapeutic research. The studies presented in this dissertation will demonstrate that FTCD is a novel predictive biomarker for pemetrexed sensitivity in lung cancer.

THESIS OBJECTIVES (SPECIFIC AIMS)

Objective One: To establish a clinically relevant pemetrexed preclinical *in vitro* assay and dose schedule to identify NSCLC response phenotypes in a large panel of lung cancer lines.

Objective Two: To identify clinical indications, oncogenotypes and histotypes that correlate with NSCLC response to pemetrexed.

Objective Three: To determine for mouse xenograft studies well tolerated murine doses of pemetrexed *in vivo* and then determine if NSCLC *in vitro* response phenotypes are matched by NSCLC xenograft responses *in vivo*.

Objective Four: To determine NSCLC gene expression signatures that correlate with pemetrexed response phenotype, and validate these expression differences in secondary assays.

Objective Five: To collect and test a retrospective dataset of lung cancer patient archival samples for biomarkers predicting pemetrexed response.

PEMETREXED PERSONALIZED MEDICINE:

IN VITRO SCREEN DETERMINATION

ABSTRACT

In this chapter, I examine the drug responses of pemetrexed by two independent *in vitro* assays, MTS and liquid colony formation to determine the most optimal assay for screening lung cancer cell lines. The results are suggestive that the liquid colony formation assay better mimicked clinical results with respect to squamous cell histology, while MTS assay results for pemetrexed were not as well correlated. However, one limitation of the clonogenic drug model was the lack of colony formation in ~10% of NSCLC line with our current culture conditions. There were three distinct pemetrexed response phenotypes found by testing with liquid colony formation across our large NSCLC cell line panel (n~75), spanning nearly 10,000-fold differences in IC50s. Histology-dependent sensitivity to pemetrexed was observed in large cell carcinomas. Furthermore, cell lines established from the same patient's tumor/normal pair exhibited drastic differences in response to pemetrexed. These results suggest that within our colony formation model there is a large therapeutic window and tumor specificity for pemetrexed.

MATERIALS AND METHODS

Reagents

Drugs used were obtained from the UT Southwestern Campus Pharmacy (Dallas, TX), and handled with aseptic technique. Pemetrexed/Alimta®, Eli Lilly (Indianapolis, IN), LC Laboratories (Woburn, MA), was reconstituted in 0.85% sterile sodium chloride, as per manufacturer's instructions, to make 83 μM solution (MW 597).

Cell Preparation

NSCLC and HBEC cell lines were obtained from Hamon Center Collection (University of Texas Southwestern Medical Center) (Phelps et al., 1996). NSCLC cells were grown in sterile, filtered RPMI 1640 with L-glutamine, Cellgro (Manassas, VA) supplemented with 5% fetal bovine serum, Gemini Biotech (Alachua, FL). HBECs were grown in keratinocyte serum free media (KSFM) supplemented with epidermal growth factor 1-53 (5 ng/mL) and bovine pituitary extract (50 μg/mL), and all reagents are from Life Technologies (Gaithersburg, MD). Oncogenically manipulated HBECs were grown in sterile, filtered RPMI 1640 with L-glutamine supplemented with 10% fetal bovine serum. The cells were incubated at 37°C in a 5% CO_2, and split with 0.05% trypsin EDTA, Gibco, Invitrogen (Carlsbad, CA) when confluent. Trypsin is neutralized after sufficient cell detachment from the dish, by addition of trypsin neutralizing solution, Lifeline Cell Technology (Fredrick, MD). Cell lines have been DNA fingerprinted by PowerPlex 1.2 System, Promega (Madison, WI) for identity confirmation, and tested for

mycoplasma contamination by e-MycoPCR Mycoplasma Detection Kit, Boca Scientific Inc (Boca Raton, FL).

MTS Assay

In vitro MTS drug response assay was carried out in 96-well flat bottom plates, in octuplicate replicas per dose per plate, with up to four replicas per cell line. Cells were seeded (500 cells up to 4000 cells per well), using an 8-channel multipipettor depending on the empirically determined proliferative nature of each cell line on day 0. On day 1, reconstituted descending four-fold dilutions of drug beginning with 250 μM for pemetrexed in either R5 or KSFM media and added to the cells, excluding "no drug" control and "blank" wells, for a final volume of 100 μL in every well. On day 5, MTS reagent is warmed to 37ºC and complexed with PMS electron coupling reagent at a 20/1 ratio, and added to the cells, 20 μL per well. The plates are incubated at 37ºC for up to 1 hour, and absorbance is measured by a spectrophotometer at 490 nm. IC50 values are determined by in-house software, DIVISA.

Colony Formation Assay

In vitro drug response was carried out in 6-well plates, with at least four replicas. All cells were plated at 500 cells per well on day 0, and on day 1, pemetrexed is added in media in five serial dilutions, beginning with 240 μM. Only media is added to the control, or the "no drug" well. The drug is removed after 24 hours, and replaced with fresh media. The cells are incubated for two weeks, media is removed, cells fixed with 0.05% crystal violet/glutaraldehyde for 30 minutes and colonies counted. Imaging of

colonies and IC50 value determination were calculated using Quantity One 4.6.5 software.

RESULTS

In Vitro MTS Pemetrexed Drug Response Assay

I screened a large panel of cell lines (lung cancer and normal lung lines) simultaneously by MTS and liquid colony formation assays to determine the most clinically relevant *in vitro* model. 48 NSCLC lines and 3 HBECs were tested by MTS assay, with at least three replicas each (Figure 1). All of the HBECs tested were resistant to treatment, and failed to exhibit an IC50 dose (Figure 2). Squamous cell carcinomas exhibited a highly variable response to pemetrexed with IC50 values ranging from greater than 250 μM (SD ± 1) to 0.843 μM (SD ± 7.5).

Cell Line	Assays	Median	SD
A549	5	250	1
Calu-1	8	250	1
Calu-3	5	250	1
EKVX	4	250	1
H1155	5	0.019	1.4
H125	4	0.0452	1.7
H1299	3	0.018	1.6
H1355	7	250	1
H1395	6	250	1
H1568	6	0.0315	2
H1573	4	250	1
H1650	4	245	1.1
H1703	4	6.52	69
H1792	4	250	93
H1819	4	250	19
H1944	4	0.0675	2.9
H1993	3	0.009	1.9
H2009	4	0.0179	27
H2030	4	250	1
H2052	4	0.0076	1.2
H2073	4	0.0306	2.9
H2087	4	250	1
H2126	4	11.9	71
H226	4	0.843	7.5
H2342	4	250	1
H2882	4	250	1
H2887	4	250	1.1
H290	4	0.0101	1.9

Cell Line	Assays	Median	SD
H3122	4	0.0157	2.8
H322	4	250	1
H324	3	250	1.2
H358	5	0.014	4.7
H441	4	250	1
H460	4	0.145	1.7
H647	4	0.39	35
H650	4	250	1
H969	4	250	1.2
HBEC17KT	4	250	1
HBEC30KT	4	250	1
HBEC34KT	4	250	1
HCC1195	4	250	1
HCC2429	4	0.0113	5.6
HCC2450	6	250	1
HCC2935	3	250	1.1
HCC366	4	250	1
HCC4006	4	34.9	110
HCC4011	8	7.48	27
HCC4017	4	1.58	370
HCC4019	6	0.012	53
HCC44	8	13.5	110
HCC461	3	0.025	1.7
HCC515	4	33.9	28

Figure 1. Pemetrexed Drug Response Phenotypes by MTS Assay. Cells were treated for 96 hours, and viability was determined using a spectrophotometer after 1 hr incubation with MTS/PMS. The median IC50 value and standard deviation (SD) of the replicas for each cell line are plotted above, with at least three replicas per cell line.

Cell Line	Assays	Median	SD
HBEC17KT	4	250	1
HBEC30KT	4	250	1
HBEC34KT	4	250	1

Cell Line	Assays	Median	SD
Calu-1	8	250	1
H1703	4	6.52	69
H226	4	0.843	7.5
HCC2450	6	250	1

Figure 2. Analysis of MTS Data Suggests Response of Squamous Cell Carcinomas is Highly Variable, Inconsistent with Clinical Indications. Cells were treated for the MTS assay, as stated previously. The median IC50 value and SD of the replicas for each cell line are plotted above, with at least four replicas per cell line.

In Vitro Pemetrexed Liquid Colony Formation Assay

I screened a large panel of cell lines (lung cancer and normal lung lines) simultaneously by liquid colony formation assays (CFA) (Figure 3). For the development of the liquid colony formation model, HBEC34KT and H226 were used as controls that should show no response to pemetrexed. In fact, no effect of pemetrexed treatment was seen at all doses of pemetrexed in normal immortalized line, HBEC34KT, or for squamous cell carcinoma H226.

In contrast, colony formation was completely inhibited by pemetrexed at 2.4 μM in H2122 cells (Figure 3). The concentration effects showed a steep curve with no inhibition seen at 0.24 μM and complete inhibition at 2.4 μM pemetrexed.

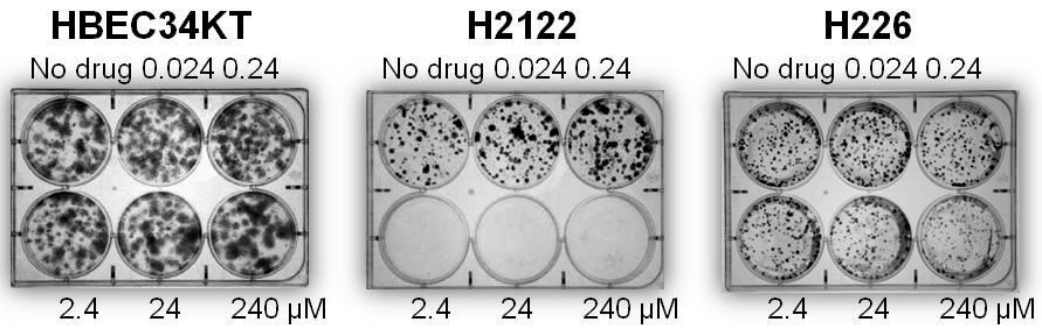

Figure 3. Establishment of Pemetrexed Liquid Colony Formation Assay. Cells were treated after adherence with five 10-fold dilutions of pemetrexed (240, 24, 2.4, 0.24, 0.024 µM) and no drug control. Media was exchanged after 24 hours. Cell lines were tested with at least four replicas. HBEC34KT, normal lung cell line; H2122, adenocarcinoma; H226, squamous cell carcinoma.

Identification of Three Distinct Response Phenotypes

Upon screening NSCLC and HBEC lines by CFA, three unique pemetrexed response phenotypes were identified: sensitive, intermediate, and resistant (Figure 4). Sensitive lines showed a complete response upon treatment, where no colonies remained above their respective IC50 doses. Intermediate lines exhibited a partial response at IC50 doses; however, there are several remaining colonies at all doses. Resistant lines fail to exhibit a response to pemetrexed, and do not have an identifiable IC50 dose.

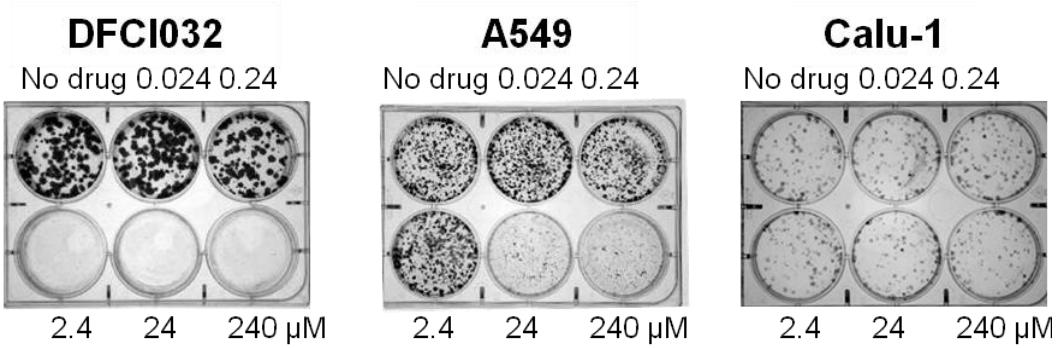

Figure 4. Pemetrexed Liquid Colony Formation Elucidates Three Distinct Response Phenotypes: Sensitive, Intermediate, and Resistant. Cells were treated using colony formation assay protocol with at least four replicas. Response phenotypes: DFCI032, sensitive; A549, intermediate; Calu-1, resistant.

Heterogeneous Response to Pemetrexed at 240 µM Across Cell Line Panel

Upon completion of the colony formation assay screen, I determined that the cell lines showed reproducible response phenotypes that varied dramatically across the panel. I quantified colonies at the highest pemetrexed treatment level (240 µM), and plotted these values as a percent of control (Figure 5). There were over two-logs (log_{10}) of kill at 240 µM pemetrexed in the sensitive lines, as compared to the inhibition of colony formation in the resistant lines.

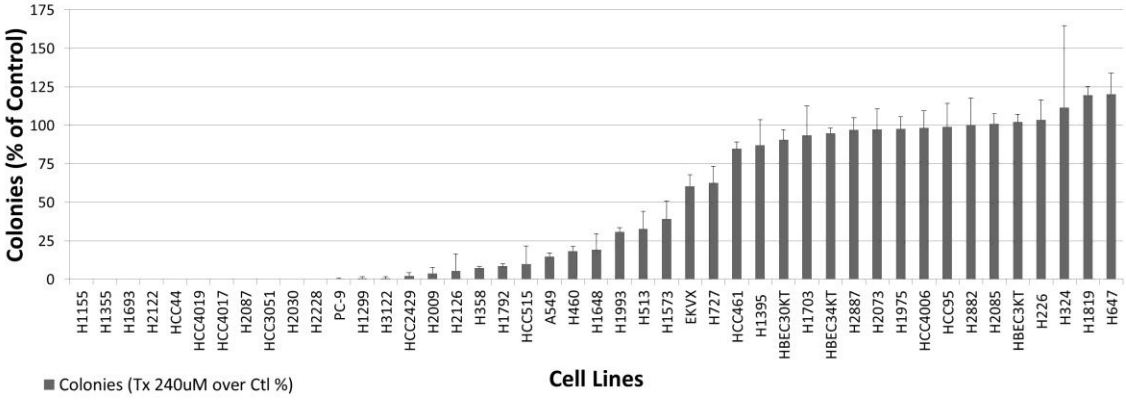

Figure 5. Response to Pemetrexed at 240 µM is Dramatically Heterogeneous Across the Lung Cancer Cell Line Panel. Quantified average colony formation are displayed as a waterfall plot of highest treatment dose (240 µM) as a percent of control (± SD). Results are the average of four or more replicate experiments.

Histology-Dependent and -Independent Responses to Pemetrexed

Interestingly, there appears to be pemetrexed responses which are histotype-dependent and -independent across the lung cancer panel (Figure 6). For example, all of the large cell carcinomas (LC) exhibit sensitive or intermediate phenotypes. By contrast, all of the normal HBECs tested and the squamous cell carcinoma cell lines were resistant to pemetrexed treatment with IC50 values greater than 240 µM (Figure 6). Correlation

analysis of our cell line panel revealed statistically significant correlation of squamous cell carcinoma histology with resistance to pemetrexed (correlation -0.38, p-value 0.007), large cell carcinoma histotypes are statistically significantly correlated with sensitivity to pemetrexed by the CFA (correlation coefficient 0.32, p-value 0.02), while adenocarcinomas (AC) were split evenly into all three response phenotypes (correlation 0.23, p-value 0.11) (Figure 6).

Sensitive	Intermediate	Resistant
DFCI032	A549	Calu-1
H23	Calu-6	H226
H1155	EKVX	H290
H1299	H358	H324
H1355	H460	H596
H1648	H1573	H647
H1693	H1993	H650
H1792	HCC515	H820
H1944		H969
H2009		H1395
H2023		H1650
H2030		H1703
H2087		H1819
H2122		H1975
H2228		H2073
H2347		H2085
H3122		H2882
HCC44		H2887
HCC2429		**HBEC3KT**
HCC3051		**HBEC30KT**
HCC4017		**HBEC34KT**
HCC4019		HCC95
PC-9		HCC461
		HCC827
		HCC2450
		HCC4006

Figure 6. Response to Pemetrexed May Be Dependent on Histology for Large Cell and Squamous Cell Carcinomas, But Not Adenocarcinomas. Pemetrexed response

phenotypes were determined using the CFA with four or more independent experiments. Green, large cell carcinoma; Red, squamous or adenosquamous cell carcinoma; Black bolded, HBECs; Black, adenocarcinoma or NSCLC-NOS.

Response of Cell Lines Which Do Not Form Colonies

There was also a subset of NSCLC lines (n=12, ~10% of total tested) which were unable to form colonies at 500 or 5,000 cells per well (Figure 7).

Cell Line	
H1734	HCC1359
H1869	HCC1588
H2250	HCC2374
H2258	HCC2935
H2342	HCC4011
HBEC17KT	HCC4018

Figure 7. Cell Lines That Were Not Able to Form Colonies. Cells were tested for their clonogenic potential using colony formation assay protocol, with at least four replicates.

Paired Samples from the Same Patient Exhibited Differences in Pemetrexed Response

Paired samples from the same patient were tested simultaneously to assess whether there were differences in response. Paired samples of lung cancer and normal lung epithelial cell lines (HCC4017/HBEC30KT) were tested, and exhibited a near ~10,000-fold difference in pemetrexed response (Figure 8). HCC4017 was very sensitive to pemetrexed, and there was a complete inhibition of colony formation at 0.24 μM, while HBEC30KT was resistant to pemetrexed, and failed to show inhibition of colony formation at 240 μM.

Paired tumor samples from the same patient (H1693/H1819) had a near 1,000-fold difference in response (Figure 8). H1693 was very sensitive to pemetrexed with a complete inhibition of colony formation at 2.4 µM, while H1819 did not exhibit colony inhibition at all doses tested (IC50 > 240 µM). In fact, H1819 actually showed statistically significant improvement in clonogenicity with increasing doses of pemetrexed.

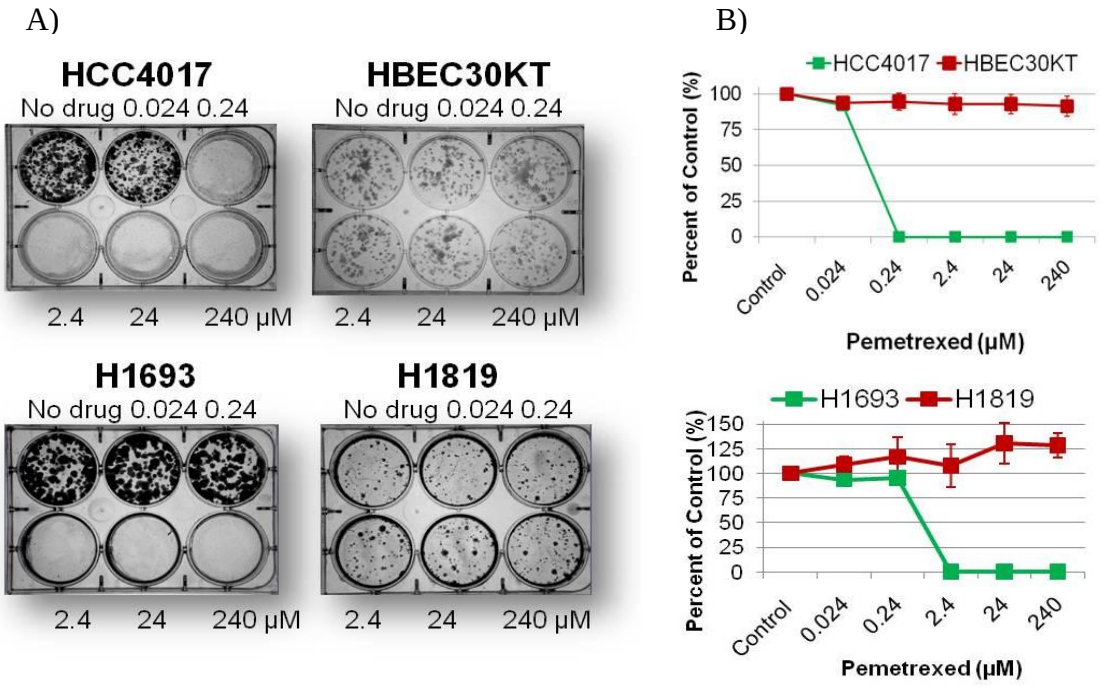

Figure 8. Paired Samples HCC4017/HBEC30KT and H1693/H1819 Exhibit Significant Differences in Response to Pemetrexed. A) Cells were treated using colony formation assay protocol with at least four replicates. B) Colonies were counted and plotted graphically (± SD). Green, sensitive; Red, resistant.

DISCUSSION

The purpose of this thesis proposal was to identify molecular mechanisms driving drug response to pemetrexed in NSCLC. To determine these factors, I needed to develop a clinically relevant *in vitro* drug response screen to test a large panel of lung cancer cell lines. There have been previous studies that have tested the response of pemetrexed in lung cancer lines. However, in general, these studies did not use conditions (dose, drug exposure) that mirrored those used in the clinic treating patients. The clinical relevance of these studies is questionable, in large part, due to elevated drug exposure times *in vitro* in the majority of prior studies. For example, one research group treated cells with pemetrexed by MTS assay for 72 hours to determine the IC50 of NSCLC lines (Takezawa et al., 2011), thus exposing the cells to drug longer than clinically achievable.

Cell Line	Shields et al., 2011	Previous Studies			
	Colony Formation Assay (CF) IC50 (μM)	IC50 (μM)	Drug Assay	Duration of Treatment	Reference
A549	2.4	0.15	CF	72 hrs	Lu et al., 2001
	2.4	0.65	CF	72 hrs	Yang et al., 2011
	2.4	< 7	SRB/MTS	72 hrs	Smith et al., 2001
	2.4	0.07	MTS	72 hrs	Takezawa et al., 2011
	2.4	0.4	Mass culture	24 hrs	Giovannetti et al., 2004
Calu-1	> 240	57.12	Mass culture	24 hrs	
Calu-6	2.4	8.08	Mass culture	24 hrs	
H1299	24	0.08	MTS	72 hrs	Takezawa et al., 2011
H23	2.4	0.072	MTS	96 hrs	Uemura et al., 2010
PC-9	2.4	0.014	MTS	96 hrs	
	2.4	0.03	MTS	72 hrs	Takezawa et al., 2011

Figure 9. Direct Comparison of Previous Pemetrexed IC50 Values with Shields et al. 2011 Research Findings on NSCLC Cell Lines. The comprehensive table above summarizes previous data on NSCLC lines treated with pemetrexed, as compared to our research findings. CF, pemetrexed colony formation assay; SRB, cytotoxicity reagent.

If these research studies failed to mimic clinical exposure to pemetrexed, then therefore these findings cannot be applied to patients and should be reevaluated with different, usually shorter, treatment schedules (Hanauske et al., 2007; Smith et al., 2001; Tonkinson et al., 1999); (Uemura et al., 2010) (Lu et al., 2001; Rothbart et al., 2010; Yang et al., 2011). I also discovered this occurrence in our own results when I simultaneously tested MTS alongside liquid colony formation (Figure 1), and determined that cellular responses of squamous cell carcinomas were inconsistent with clinical indications (Figure 2). The cells were being exposed to drug for 96 hours, which is 72 hours longer than clinically achievable in patients.

There have been three studies that have used doses of pemetrexed near the MTD, (Hanauske et al., 2007), (Giovannetti et al., 2004) and (Mercalli et al., 2007). The Hanauske and Giovannetti studies were designed in conjunction with Eli Lilly. Pancreatic cancer researchers Mercalli et al. used up to the pemetrexed MTD of 229 μM; however, the pancreatic cancer cells were treated for 48 hours (Mercalli et al., 2007). Groups of Hanauske and Giovannetti used doses of up to 100 μg/mL pemetrexed (167 μM) (Giovannetti et al., 2004; Hanauske et al., 2007). To date, Giovannetti et al. has been the most appropriately designed experimentation for pemetrexed drug response in lung cancer, and it was performed on A549, Calu-1, and Calu-6 for 24 hours of treatment (Giovannetti et al., 2004). Unfortunately, there are apparent miscalculations in the extrapolation of the highest dose in the Giovannetti study from μg/mL to μM, where 100 μg/mL is 167 μM, not 212 μM as stated, which is still well below the MTD of pemetrexed of 229 μM (Britten et al., 1999; Mercalli et al., 2007). The design of the

novel pemetrexed colony formation assay detailed in this dissertation more closely imitates clinically achievable doses and treatment duration than previous pemetrexed studies.

The rationale for utilizing the Cpmax as the achievable concentration in tissue was confirmed by attempting to model the pemetrexed pharmacokinetics using a one-, two-, or three-compartment model using WinNonlin software. The best fit with a two-compartment model; however, the Cpmax generated by the software for a 10-minute infusion was well above the predicted theoretical maximum plasma concentration given the administered dose, suggesting a large error in the theoretical model. Furthermore, the two-compartment model did not provide a calculation of area under the curve (AUC) for the extravascular compartment, but it provides the plasma concentration when it is at equilibrium with tissue. However, one would argue that tissue concentrations would be predicted to show a higher AUC than plasma, as pemetrexed is activated by polyglutamation and retained in the cancer cell. If the drug is retained once activated, then this supports the argument that the cancer cells in culture only need to be exposed to pemetrexed for a short period of time (24 hours) to cause significant toxicity, lending reason as to why cancer patients are treated only once every three weeks and rapid clearance observed in the Rinaldi Phase I study. Hence, the Cpmax observed in patients is probably the relevant concentration to correlate with activity, as theoretical model calculations were unable to predict achievable concentrations in tissues.

Therefore, I decided to utilize this novel pemetrexed CFA across our panel of cell lines. All normal human bronchial epithelial cells I tested were resistant to pemetrexed treatment (IC50 > 240 μM) (Figures 3, 5, 6), suggesting low toxicity to normal lung, as expected based on the minimal side effects of pemetrexed in patients. Additionally, our CFA was consistent with clinical indications, where squamous cell carcinoma lines were resistant to pemetrexed (Figures 3, 5, 6). Unfortunately, the use of colony formation as our *in vitro* model does eliminate the testing of lines that do not form colonies (Figure 7).

I identified that there were three unique response phenotypes associated with pemetrexed treatment: sensitive, intermediate and resistant (Figure 4). Because the dose schedule is theoretically clinically achievable, the response phenotypes could be thought to correlate with clinical responses. Therefore, sensitive lines such as H2122 or DFCI032 exhibit essentially a complete response (CR), where at a certain dose below the MTD, the ability of the cell line to form colonies is sharply and completely inhibited (Figures 3 and 4). Intermediate lines such as A549 or EKVX exhibit a measureable IC50; however, there are existing colonies at all tested doses (Figures 3 and 4), and this phenotype is similar to a partial response (PR) seen in patients, where considerable but incomplete growth inhibition occurs. Resistant lines such as H226 or Calu-1 failed to exhibit significant growth inhibition, and this response phenotype is similar to stable disease (SD), where the tumor burden is unchanged after treatment. Where there is significant growth promotion with 240 μM pemetrexed treatment, such as H1819, there may be indications of early progressive disease (PD) *in vitro* (Figure 5).

In addition to identifying clinically indicated squamous cell carcinoma lines as resistant, I determined that there were responses among our panel that correlated with histology. We found that large cell carcinomas were typically very sensitive to treatment (IC50 < 2.4 μM) while squamous cell carcinomas were resistant (Figure 6). Both of the histological-dependent response phenotypes (squamous, large cell carcinomas) were statistically significant by two-tailed t-test (p-values 0.007, and 0.02). These results are consistent with observations made for pemetrexed/cisplatin versus gemcitabine/cisplatin combination, where large cell carcinomas have statistically significantly longer overall survival on pemetrexed-based therapy than on gemcitabine-based therapy (n=153 patients, OS 10.4 vs. 6.7 months, pem/cis vs. gem/cis) (Scagliotti et al., 2008). Conversely, in this same study, patients with squamous cell carcinoma histology had improved overall survival on gemcitabine-based therapy as compared to pemetrexed-based therapy (n=473, OS 9.4 vs. 10.8 months, pem/cis vs. gem/cis). Interestingly, I identified that the response of adenocarcinomas was histologically-independent, and there appears to be slightly more adenocarcinomas that are sensitive (n=20) versus resistant (n=17) (Figure 6). These results are also consistent with Scagliotti et al. findings where pemetrexed-based combination therapy is statistically superior for adenocarcinomas over gemcitabine-based combination therapy (n=847, OS 12.6 vs. 10.9 months, pem/cis vs. gem/cis) (Scagliotti et al., 2008).

I also evaluated three pairs of cell lines, which were each from the same patient respectively. First, I tested paired samples HCC4017/HBEC30KT (Figure 8A), which are a tumor/normal pair from a woman who had Stage IA large cell carcinoma lung cancer,

and was subsequently curatively resected. The dramatic difference in pemetrexed response nearly exceeded 10,000-fold suggesting that there is an achievable therapeutic window for pemetrexed with this dose schedule that is large and tumor-specific.

Conversely, the second set of paired samples I tested was H1693/H1819, which is a tumor/tumor pair from a woman who had Stage IIIB adenocarcinoma lung cancer (Figure 8B). This patient was biopsied at a regional lymph node (H1693 established), treated with cisplatin, etoposide and radiotherapy, and residual primary lung tumor was resected (H1819 established). There was nearly a 1,000-fold difference in response within the pair suggesting that there were specific differences or changes specific to either chemotherapy, radiotherapy or tumor location which caused such dramatic response diversity.

The third pair of patient samples I tested was H1993/H2073, which is a tumor/tumor pair from a woman who had Stage IIIA adenocarcinoma lung cancer. This patient was biopsied at a regional lymph node (H1993 established), treated with cisplatin, etoposide, and residual primary lung tumor was resected (H2073 established). I did not observe a dramatic difference that I saw in the first two pairs, but there was a definitive difference in response phenotypes, where H1993 was an intermediate responder and H2073 failed to exhibit any response (Figure 6).

I tested two more sets of paired samples HCC4018/HBEC34KT and H2250/H2258, but response was unable to be evaluated as HCC4018 and the

H2250/H2258 NSCLC lines do not form colonies under typical tissue culture conditions (Figure 7). Our lab is further exploring potential conditions to optimize clonogenicity of these non-colony forming lines, by the addition of osteopontin as well as other growth factors and serum concentrations.

PEMETREXED PERSONALIZED MEDICINE:

ONCOGENOTYPES AND CLINICAL

FEATURES OF RESPONSE

ABSTRACT

In this chapter, the clinical features of the NSCLC lines were characterized for their potential associations with the pemetrexed response phenotypes. This was of interest clinically to determine whether an oncogenotype could behave as a predictive biomarker for pemetrexed treatment. Interestingly, there was a significant imbalance in the distribution of *EGFR* mutant/overexpressed lines with a positive correlation to pemetrexed resistance, with the exception of PC-9, as identified by sequencing and microarray expression profiling. Independent reverse phase protein array analysis highlighted EGFR, and ERK1, protein expression significantly associated with pemetrexed resistance. Furthermore, I observed that all three ALK+ lung cancer cell lines in our panel were sensitive to pemetrexed, consistent with current retrospective clinical findings. There were no associations with pemetrexed response to the patient's gender, or *TP53*, *RB* or *STK11* status. Additionally, further clinical feature analysis exhibited significant correlations of mutant *KRAS* to pemetrexed sensitivity, and the occurrence of specific 12TGT transversion mutations in *KRAS* was significantly higher in pemetrexed sensitive lines.

MATERIALS AND METHODS

Genetic Mutational Analysis of Panel

Somatic mutations of genes were defined as data provided in the Catalogue of Somatic Mutations in Cancer (COSMIC) of the Wellcome Trust Sanger Institute (Forbes et al., 2008 and Forbes et al., 2011). Most genes were analyzed for small intragenic mutations, such as base substitutions and base insertions/deletions, whereas others (for example, *TP53*) were characterized for hot spot mutations at known high-frequency mutational sites. The dataset of COSMIC is composed of sequencing extracted from primary scientific literature previously published. Correlation analysis was performed on liquid colony formation response phenotype groups, sensitive and resistant only, where intermediate lines were excluded. Analysis was performed with binary code, where mutant lines were denoted as "1", and wild-type lines were "0." Similarly, pemetrexed response was denoted as a binary variable where pemetrexed sensitive lines were denoted as "0", and resistant lines as "1." Correlation coefficients were calculated for each gene with pemetrexed response, and two-tailed Student's t-test for p-values, where p-value < 0.05 was considered statistically significant.

Reverse Phase Protein Array (RPPA) Analysis

Endogenous protein expression was analyzed by RPPA independently at the John Heymach laboratory (MD Anderson, Houston, TX), as part of the Specialized Program of Research Excellence (SPORE) research collaboration with our laboratory. Methods and procedures for establishment of pellets lysates and execution of RPPA arrays have been

mentioned previously (Byers et al., 2009). Briefly, protein lysates from cell pellets were serially diluted with SDS, and equally added to 80% glycerol/2X PBS, and transferred to 384-well plates for analysis. RPPA arrays were printed on nitrocellulose coated glass FAST Slides in a 48 grid format, where each grid contained 24 protein dots, in duplicates with five concentrations. Automated Bio-Genex autostainer was used to block, and stain for primary and secondary antibodies, and signal was detected using the catalyzed signal amplification (CSA) system, Dako Cytomation (Carpinteria, CA). Between steps, each slide was washed with TBS containing 0.1% Tween-20 (TBST). The slides were incubated with streptavidin-biotin complex and biotinyl-tyramide (for amplification) for 15 min each, streptavidinperoxidase for 15 min, and 3,3-diaminobenzidine tetrahydrochloride chromogen for 5 min. Spot images were quantified using imaging analysis with a Hewlett Packard Scanjet 8200 scanner with a 256-shade gray scale at 600 dots per inch. RPPA data were quantified using a SuperCurve method which detects changes in protein level by Microvigene software, VigeneTech (Carlisle, MA).

RESULTS

EGFR Status May Predict for Resistance to Pemetrexed

Seven *EGFR* mutant or amplified adenocarcinomas in our lung cancer panel were found to form colonies and thus accessible for response by pemetrexed liquid colony formation assay (Figure 1A). Remarkably, all of these lines were resistant to pemetrexed, with the exception of PC-9. PC-9 displayed a complete response at 2.4 μM, whereas all of the other EGFR mutants/overexpressors failed to exhibit an IC50 (IC50 > 240 μM) (Figure 1A and 1B).

A)

Sensitive	Resistant
PC-9	H820
	H1650
	H1975
	H2073
	HCC827
	HCC4006

B)

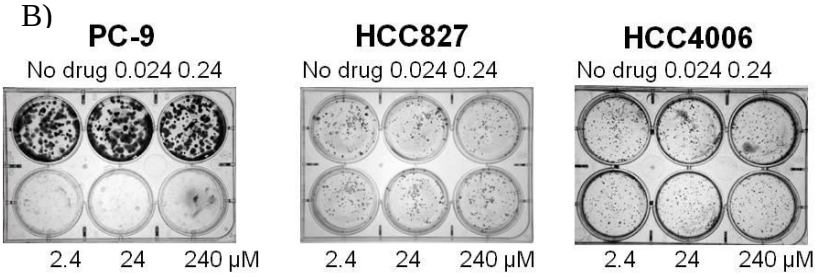

Figure 1. Mutant or Overexpressed EGFR Cell Lines That Form Colonies, Except PC-9, are Resistant to Pemetrexed. Cells were treated using colony formation protocol, as previously stated, with at least four replicas. Black bolded, Mutant EGFR; Black, Overexpressed EGFR.

RPPA Independently Associates with EGFR Protein Expression with Resistance

Interestingly, independent RPPA analysis of our lung cancer panel elucidated statistically significant correlations of endogenous protein expression of EGFR and ERK1 with pemetrexed resistance (Figure 2). EGFR protein was significantly higher in the pemetrexed resistant population, with a $\log_2$ ratio of -0.723 (p-value 0.007).

Additionally, I observed a similar result for ERK1 (MAPK3) protein, with a $\log_2$ ratio of -0.698 (p-value 0.009).

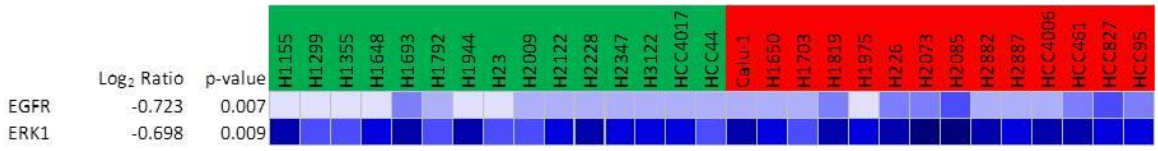

Figure 2. EGFR and ERK1 Expression Correlate with Resistance to Pemetrexed. Cell pellets were analyzed for protein expression by RPPA. Experiments were performed exclusively by the laboratory of John Heymach (MD Anderson, Houston, TX). Values are color-coated on a continuous gradient, where white is representative of no/low expression and dark blue is high expression. Log ratios were determined as average $\log_2$ values of the sensitive population minus those of the resistant, and p-values were determined by Student's t-test.

EML4/ALK Fusion Status May Predict Sensitivity to Pemetrexed

Oncoprotein-driven EML4/ALK positive lung cancer lines were assessed for their response to pemetrexed by liquid colony formation. All three tested lines exhibited sensitive phenotypes, with complete responses to treatment at 2.4 μM (Figure 3). H3122 appeared to be potentially more sensitive than the other two EML4/ALK fusion lines where some response was observed at 0.24 μM pemetrexed. I did not observe any EML4/ALK lines that failed to respond to pemetrexed treatment.

Figure 3. ALK+ Cell Lines are Sensitive to Pemetrexed. Cells were treated using

colony formation protocol, as previously stated. Cell lines were tested with at least four replicas.

Analysis by Oncogenotypes Elucidates General Predictive Factors for Response

Other clinical features of our lung cancer panel were annotated and analyzed for any significant correlations of the two pemetrexed response populations, as total samples (Figure 4). Significant differences in EGFR status (mutation, amplification) was our expected positive control, with positive correlation to the resistant population as previously elucidated (Figure 1). As expected, *EGFR* status was altered in 4.5% of all sensitive lines compared to 23.8% of all resistant lines, with a statistically significant p-value of 0.03.

Gender representation between the two response groups was evenly balanced, with both groups comprised of approximately 40% females and 60% males. The mutational status (including LOH, null, mutant) of *TP53*, *RB1*, and *STK11* were evenly balanced among the two phenotypes, with no statistical correlation to response (Figure 4). There was a positive trend of number of pack years the patient smoked with response to pemetrexed, however not significant (p-value 0.11). On the contrary, *CDKN2A* (*p16*) status nearly significantly correlated with resistance to pemetrexed (p-value 0.12). Overall, EML4/ALK translocations were nearly statistically significantly correlated with sensitivity to pemetrexed, with a p-value of 0.053 (Figure 4).

Unexpectedly, mutant *KRAS* had significant correlation with sensitivity to pemetrexed, where 50% of all sensitive lines were *KRAS* mutant, compared to only 20%

of resistant lines (p-value 0.030) (Figure 4). *KRAS* mutational status was available for all 22 sensitive lines, and 25 out of the 26 resistant lines.

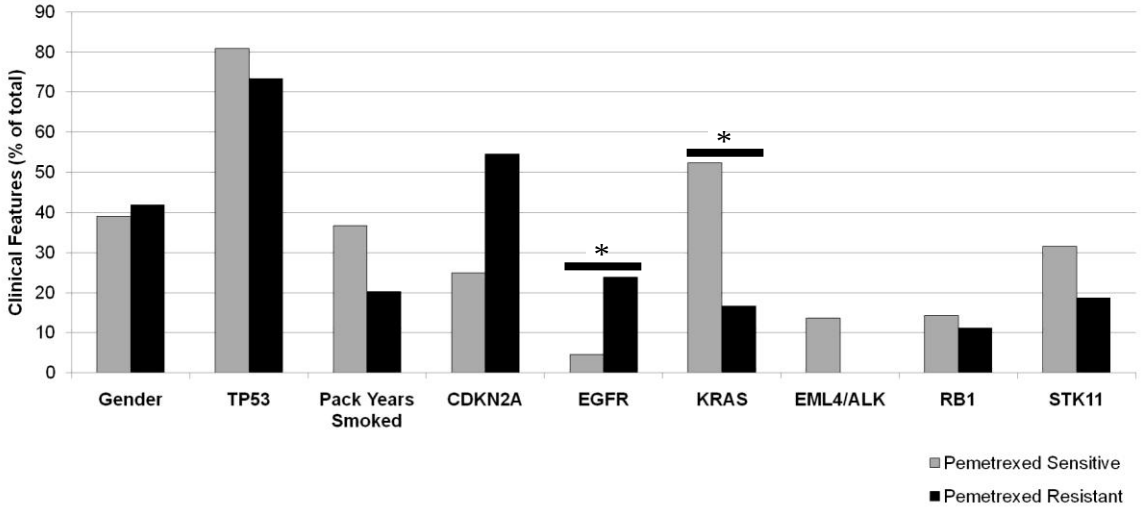

Figure 4. Clinical Features of Panel Exhibits Significant Correlation of Mutant *KRAS* and Sensitivity to Pemetrexed. The percentage of lines with the clinical feature within their respective response group (% of total) is graphically represented above. Gender is displayed as percentage of females within the group (male population is the remainder of the total percentage). Grey, sensitive; Black, resistant. ***** denotes statistically significant differences between response phenotypes (p-values < 0.05).

Specific 12TGT *KRAS* Genetic Alteration Significantly Correlates with Sensitivity

I wanted to further investigate *KRAS* status across our panel, specifically by observing whether the genetic alteration in each cell line was 12TGT, other potential *KRAS* mutations, or wild-type. Interestingly, there was a significant difference in the distribution of the 12TGT *KRAS* mutations with relation to pemetrexed response (Figure 5), where 31.8% of the sensitive lines harbored the specific 12TGT *KRAS* mutation, as compared to 8% of the resistant lines (p-value 0.039). This result was also consistent with the previous oncogenotype correlation for *KRAS* against pemetrexed response (Figure 4). In fact, 7 of the 11 (63%) *KRAS* mutant pemetrexed-sensitive lines harbored 12TGT

mutations, compared to 2 of the 5 (40%) *KRAS* mutant pemetrexed-resistant lines. However, correlation analysis of only the different individual *KRAS* mutant lines versus *KRAS* 12TGT mutants could not alone predict response to pemetrexed.

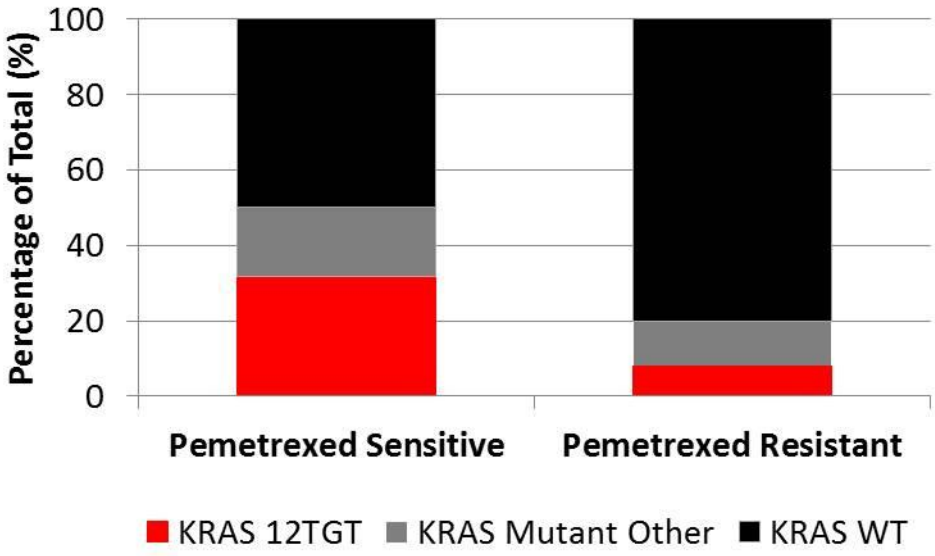

Figure 5. Specific 12TGT *KRAS* Mutation is Significantly More Frequently Observed in Lines with Sensitivity to Pemetrexed. The percentage of lines with the clinical feature within their respective response group (% of total) is graphically represented above. Red, *KRAS* mutants with 12TGT alteration, Grey, *KRAS* mutant with other known mutations, Black, *KRAS* wild-type.

DISCUSSION

Pemetrexed response has not yet been clearly linked to oncogenotypes *p53, KRAS* or *EGFR* in lung cancer. One research study by Lu et al. claimed mutant *p53* status may play a role in the resistance of pemetrexed, where that two WT *p53* cancer lines HCT-116 and A2780 (colon and ovarian, respectively) with their isogeneic mutant *p53* pairs were examined (Lu et al., 2001). They found that introduction of mutant *p53* lead to a relative increase in the IC50 of both paired samples; WT *p53* HCT-116 IC50 was 59 $\pm$ 28 nM to HCT-116/N7 IC50 > 10 μM, and WT *p53* A2780 IC50 was 136 $\pm$ 82 nM to A2780/CP70 IC50 850 $\pm$ 96 nM. Unfortunately, the doses employed in this study were all less than the clinically achievable MTD, and therefore, by that definition, true pemetrexed resistance was never achieved (Lu et al., 2001).

In this study, I examined the somatic oncogenotypes of the response phenotypes observed with our clinically relevant *in vitro* pemetrexed model (Figure 4). The clinical features of our lung cancer panel were further annotated and analyzed for any significant correlations with responses of resistance or sensitivity to pemetrexed. Unexpectedly, gender was evenly balanced, as was mutational status (including LOH, null, mutant) of *TP53*, inconsistent with previously published *in vitro* results (Lu et al., 2001).

I first noticed a general imbalance in the distribution of *EGFR* mutants (including both activating and resistance mutations) among the response phenotypes, where all, but one, of the known mutant lines are completely resistant to pemetrexed therapy (Figures 1

and 3). EGFR mutant tumor resistance to pemetrexed has not been conclusively studied nor clinically indicated for pemetrexed-enrollment exclusion criteria. However, Phase II study results from the combination of pemetrexed and EGFR-neutralizing monoclonal antibody matuzumab exhibits an improved overall response rate (ORR) in the combination treated patients versus pemetrexed alone (ORR 11% vs. 5%, pem/matuzumab versus pem, respectively) (Schiller et al., 2010), suggesting patients with EGFR mutant cancers are not responding to pemetrexed alone.

Furthermore, in a retrospective analysis of pemetrexed-treated patients (n=89) where ALK positivity, *EGFR* and *KRAS* status of each patient were known, mutant *EGFR* status had the shortest progression-free survival among the three molecular subtypes (mutant *EGFR* PFS 5.5, *KRAS* PFS 7, ALK+ PFS 9 months), with exclusion of the triple-negative remaining population (PFS 4 months). The hazard ratio of mutant *EGFR* versus the triple-negative group for pemetrexed treatment was 1.0 (p-value 0.99) (Camidge et al., 2011). This clinical result is consistent with recent clinical findings from Lee et al. where patients (n=95) were genotyped for *EGFR* mutation (45%), *ALK* translocation (16%), or WT (39%), in addition to response to second-line pemetrexed. They discovered that patients with *EGFR* mutant tumors had shorter time to progression (TTP 1.4 vs. 2.9 months, MT versus control, respectively), and worse overall response rates (ORR 4.7% vs. 16.2%, MT versus control, respectively) compared to patients with *EGFR* WT tumors (Lee et al., 2011).

Additionally, I found *EGFR* mRNA and protein expression to also be statistically significantly correlated with resistance to pemetrexed, by microarray, and RPPA analysis (collaboration with John Heymach, MD Anderson) across our lung cancer panel. The trend of pemetrexed response in *EGFR* mutants (both activating and resistant alterations) has never been implicated in a clinically relevant *in vitro* model prior to our study. Therefore, I hypothesize oncogenic addiction to mutant *EGFR* is playing a key role in resistance to pemetrexed, as seen in our *in vitro* colony formation model and as suggested from patient response data in the Schiller, Camidge, and Lee et al. clinical reports.

EML4-ALK translocations (t(2;5) (p23;q35)) are the most newly discovered and characterized oncoprotein in the field of thoracic clinical oncology (Gerber and Minna, 2010). ALK rearrangements took only three years from discovery to the bedside with the application of a previously FDA-approved targeted therapy, crizotinib (PF-02341066, Pfizer), a dual ALK and MET inhibitor (Gerber and Minna, 2010). *ALK* (2p23) is only expressed in certain neuronal cells, testes and the small intestine (Morris et al., 1994), and therefore patients with *ALK* rearrangements, or *ALK*+ lung tumors can be easily identified by fluorescence *in situ* hybridization (Camidge et al., 2011). Within our lung cancer panel, there are three known *ALK*+ cell lines to date: H2228 (variant 3a), H3122 and DFCI032 (both variant 1) (Koivunen et al., 2008). I decided to test the pemetrexed response phenotypes of these three lines, and found all three to be sensitive to pemetrexed treatment (IC50 < 2.4 μM) (Figure 3). I found this result to be intriguing as patients with *ALK*+ tumors were recently clinically identified to have survival benefits with pemetrexed treatment. Specifically, in the Camidge et al. clinical study previously

mentioned, *ALK*+ lung cancer patients treated with pemetrexed exhibited a statistically significant difference in median PFS of 9 months, compared to 4 months for patients with WT disease, and the HR for *ALK*+ compared to WT was 0.36 (p-value 0.005) (Camidge et al., 2011). This indication is consistent with Lee et al. findings, where patients with *ALK*+ tumors treated with pemetrexed had superior overall response rates (ORR 46.7 vs. 16.2, *ALK*+ versus WT, p-value 0.001), longer time-to-progression (TTP 9.2 vs. 2.9 months, *ALK*+ versus WT, p-value 0.001) and *ALK* positivity alone was a significant predictor for ORR (HR 0.07, p-value 0.001). *ALK*+ patients' sensitivity could be pemetrexed specific or could be an indicator of general chemotherapeutic sensitivity, and to answer this question, more *ALK*+/WT randomized clinical trials will need to be performed.

It has been well established that *KRAS* mutations are mutually exclusive to *EGFR* mutations and ALK positivity in lung cancer (Kim et al., 2011), and therefore, I wanted to know whether *KRAS* mutations would correlate with sensitivity to pemetrexed, since *EGFR* status (mutations, amplification), message and protein correlated with resistance within our cell line panel (Figures 1, 2 and 4). Oncogenotype analysis of our panel elucidated that 50% of the sensitive lines tested harbored *KRAS* mutations, whereas only 20% of the resistant lines were *KRAS* mutant, a statistically significant difference in *KRAS* mutant representation (Figure 4). I did indeed wonder why there were some *KRAS* mutants in the resistant population, if these genetic alterations were mutually exclusive with *EGFR*. The previously mentioned retrospective study helped us to bear insight on this observation with independently observed clinical significance (Camidge et al., 2011).

In that study's discussion, the authors stated that although *KRAS* mutation is not quite statistically significant in terms of hazard ratio (HR 0.55, p-value 0.095), they felt it was worthy to mention that there were two distinct groups of responses within the *KRAS* mutant patient cohort, split 50:50, where there were clearly evident rapid progressors versus longer PFS outcomes with pemetrexed treatment. The authors further stated that the basis of which is currently unknown.

Furthermore, another interesting correlation with pemetrexed response was the number of pack years smoked by the patient, such that higher frequency of smoking was nearly associated with sensitivity to pemetrexed (Figure 4). The average number of mutations found in the tumors of smokers was 3-fold higher, than those in never smokers (p-value 0.021), among the 623 candidate genes and 188 tumors sequenced (Ding et al., 2008). More importantly, *KRAS* mutations were found to significantly correlate with smoking status (p-value 0.021) (Ding et al., 2008), thus suggestive to us that these two clinical features (smoking, *KRAS* status) were not exclusive of one another in their prediction of pemetrexed response.

G-to-T transversion mutations in codon 12 of *KRAS* specifically, are strongly associated with smoking status, whereas G-to-A transition mutations are found in never, former and current smokers (Riely et al., 2008). Systematic review by meta-analysis of *KRAS* mutations found such mutations to be associated with poor prognostic significance for survival in lung cancer patients globally, and with adenocarcinoma, not squamous cell carcinoma (Mascaux et al., 2005). Thus, by correlations in oncogenotype to response, I

hypothesized that pemetrexed sensitivity is associated with *KRAS* G-to-T transversion mutations in codon 12, current or former smoking patients, with aggressive, invasive tumors predicted to have poor survival, and that pemetrexed is the targeted therapy appropriate for this subgroup of NSCLC patients. I determined that indeed *KRAS* 12TGT mutations occurred more frequently in lines sensitive to pemetrexed (31.8% of sensitive lines versus 8% of resistant lines), and there was a significant correlation of 12TGT *KRAS* mutations to pemetrexed sensitivity (Figure 5). However, in a comparison of only *KRAS* mutants, 12TGT mutations in *KRAS* were not sufficient to predict response. I believe this insignificant correlation is due to the small number of *KRAS* mutant lines that are resistant to pemetrexed, and that is why there is significant correlation when wild-type *KRAS* lines are also considered in our analysis. I found this result, in addition to relationships of ALK+, *EGFR* and *KRAS* statuses with pemetrexed response, to be very exciting and have clinical potential for application in a biomarker-specific enrollment of patients for pemetrexed treatment.

PEMETREXED PERSONALIZED MEDICINE:

IN VIVO TOXICITY STUDY, TUMORIGENICITY OF LINES,

AND DOSE ESCALATION XENOGRAFTS

ABSTRACT

In this chapter, to test whether the *in vitro* pemetrexed response phenotypes could be recapitulated *in vivo*, "Phase I toxicity trials" of pemetrexed or cisplatin were completed to identify maximum tolerated achievable doses *in vivo*. I determined that all nine doses of pemetrexed tested (26.6 mg/kg to 1000 mg/kg) *qwx3* are safe and well tolerated in *NOD/SCID* mice. On the other hand, toxicities were observed in 6 and 8 mg/kg doses of cisplatin, and the maximum tolerated dose of cisplatin tested was 4 mg/kg *qwx3*. Next, to determine an effective dose, "Phase II small scale dose escalation efficacy trials" were performed on pemetrexed sensitive H2009 xenografts, and observed tumor response after treatment with seven different dose schedules of pemetrexed: saline control or 150, 200, 250, 500, 750, 1000 mg/kg. I elucidated that doses of pemetrexed 500 mg/kg or higher were sufficient to mimic *in vitro* response. Finally, to determine whether *in vitro* pemetrexed resistant were also resistant at effective *in vivo* doses, "Phase III large scale efficacy trials" were performed on pemetrexed resistant H2882 and H226 xenografts, and tumor burden after treatment with established doses of saline control or 500, 750 and 1000 mg/kg pemetrexed was observed. All treatment doses were insufficient to reduce tumor burden in these pemetrexed resistant models. Furthermore, tumor burden post-sacrifice was significantly reduced in H2009, and not in H226 tumors, after treatment with our established pemetrexed dose schedule. From these studies, I can define that the response phenotypes observed *in vitro* by liquid colony formation were also able to be recapitulated *in vivo*.

MATERIALS AND METHODS

Mice

Female *NOD/SCID* mice were obtained from Wakeland laboratories, UT Southwestern Mouse Breeding Core (Dallas, TX) at approximately 6-8 weeks of age.

Reagents

Drugs used were obtained from the UT Southwestern Campus Pharmacy (Dallas, TX), and handled with aseptic technique. Pemetrexed from Eli Lilly, or LC Laboratories, was reconstituted in 0.85% sterile sodium chloride, as per manufacturer's instructions, to make 50 mg/mL solution. Cisplatin/CDDP, Teva Parenteral Medicines, Inc. (Irvine, CA) is available in 1 mg/mL solution, and kept with minimum exposure to light. Control groups for pemetrexed or cisplatin were injected with equivalent volumes of 0.85% sterile sodium chloride vehicle *i.p.*

In vivo Toxicity Assays

Mice received treatments weekly for three weeks and were monitored up to two weeks post-treatment for extensive adverse events or mortalities. Body weight was quantified using a scale, each week after receiving treatment, averaged, and recorded as compared to the average starting control weight. Toxicity was assessed as loss of 10% or more body weight (as denoted by a black line), or mortality.

Xenograft Studies

$1x10^6$ cells per cell line were injected subcutaneously into the shaved right flank of *NOD/SCID* mice, and monitored by calipers ($v = \pi/6*l*w^2$; v, volume; l, length, w, width, where width is the smallest dimension) weekly. When tumor burden averaged between 250-500 mm^3, the mice were randomized to four non-statistically different groups: control, 150, 200, and 250 mg/kg or control, 500, 750, and 1000 mg/kg. All mouse procedures are in compliance with UT Southwestern IACUC policies (APN 0575-06-1 and APN 2009-0178). Mice were sacrificed when tumor burden was near or exceeded 2,000 mm^3 in volume.

Measurement of Tumor Burden at Sacrifice

After the completion of the third and final week of pemetrexed treatment, the tumor burden was measured subcutaneously with calipers, and then sacrificed by CO_2 exposure as per the UT Southwestern IACUC guidelines. The mice were lacerated and the entire tumor burden was excised. The tumor burden was measured via laboratory scale, prior to any cryopreservation and formalin-fixation. The average tumor burden, sample size, and standard deviations were used to determine the statistical significance by Student's t-test.

RESULTS

"Phase I Toxicity Trial" of Pemetrexed and Cisplatin Single Agents

To determine if the responses observed in tissue culture were conserved, I decided to first establish an *in vivo* toxicity model for pemetrexed in *NOD/SCID* mice (Figure 1). I tested nine treatments (26.6, 40, 53.3, 150, 200, 250, 500, 750, 1000 mg/kg) of pemetrexed with a *qwx3* dose schedule, and three treatments (4, 6, 8 mg/kg) of cisplatin were used as a positive control. Toxicity was determined by greater than 10% weight loss from starting weights or mortality. Toxicity was observed at 6 and 8 mg/kg of cisplatin, and the MTD of cisplatin tested was 4 mg/kg *qwx3* (Figure 2). Alternatively, based on this study, pemetrexed was well tolerated at all doses tested with no observable toxicities, and no MTD was identified (Figure 1).

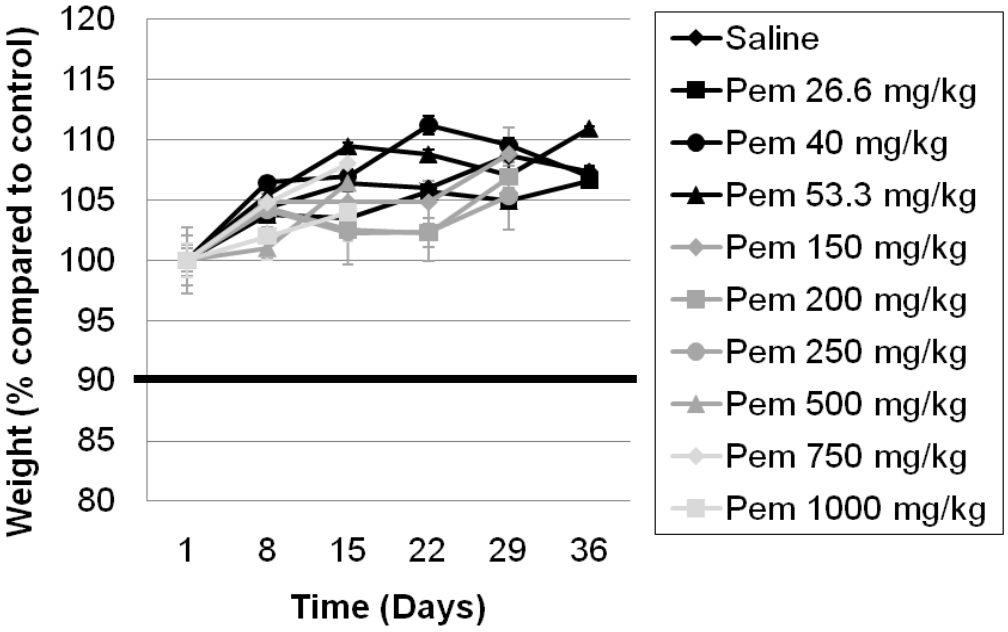

Figure 1. *In vivo* Toxicity Profile of Pemetrexed. Nine treatments of pemetrexed (26.6, 40, 53.3, 150, 200, 250, 500, 750, 1000 mg/kg) or saline control, were administered *i.p.* to *NOD/SCID* female mice (n=5/group) under a *qwx3* dose schedule.

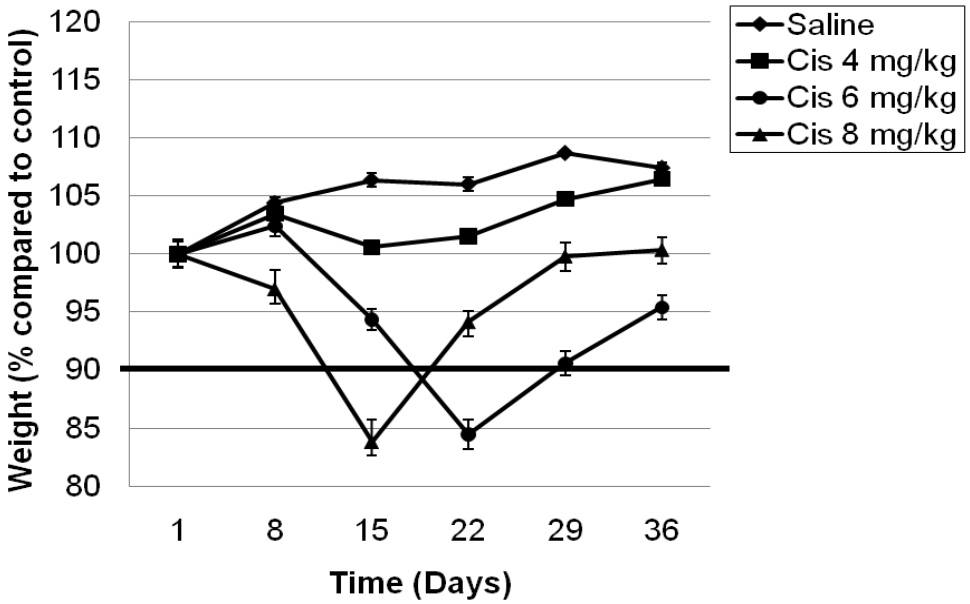

Figure 2. *In Vivo* Toxicity Profile of Cisplatin. Three treatments of cisplatin (4, 6, and 8 mg/kg) or saline control, were administered *i.p.* to NOD/SCID female mice (n=5/group) under a *qwx3* dose schedule.

"Phase II Small Scale Dose Escalation Trial" with Pemetrexed-Sensitive H2009

Based on our toxicity data, I decided to test three low doses and three high doses for our preclinical xenograft trials to determine an efficacious dose schedule of pemetrexed *in vivo* (Figure 3). I chose a pemetrexed-sensitive line H2009 based on consistent CF assay data and their ability to form xenografts in immunocompromised mice. Two independent experiments were performed for "low doses" and "high doses" of pemetrexed, where mice were randomized into two phases of increasing doses of pemetrexed (150, 200, 250 mg/kg and saline control; 500, 750, 1000 mg/kg and saline control) mimicking a small scale Phase II dose escalation efficacy trial (Figure 3).

After completion of the third dose of the "lower" pemetrexed treatments, H2009 control average was 977.91 mm^3, whereas 150, 200 and 250 mg/kg group averages were

772.41, 542.89, and 577.90 mm^3, respectively (Figure 3A). Treatment/control ratios for the treatment arms were 0.78, 0.55, 0.59 for pemetrexed 150, 200 and 250 mg/kg, comparatively. There were no large statistically significant differences between all three treatments and control.

Whereas, after completion of the final dose of the "higher" pemetrexed treatments, H2009 control average was 1246.07 mm^3, whereas 500, 750 and 1000 mg/kg group averages were 509.30, 539.55, and 453.23 mm^3, respectively (Figure 3B). Treatment/control ratios for the treatment arms were 0.40, 0.43, 0.36 for pemetrexed 500, 750 and 1000 mg/kg, comparatively. There were large statistically significant differences between all three treatments and control (p-value equaled to 0.003, 0.001, and 0.001, respectively).

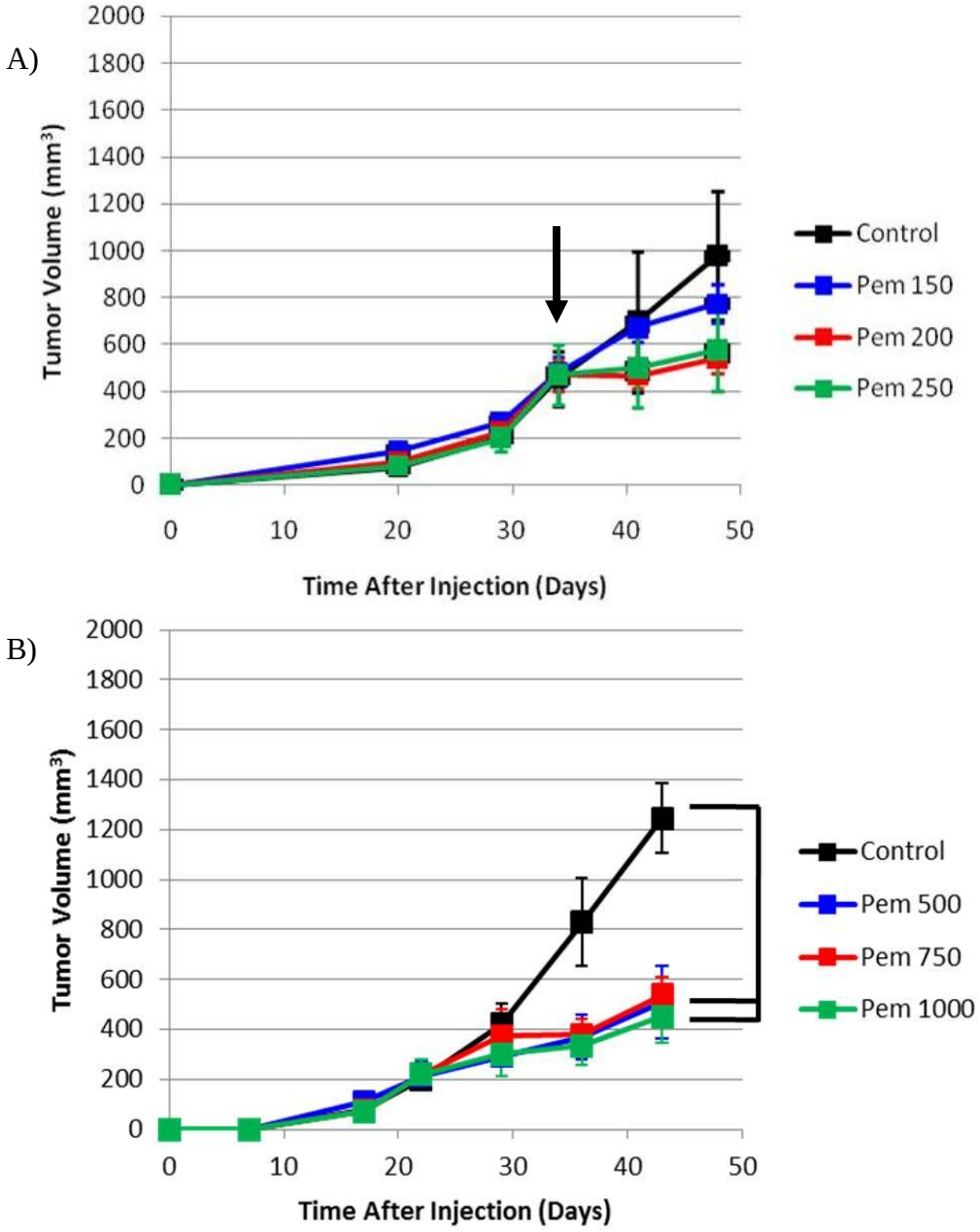

Figure 3. *In Vivo* Dose Schedules Greater Than 250 mg/kg *qwx3* Mimic *In Vitro* Sensitive Response Phenotype for H2009 Xenografts. Independent experiments were performed on H2009 xenografts, where mice (n=5/group) received either "low" doses or "high doses" of pemetrexed treatment. Black arrow denotes beginning of *qwx3* pemetrexed treatment. * denotes p-value < 0.003. ** denotes p-value < 0.001.

"Phase III Large Scale Efficacy Trial" for Pemetrexed-Resistant H2882 and H226

Based on our toxicity data, I decided to use three of the highest doses tested for our preclinical xenograft trials designed to mimic a dose escalation study. Two

pemetrexed-resistant lines (H226 and H2882) were chosen based on consistent CF assay data and their ability to form xenografts in immunocompromised mice (Figure 4). Twenty *NOD/SCID* female mice were subcutaneously injected per line, and tumor burden was measured once weekly. When tumor burden averaged between 250-500 mm^3, the mice were randomized to four non-statistically different groups: control, 500, 750, and 1000 mg/kg.

After the completion of the third treatment cycle, H2882 control average was 1267.04 mm^3, whereas 500, 750 and 1000 mg/kg group averages were 980.81, 1681.14, and 1956.50 mm^3, respectively (Figure 4A). Treatment/control ratios for the treatment arms were 0.77, 1.32, 1.54 for pemetrexed 500, 750 and 1000 mg/kg, comparatively. There was no statistical significance between any of the treatments and control (p-value equaled to 0.49, 0.65, and 0.46, respectively).

Finally, after the completion of the third treatment cycle, H226 control average was 647.68 mm^3, whereas 500, 750 and 1000 mg/kg group averages were 669.96, 762.18, and 903.88 mm^3, respectively (Figure 4B). Treatment/control ratios for the treatment arms were 1.03, 1.17, 1.39 for pemetrexed 500, 750 and 1000 mg/kg, comparatively. There was no statistical significance between any of the treatments and control (p-value equaled to 0.88, 0.677, and 0.27, respectively).

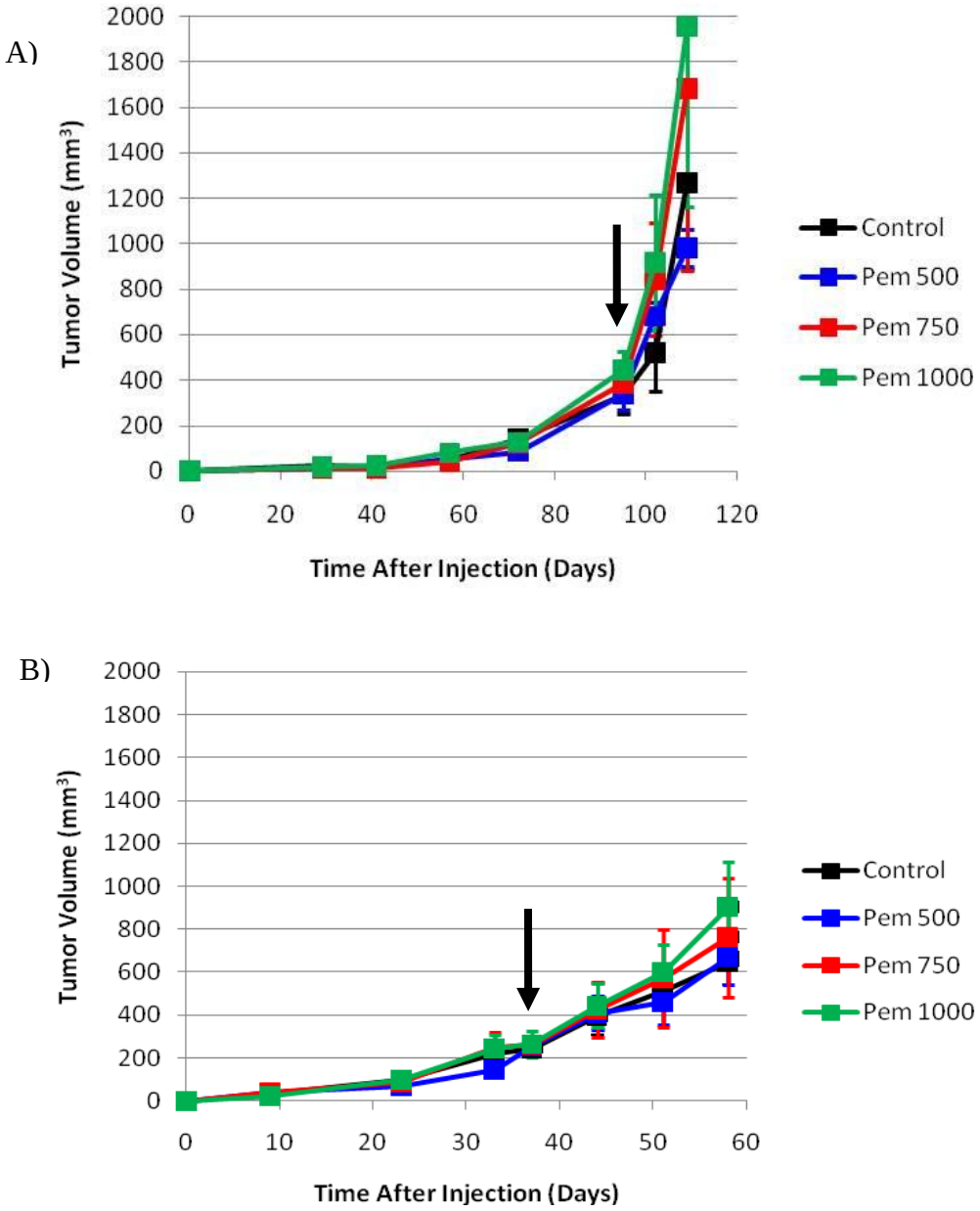

Figure 4. *In Vivo* Dose Schedule Mimics *In Vitro* Resistant Response Phenotypes. Mice were randomized into four treatment groups of pemetrexed (500, 750, 1000 mg/kg) or saline control. Tx were administered *i.p.* to *NOD/SCID* female mice (n=5/group) under a *qwx3* dose schedule. A) H2882 Xenografts. B) H226 Xenografts. Black arrow denotes beginning of *qwx3* pemetrexed treatment.

Xenograft Tumor Burden Post-Sacrifice is Also Consistent with *In Vitro* Phenotypes

After the completion of the third and final week of pemetrexed treatment, the mice were sacrificed and tumors were extracted for weight measurement. H2009 treated and control tumors were statistically significant in tumor size post-extraction (Figure 5A). Tumor burden weight averages (in grams) were 1.11 (control), 0.59 (500), 0.36 (750), 0.32 (1000 mg/kg), with p-values of 0.052, 0.001, and 0.001, respectively, compared to control. Tumor/control ratios for tumors extracted from H2009 pemetrexed treated mice with 500, 750 and 1000 mg/kg were 0.53, 0.32, and 0.28, respectively.

Furthermore, H226 treated and control tumors were not statistically significant in tumor size post-extraction (Figure 5B). Tumor burden weight averages (in grams) were 0.35 (control), 0.27 (500), 0.34 (750), 0.37 (1000 mg/kg), and there was no statistical significance between any of the treatments and control (p-value equaled to 0.22, 0.88, and 0.80, respectively). Tumor/control ratios for tumors extracted from H226 pemetrexed treated mice with 500, 750 and 1000 mg/kg were 0.77, 0.97, and 1.05, respectively.

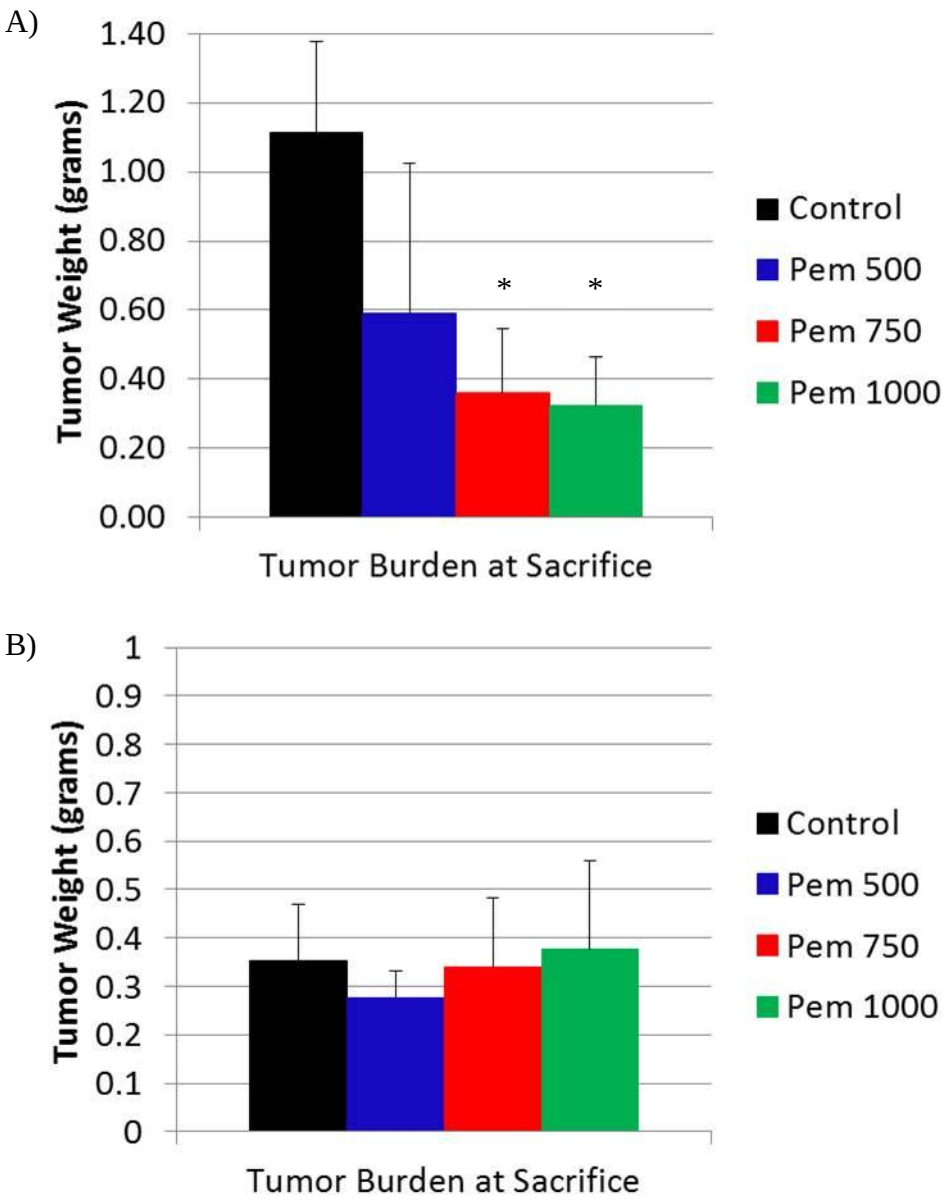

Figure 5. Xenograft Tumor Burden Post-Sacrifice is Consistent with Response Phenotypes *In Vitro*. Mice were randomized into four treatment groups of pemetrexed (500, 750, 1000 mg/kg) or saline control. Tx were administered *i.p.* to *NOD/SCID* female mice (n=5/group) under a *qwx3* dose schedule, and tumors were extracted post-sacrifice for measurement of final tumor burden weight. A) H2009 Xenografts. B) H226 Xenografts. * denotes p-value < 0.001.

DISCUSSION

The purpose of this study was to determine whether *in vitro* pemetrexed response phenotypes were consistent when tested *in vivo* in the mouse. Although the design of the *in vitro* screen was based on clinical pharmacokinetics, and many of the response phenotype features (*EGFR* and *KRAS* mutations, *ALK* positivity, squamous cell carcinomas) mimic clinical indications, I wanted to bridge the gap between tissue culture and patients, by also testing and confirming our results through *in vivo* mouse hospital trials of pemetrexed treatment.

The first obstacle I encountered was choosing the appropriate dose schedule of pemetrexed to use in mice. There have been a several pilot studies of *in vivo* treatment of xenografts with pemetrexed, although no naïve toxicity studies at several doses have been performed. Several studies adopted a 100 mg/kg *i.p.* dose with varying schedules of treatment, either daily for three days (Tonkinson et al., 1999), five days at 50 mg/kg (Bareford et al., 2011), ten days (Mercalli et al., 2007; Schultz et al., 1999) or weekly (Takezawa et al., 2011; Wang et al., 2006). A few studies adopted dose schedules of several days of treatment on and then subsequently off, for one or two weeks, such as *qd4* with 3 days off, and *qd4* tx once again (Teicher et al., 2000) or *qd5* x 2 cycles at 150 mg/kg (Izbicka et al., 2009). Interestingly, there was only one previous study, where a higher dose of pemetrexed was tested *in vivo*, with a dose schedule of 1000 mg/kg *qwx3 i.p* in CD1 nude mice (Thomas et al., 2009). This study was intriguing to us for many reasons. First, there was no naïve mouse toxicity data published with this study, but the

mice did complete the xenograft treatments with no apparent mortalities noted, suggesting the dose schedule was most likely well tolerated. Second, this dose was significantly higher than any other doses previously attempted, and third, the 1000 mg/kg dose had no apparent effect on tumor volume of these CORL23 lung cancer xenografts suggesting potential pemetrexed resistance. The final piece of interest to us was the decision of the researchers to extend the treatment schedule to weekly injections. I also felt that weekly injections of mice were more clinically applicable to cytotoxic chemotherapeutics, where a patient receives treatments every three weeks, than a daily injection schedule for mice, which I believe more so mimics orally available, targeted therapeutics that are taken daily by patients.

Therefore, preclinical mouse hospital Phase I trials were performed to determine the MTD of pemetrexed in *NOD/SCID* mice, with doses of pemetrexed ranging from 26.6 mg/kg up to 1000 mg/kg *qwx3 i.p.* (Figure 1). The lower doses of pemetrexed (26.6, 40, 53.3 mg/kg) were tested as single agents, to be given later in combination studies with cisplatin at a clinically relevant ratio of 20:3 (pem/cis). Higher doses of pemetrexed (150, 200, 250, 500, 750, 1000 mg/kg and saline control) were tested for pemetrexed single agent application. I was delighted to discover that all doses of pemetrexed were tolerable (Figure 1). I did encounter toxicity (mortality and weight loss) with cisplatin single agent treatment at 6 and 8 mg/kg *qwx3 i.p.* treated simultaneously with the pemetrexed dose trials (Figure 2). This is the first study to exhibit that doses up to 1000 mg/kg *qwx3 i.p.* for pemetrexed in *NOD/SCID* mice are safe and well tolerated.

After the establishment of a safe pemetrexed dose schedule, I wanted to know how much pemetrexed treatment (if possible) was required to segregate response phenotypes *in vivo*. To answer this question, I injected H2009 adenocarcinoma (pem sensitive) cells into mice, and randomized the mice into two phases of increasing doses of pemetrexed (150, 200, 250 mg/kg and saline control; 500, 750, 1000 mg/kg and saline control), thus mimicking a Phase II small scale efficacy trial (Figure 3). Interestingly, H2009 xenograft sizes at the three lower doses of pemetrexed failed to be statistically significantly different from the control group (Figure 3A). However, H2009 xenografts treated with 500, 750, and 1000 mg/kg were statistically significantly different in size than control (Figure 3B). These results suggested to us that doses of 250 mg/kg or less cannot recapitulate the *in vitro* response phenotypes exhibited in the colony formation assay.

I further tested two pemetrexed-resistant lines, H2882 (NSCLC-NOS) and H226 (SQ), and found that neither displayed sensitivity to pemetrexed *in vivo* (Figures 4 and 5). These results support the use of the CFA as an accurate measure of pemetrexed drug response.

This is the first research study to determine a "bench to cage to bedside" approach for pemetrexed response phenotypes at clinically achievable dose schedules *in vitro* with secondary validation by *in vivo* xenografts. With these results, I believe further indications and observations identified in our *in vitro* liquid colony formation model now could be potentially applied to clinical settings.

PEMETREXED PERSONALIZED MEDICINE: FTCD AND PEMETREXED-RELATED GENE EXPRESSION ACROSS CELL LINE PANEL

ABSTRACT

In this chapter, I explore canonical and alternative mechanisms of response by looking at the expression of pemetrexed-related genes, in addition to top hits from unsupervised expression profiling of pemetrexed sensitive and resistant lines. mRNA expression levels of *TYMS* and other pemetrexed-related genes in lung cancer xenografts failed to identify if there are any significant relationships with respective gene expression and pemetrexed response by colony formation assay. Unsupervised microarray expression profiling identified high FTCD levels had significant correlation to pemetrexed sensitivity, and high EGFR expression correlated with pemetrexed resistance. Furthermore, I performed RNA-Seq whole transcriptome analysis on a set of paired samples with differential response to pemetrexed and revealed that there were dramatic differences in FTCD gene expression, but no significant differences in other pemetrexed-related genes. Western blot analysis confirmed that FTCD was overexpressed in pemetrexed-sensitive lines, compared to pemetrexed-resistant lines. Interestingly, I determined that FTCD was overexpressed in a pemetrexed-sensitive EGFR mutant PC-9, and not in pemetrexed-resistant EGFR mutants H1975 and HCC4006, consistent with my recent findings. Moreover, spontaneous overexpression of FTCD was observed in pemetrexed-sensitive 3KTRL53 clone 5, and not in pemetrexed-resistant 3KTRL53 parental population and clone 7. I wanted to determine whether FTCD overexpression was playing a functional role in pemetrexed response. However, FTCD shRNA-mediated knockdown in FTCD-positive HCC4017, but not in FTCD-null HCC3051, resulted in acute cell death, suggesting a potential oncogenic role of FTCD in lung cancer survival.

MATERIALS AND METHODS

RNA/cDNA Preparation and Quantitative Real Time Polymerase Chain Reaction

Total RNA was extracted from cultured cell pellets or tumor tissues by trizol/chloroform addition, resuspended in RNase-free water, and quantified at OD260. 2 μg RNA was reverse transcribed with iScript cDNA Synthesis Kit (Bio-Rad Laboratories, Hercules, CA), according to the manufacturer's protocol. iTaq Supermix Kit with ROX, Bio-Rad Laboratories was used to perform qRT-PCR with 1 μg cDNA per reaction, and was performed in quadruplicate. The Taqman Gene Expression Probes, Applied Biosystems, Life Technologies (Carlsbad, CA) used were: FPGS (Hs00191956_m1), GART (Hs00531926_m1), 18S (4319413E), RFC1 (Hs00161340_m1), and TYMS (Hs00426591_m1). The ΔΔCt was calculated relative to H2073 tumor.

Gene Expression Profiling by Microarray

I performed whole genome expression profiling on our panel of lung cancer cell lines. RNA was extracted (as stated previously) from cell pellets, reverse transcribed and labeled with TargetAmp Nano-g Biotin-aRNA Labeling Kit #TAN07924-142 Illumina (San Diego, CA), and directly hybridized onto Human-6 v2 or HumanWG6-v3.0 Beadchips Illumina (48,000 probes per sample). Expression levels were normalized between samples, by internal controls, converted to $\log_2$ values, and Student's T-test was performed for each gene between the average of sensitive and resistant groups (with p-

value < 0.05, and difference > 2 $\log_2$ as criteria) using Matrix software (Girard et al., in preparation).

Western Blot Analysis

Protein lysates were made from NSCLC cell lines grown on sterile 10 cm^2 dishes and harvested at sub-confluency. Lysis buffer contained 0.1% sodium dodecyl sulfate (SDS) and complete protease/phosphatase inhibitors. The lysates were incubated on ice for 30 minutes, centrifuged for 15 minutes at 4°C, and the supernatant was snap-frozen. Protein concentrations were quantified by addition of Bradford reagent, Sigma-Aldrich (St. Louis, MO) and absorbance was measured at 595 nm, with bovine serum albumin dilutions (0.625-10 mg/mL) for standard curve generation. 5X SDS, supplemented with β-mercaptoethanol and bromophenol blue dye, was added to supernatants and boiled at 95°C for 5 minutes. Stable lysates were stored at -20°C for long term storage. 40 µg of protein lysates were loaded onto 10 or 12% Tris-HCl precast polyacrylamide gels, Bio-Rad Laboratories, and run at 50-200 volts. Protein was transferred to nitrocellulose membranes at 50 volts for 2 hours at 4°C. Blots were blocked for 1 hour at RT in 5% milk supplemented with 1% BSA in 1X TBST. Primary antibodies were incubated in the same blocking buffer overnight at 4°C with shaking. Primary antibodies used were FTCD (1:100) sc-47885 and HSP90 (1:1000) sc-13119, Santa Cruz Biotechnology (Santa Cruz, CA). Secondary antibodies were added to 1X TBST for 1 hour at RT with shaking. Secondary antibodies used were: HRP IgG goat anti-rabbit #32460 (1:2000) and HRP IgG goat anti-mouse #32430 (1:2000), Thermo Scientific (Portsmouth, NH).

RNA-Seq Whole Transcriptome Analysis

The mRNA-Seq library was prepared and performed by the Genomics and Microarray Core Facility (UT Southwestern). Briefly, mRNA (1-5 μg) was isolated, cDNA was synthesized, adaptors were added, and underwent size selection. The cDNA was amplified and quality controlled. Both samples were sequenced for 35 bp reads with 1 lane of paired ends and 3 lanes of single end reads on an Illumina GAIIx platform (San Diego, CA). Sample sequences were mapped with Bowtie software (version 0.12.7, Baltimore, MD), to human genome reference sequence (version hg18) with the –best option. Bowtie mapping generated a BAM file, which was exported and analyzed with PARTEK Genomics Suite (St. Louis, MO). Expression was calculated by RPKM (reads per kilobase per million reads) for each transcript analyzed (Mortazavi et al. 2008). Chi squared analysis was used to determine the statistical significance of differential expressed transcripts for p-values < 0.05. Relative paired-expression was determined by HCC4017 over HBEC30KT.

Knockdown by shRNA Transfection

To establish stable knockdown of FTCD expression, I utilized shRNA constructs that included three different shRNA plasmids targeting FTCD #sc-60662-SH Santa Cruz (0.1 μg/uL). Control cells were transfected with mock scrambled shRNA plasmid A #sc-108060, Santa Cruz (0.1 μg/uL) concurrently. Three dilutions of Fugene 6 transfection reagent #05061377001 Roche Applied Science (Indianapolis, IN) to plasmid DNA (μg) were tested (3:2, 3:1, 6:1) for each cell line, and puromycin selection was optimized prior

to transfection. Puromycin was added 72 hours post transfection and maintained for at least 10 days.

RESULTS

Expression of *TYMS* and Pemetrexed Related Genes by qRT-PCR

Relative gene expression levels were observed across a panel of extracted NSCLC xenograft tumors for *TYMS* and pemetrexed related genes by qRT-PCR (Figure 1). A resistant line, H2073, was used as the reference sample. As would be predicted for resistance, I would expect lower levels of *TYMS*, and higher levels of *FPGS* and *RFC1* in the sensitive samples. Alternatively, levels of *TYMS* were either similar or higher in the sensitive samples as compared to control, and the inverse relationships (lower levels) were seen for *FPGS* and *RFC1*.

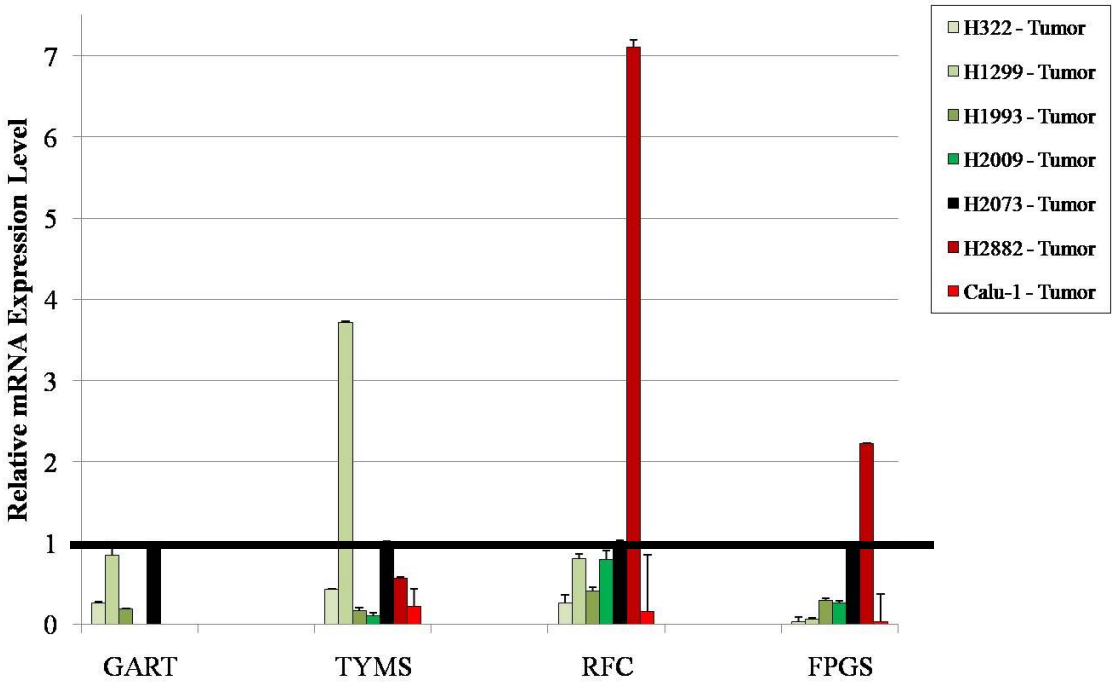

Figure 1. *TYMS* and Other Pemetrexed Related Gene Expression Levels, of Lung Cancer Lines Grown as Xenografts, Do Not Associate with Response to Pemetrexed by CFA. qPCR analysis of RNA from untreated xenografts of lung cancer cell lines. A resistant line H2073 was set as the reference sample, and 18S was used as the housekeeping gene. Green, sensitive; Red, resistant; Black, reference sample. RNA and cDNA synthesis, and qPCR were kindly performed by Jihan Osborne (UT Southwestern).

Gene Expression Profiling by Microarray

I performed mRNA expression profiling on cell lines from our panel of pemetrexed CF results (sensitive H1155, H1299, H1355, H1648, H23, H2009, H2030, H2122, H2228, H3122, HCC2429, HCC4017, HCC4019, PC-9; resistant Calu-1, H1395, H1650, H1703, H1819, H226, H290, H2073, H2882, H2887, H324, H596, H647, H650, H969, HCC95, HCC461, HCC827, HCC2450, HCC4006). Sensitive and resistant group averages were compared for statistically significant differences, and hits that were greater than two $\log_2$ fold different were mentioned (Figure 2). In reference to the sensitive group, there were 5 upregulated genes (*CRIP1, NUDT11, ULBP1, SYK* and *FTCD)* and 20 downregulated genes *(IFI44L, LBH, IGFBP5, IFI6, COL5A1, EFEMP1, COL4A1, GPNMB, BST2, RFTN1, LOX, KAL1, DNER, FRAS1, IGFBP7, PRKCDBP, MSLN, OLR1, FSTL1,* and *SPARC*) that fit these criteria.

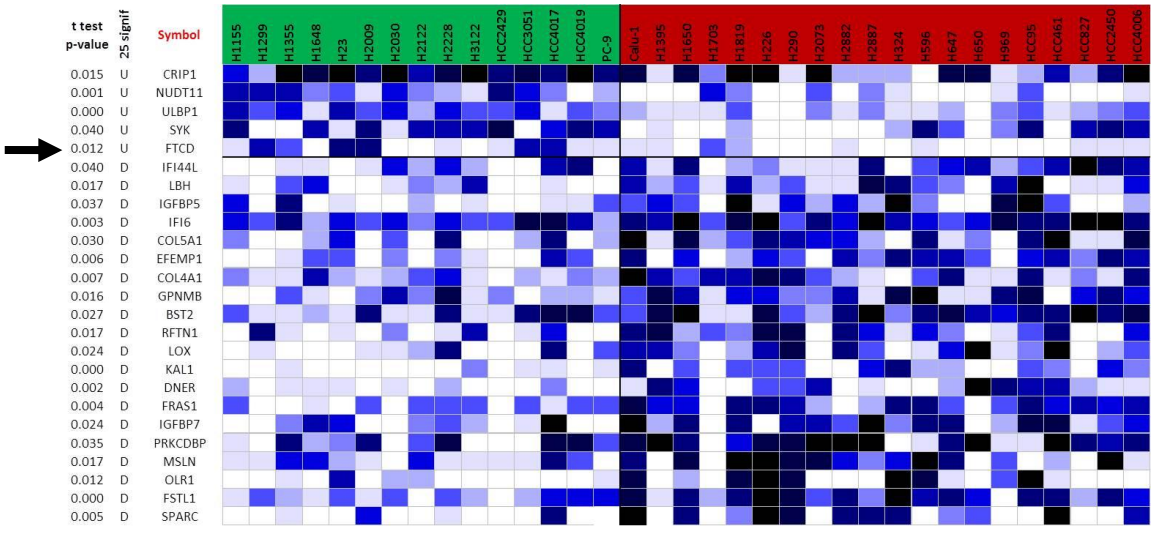

Figure 2. mRNA Microarray Signature Highlights Statistically Significant Genes with Differential Expression Between Sensitive and Resistant Response Phenotypes. Gene expression levels were quantile-quantile normalized across all samples and log ratios were calculated. Green, low expression; Red, high expression.

FTCD Expression by Western Blot Analysis

FTCD protein expression (58 KDa) was analyzed across our panel of cell lines. FTCD expressers were H2122 (AC), H1155 (LC), HCC4017 (LC), HBEC3KT RL53 clone 5 (tumorigenic p53 knockdown, *KRAS* mutant HBEC, forms LC tumors), whereas counterparts HBEC30KT (normal HBEC pair to HCC4017) and HBEC3KT (normal HBEC) and HBEC3KT RL53 parental population (non-tumorigenic) do not express FTCD. Very low FTCD expressers were H1299 (LC) and H2009 (AC). Interestingly, several cell lines, such as H226 (SQ), H1975 (AC, EGFR mutant), and paired samples H1693 and H1819 (ACs), expressed lower molecular weight bands that were detected by FTCD blotting.

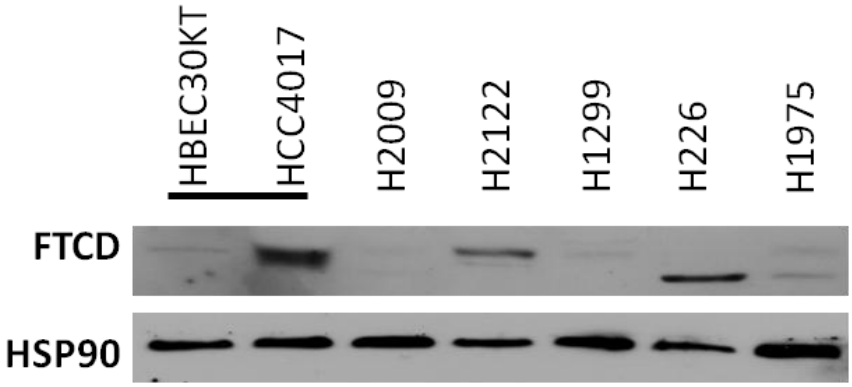

Figure 3. *In Vitro* FTCD Protein Expression Across Panel Reveals Overexpression in Sensitive, But Not Resistant, Lines. Western blot was performed on cellular protein lysates, and blotted overnight for FTCD (58 KDa) and HSP90 (90 KDa). HSP90 was used as an endogenous, loading control. Black bar denotes paired samples.

FTCD Protein Expression Significantly Associates with Sensitivity to Pemetrexed

I performed western blot analysis on a large panel of lung cancer and normal HBEC cell lines (n=24) to characterize their endogenous FTCD protein expression. I

determined that none of the squamous cell carcinomas (n=3) had overexpression of FTCD at 58 KDa, likewise for normal HBECs (n=2). Interestingly, EGFR mutants (n=3) failed to express FTCD, with the exception of the one pemetrexed-sensitive EGFR mutant, PC-9 where FTCD was endogenously overexpressed.

Cell Line	**Histology**	**FTCD Expression (at 58 KDa)**	**Response to Pem**	**IC100**
H1648	Adenocarcinoma	Null	Sensitive	2.4
H1693	Adenocarcinoma	Null	Sensitive	2.4
H1819	Adenocarcinoma	Null	Resistant	> 240
H1944	Adenocarcinoma	++++	Sensitive	2.4
H1975	Adenocarcinoma	Null	Resistant	> 240
H2009	Adenocarcinoma	+	Sensitive	2.4
H2030	Adenocarcinoma	Null	Sensitive	2.4
H2087	Adenocarcinoma	Null	Sensitive	2.4
H2122	Adenocarcinoma	++	Sensitive	2.4
HCC4006	Adenocarcinoma	Null	Resistant	> 240
PC-9	Adenocarcinoma	++++	Sensitive	2.4
H1155	Large Cell	++++	Sensitive	2.4
H1299	Large Cell	+	Sensitive	24
HCC3051	Large Cell	Null	Sensitive	2.4
HCC4017	Large Cell	++++	Sensitive	0.024
HBEC30KT	Normal Immortalized	Null	Resistant	> 240
HBEC3KT	Normal Immortalized	Null	Resistant	> 240
HBEC3KTRL53 Clone 5	Normal Immortalized	++++	Sensitive	2.4
HBEC3KTRL53 Clone 7	Normal Immortalized	+	Resistant	> 240
HBEC3KTRL53 Parental	Normal Immortalized	Null	Resistant	> 240
H2887	NSCLC-NOS	Null	Resistant	> 240
Calu-1	Squamous	Null	Resistant	> 240
H226	Squamous	Null	Resistant	> 240
H1703	Squamous	Null	Resistant	> 240

Table 1. FTCD Protein Expression Across Panel Reveals Overexpression in Sensitive, But Not Resistant, Lines. Table of FTCD protein expression from western blot analysis performed on cellular protein lysates, and blotted overnight for FTCD (58 KDa). Bolded font denotes paired samples, + denotes very low expression, ++ denotes expression, and ++++ denotes overexpression. IC100 is denoted in μM, as defined by the dose that completely inhibits colony forming ability in the liquid colony formation assay.

Next, I performed a correlation analysis on this panel with defined FTCD protein expression, for any relationship between FTCD protein expression and pemetrexed response. FTCD protein expression at 58 KDa correlated significantly with sensitivity to pemetrexed (p-value 0.007), with a correlation coefficient of 0.53.

RNA-Seq Transcriptome Analysis of Paired Samples HCC4017/HBEC30KT

I performed whole transcriptome sequencing of mRNA on paired samples HCC4017 and HBEC30KT to determine specific differences in mRNA expression patterns within the pair (Figure 4). Expression levels of *TP53, TYMS, DHFR, GARFT,* and *FPGS* were not significantly different within the pair. Another folate-dependent gene *ATIC* failed to exhibit any difference between the tumor/normal paired samples (1.21-fold change).

KRAS expression was mutant and 1.95-fold (SD $\pm$ 0.08) higher in HCC4017 than in HBEC30KT. The most dramatic difference observed was in *FTCD* expression, where there was greater than 47.5-fold (SD $\pm$ 17.9) increase of message in HCC4017 compared to HBEC30KT. Furthermore, the coding sequence of *FTCD* was unchanged, wild-type within the pair (data not shown).

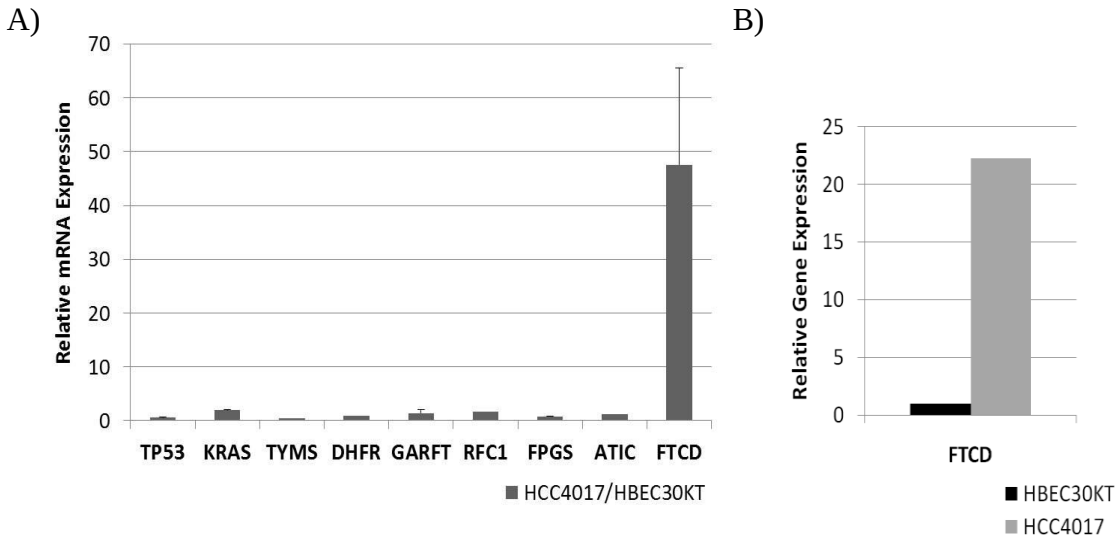

Figure 4. Expression Analysis of HCC4017/HBEC30KT Reveals Dramatic Differences in *FTCD* Expression, But Not in Pemetrexed-Related Genes. A) RNA-Seq whole transcriptome analysis. B) Microarray expression profiling of cellular mRNA. Relative mRNA expression levels are quantified above as HCC4017 relative to HBEC30KT. Values are plotted ± SD.

Response to Pemetrexed After Oncogenic Manipulation of HBECs

To determine whether the addition of oncogenic manipulations affect normal cells response to pemetrexed, I simultaneously tested normal human bronchial epithelial cell line 3KT with its paired cell line 3KTRL53 parental (constitutive siRNA knockdown of *TP53* and expression of mutant *KRAS*), and the respective soft agar colony forming clones, 3KTRL53 clones 1, 5, 7 and 8 (Figure 5A). Interestingly, HBEC3KT, 3KTRL53 parental, non-tumorigenic 3KTRL53 clones 7 and 8 were completely resistant to pemetrexed (IC50 undetermined), whereas tumorigenic 3KTRL53 clones 1 and 5 exhibited response to pemetrexed at 2.4 μM. I decided to look at the FTCD expression levels among these paired lines. I found that FTCD was null in HBEC3KT, 3KTRL53 parental, and 3KTRL53 clone 7, and dramatically overexpressed in 3KTRL53 clone 5 (Figure 5B).

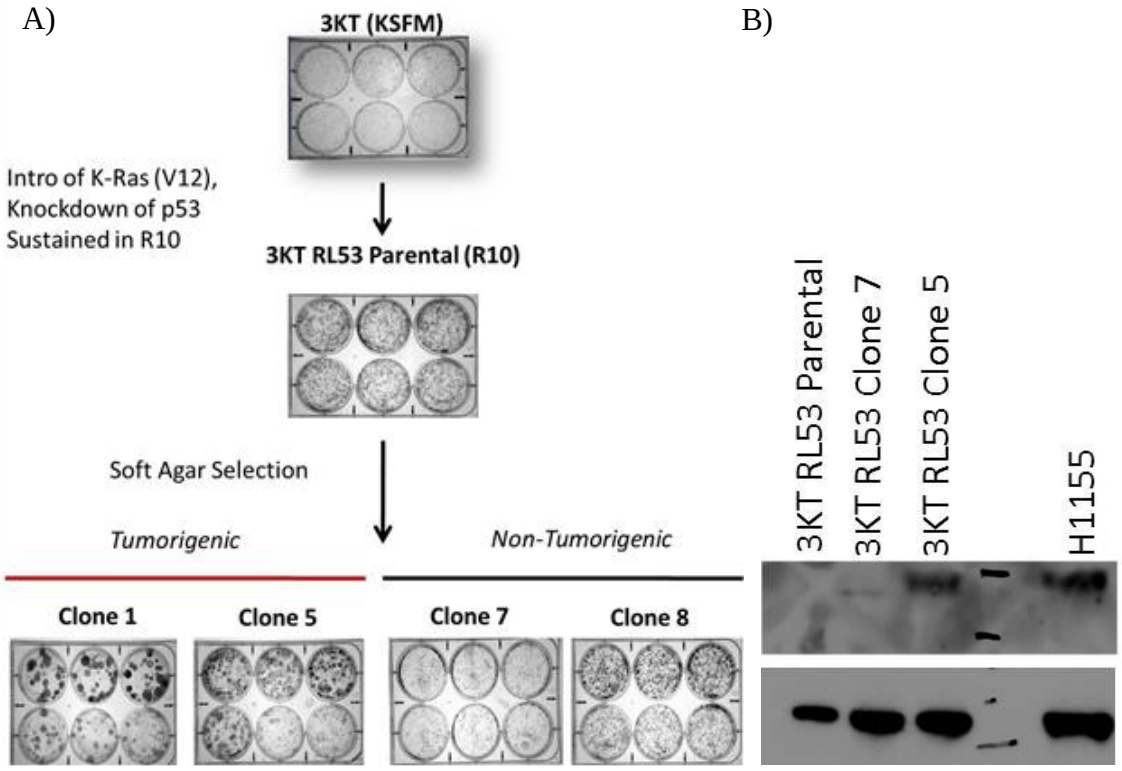

Figure 5. FTCD is Spontaneously Overexpressed in Pemetrexed-Sensitive, Tumorigenic HBEC3KTRL53 Clone 5, and Not in HBEC3KT, HBEC3KTRL53 Parental or Clone 7. A) Cells were treated using colony formation protocol, as previously stated. Cell lines were tested with at least four replicas. B) Western blot was performed on cellular protein lysates, and blotted overnight for FTCD (58 KDa) and HSP90 (90 KDa). HSP90 was used as an endogenous, loading control.

Stable Knockdown of *FTCD* Expression in HCC4017 and HCC3051

To determine the functional role of FTCD in lung cancer, I performed shRNA-mediated knockdown in a line with endogenous overexpression, HCC4017, by transfection of FTCD-specific short hairpin RNA (Figure 6). Post-selection with puromycin, I determined that there was significant cell death in the FTCD-shRNA wells compared to control non-targeting shRNA wells.

I performed *FTCD* knockdown in an FTCD-null line HCC3051 to control for off-target effects. HCC3051 cell proliferation was completely unaffected by *FTCD* knockdown, and HCC3051 KD cells had no change in sensitivity to pemetrexed upon testing with colony formation as compared to control (data not shown).

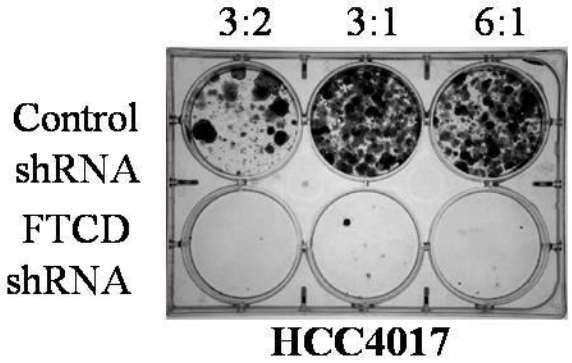

Figure 6. FTCD shRNA-mediated Knockdown in HCC4017 Results in Cell Death. Cells were plated and forward-transfected with either control non-targeting or *FTCD*-specific shRNA, placed under puromycin-selection for 10 days, and stained with crystal violet for visualization. Lipid/DNA ratio conditions tested were 3:2, 3:1 and 6:1 for each shRNA.

DISCUSSION

The purpose of this research proposal was to determine whether the expression levels of pemetrexed-related genes are driving response phenotypes, and to identify any genes with significant correlation to pemetrexed response for potential clinical application. As previously mentioned (Chapter One Introduction), the most common mechanism of resistance to pemetrexed to date is higher levels of *TYMS* (Ceppi et al., 2006). Therefore, I wanted to conclude if *TYMS* and other pemetrexed-related genes were driving resistance or sensitivity in our panel of lines, and to test this, I extracted RNA from untreated xenografted tumors with varying responses to pemetrexed, and performed qRT-PCR analysis. The experimental design of this study was important for two reasons, clinical application and *in vivo* expression. I chose to look at RNA expression, instead of protein, because RNA levels have been employed as the gold standard for *TYMS* and other pemetrexed related genes' expression in patient samples for mechanisms of resistance (Ceppi et al., 2006; Shintani et al., 2004). Furthermore, I chose to look at intratumoral RNA expression of xenografted lung cancer lines to most mimic influences from environmental factors seen clinically, such as tumor vasculature and hypoxia. I concluded that none of the genes examined had significant correlation to pemetrexed response; in fact, *TYMS* levels in pemetrexed sensitive tumors were higher or the same as pemetrexed resistant tumors (Figure 1). I was surprised to know *RFC1* and *FPGS* mRNA levels were higher in the resistant tumors, especially H2882 compared to H2009, considering the drastic differences in their *in vivo* pemetrexed responses shown previously, suggesting response is not due to how much pemetrexed enters the cell and is

subsequently activated. In addition to qRT-PCR analysis, I performed RNA-Seq on paired samples HCC4017/HBEC30KT to examine RNA expression of *TYMS* and pemetrexed-related genes by a secondary assay, and determined there were no significant differences in *TYMS, DHFR, GARFT, FPGS* or *RFC1*. Interestingly, Camidge et al. elucidates that levels of THF-dependent enzyme ATIC may trigger sensitivity to pemetrexed, through an ALK phosphorylation-dependent either indirectly or directly by *DHFR* production of THF to increase of ATIC enzymatic activity (Camidge et al., 2011). I found *ATIC* expression to have insignificant differences between the tumor/normal paired samples, suggesting *ATIC* is not playing an important role in pemetrexed response.

Since *TYMS* and pemetrexed-related genes did not significantly correlate with response among our lung cancer panel, I decided to find out genes that correlate by performing an unsupervised microarray analysis of pemetrexed sensitive and resistant lines (Figure 2). There were many genes with significant (p-value <0.05) correlation to pemetrexed response, including *EGFR*, and members of the collagen gene family (*COL4A1, COL5A1, LOX)* and extracellular matrix (*SPARC*), but the hit *FTCD* with one of the highest fold-change between the two groups was of the most interest to us.

FTCD is a bifunctional enzyme involved in folate metabolism (Bashour and Bloom, 1998). I found it to be fortuitous that a clinically relevant *in vitro* screen of an anti-folate chemotherapeutic would produce as a significant hit a gene directly involved in folate metabolism. More importantly, *FTCD* has never been implicated in any form of cancer or any anti-folate chemotherapeutic research, and in fact, to date *FTCD* has been

published on just over 50 times. Interestingly, I determined there were no significant correlations with *TYMS, DHFR, GARFT, FPGS* or *RFC1* mRNA expression, across our lung cancer panel by microarray, and response to pemetrexed. FTCD activity in this panel has not been characterized; however, *in vitro* experiments on whole cell extracts could be performed by looking either at levels of ammonia bi-product by using pH levels or production of intermediate or terminal products of FTCD enzymatic activity by spectrophotometry.

I further examined whether our microarray expression analysis results were valid, by performing western blot analysis specifically for FTCD protein (at 58 KDa) expression across our lung cancer panel. I found that there were several lines with very high protein expression as compared to normal controls. For example, I knew from our screen that HCC4017 and HBEC30KT are pemetrexed sensitive and resistant, respectively, with nearly a 10,000-fold difference in IC50 values. By western blot analysis, HCC4017 was determined to have very high levels of FTCD, whereas HBEC30KT had very low basal levels (Figure 3), consistent with microarray results suggestive of a 23-fold expression difference (Figure 4B). Furthermore, I validated both of these results with a tertiary assay RNA-Seq, which revealed a 47.5-fold (SD $\pm$ 17.9) overexpression of FTCD in HCC4017, compared to HBEC30KT (Figure 4A).

Interestingly, I discovered other characteristics of FTCD expression across our panel that I felt were worth noting. FTCD expression appeared to also be null/very low in HBEC3KT (Table 1), suggestive that FTCD levels are probably consistently, seemingly

null in normal bronchial epithelial cells, where very low, basal expression would be necessary for functional metabolism of folic acid and B12. Null/very low expression of FTCD in normal HBECs is consistent with the results of Bashour and Bloom, where FTCD expression was exclusively found in rat liver and not in other tissues, unless under high exposure conditions.

FTCD overexpression was not limited to one histological type of lung cancer, but rather apparent in adenocarcinomas (H1944, H2122, PC-9) and large cell carcinomas (H1155, HCC4017) (Table 1). I was unable to identify any overexpression of FTCD mRNA or protein in any of the tested squamous cell carcinoma lines (H226, H1703 and Calu-1) (Table 1), although a lower molecular weight band was detected in H226 (Figure 3) that may be an indication of single nucleotide polymorphisms or splice isoforms of *FTCD* that are smaller in total size.

By utilizing our in-house oncogenically manipulated HBEC3KT model, I was able to confidently compare the response phenotypes of isogeneic HBEC clones in relation to specific oncogenic alterations (loss of *TP53*, gain of mutant $KRAS^{V12}$). Interestingly, the introduction of these alterations had no effect on the pemetrexed response of HBEC3KT, where both HBEC3KT and 3KTRL53 parental were resistant (IC50 > 240 μM, data not shown). Moreover, 3KTRL53 parental clones extracted from colonies in soft agar were expanded and established as cell lines for study (Sato et al., 2006). 3KTRL53 tumorigenic clone 5 and non-tumorigenic clone 7 were tested for their response to pemetrexed. I found that 3KTRL53 tumorigenic clone 5 was sensitive to

pemetrexed IC50 < 2.4 μM, where as non-tumorigenic clone 7 was resistant to pemetrexed, like the previously tested HBEC3KT isogeneic manipulations (Figure 5A).

Therefore, when I compared 3KTRL53 parental, clone 7 and clone 5 for their FTCD protein expression by western blot, I was pleasantly surprised to find FTCD was overexpressed in the tumorigenic, pemetrexed-sensitive clone 5, and not in clone 7 or the parental population (Figure 5B). FTCD overexpression in tumorigenic 3KTRL53 clone 5 was spontaneous, and specific, as a result of anchorage-independent soft agar selection in the context of *TP53* knockdown and mutant $KRAS^{V12}$. This result was suggestive to us that FTCD overexpression may be also associated with tumorigenic ability and transformation of normal bronchial epithelial cells. Interestingly, 3KTRL53 clone 5 tumors result in large cell carcinoma malignancies (Sato et al., in preparation), consistent with pemetrexed-sensitive response phenotypes observed in this study for LC histology.

To determine whether FTCD overexpression was playing a key role in pemetrexed response, I performed shRNA-mediated knockdown of FTCD in an FTCD-overexpressed line HCC4017. Stable knockdown of FTCD resulted in acute cell death in all conditions tested; however, this result was not observed in the control plasmid conditions (Figure 6). I was unable to perform our secondary assay, liquid colony formation, to functionally test the mechanistic role of FTCD in this line. Additionally, FTCD-null line HCC3051 was unaffected by stable shRNA-mediated knockdown, and I was able to perform pemetrexed liquid CF assay after knockdown. There was no difference in pemetrexed response, between FTCD knockdown versus control plates, at

all three conditions. Western blot analysis revealed that FTCD was null in all manipulated HCC3051 lysates, including the HCC3051 parental line, suggestive that cell death by FTCD shRNA mediated knockdown of HCC4017 was specific to loss of FTCD expression. I was not expecting HCC4017 cells to die simply after FTCD knockdown, and I believe that FTCD may not only be related in pemetrexed response, but in lung cancer cell survival, as an essential oncogene. I am additionally continuing these knockdown experiments in more lines, to fully understand the scope of FTCD in pemetrexed response and its potential role as an oncogene. I am excited about the potential of FTCD as a therapeutic drug target, in addition to being a pemetrexed-specific predictive biomarker in lung cancer.

I further hypothesize that FTCD may be a direct target of pemetrexed, in addition to the canonical targets of pemetrexed, TYMS, DHFR and GARFT. Our evidence to support this hypothesis is two-fold. In the findings of Bashour and Bloom, the researchers mention that FTCD bound microtubules formed from brain tubulin, and not liver tubulin (Bashour and Bloom, 1995). They were confounded by the physiological relevance of this finding, as a liver-specific enzyme would never interact with microtubules formed from tubulin from the brain. What I found was extraordinarily interesting was that brain tubulin is polyglutamated, whereas liver tubulin is not. The second piece of information to consider is that upon shuttling into the cancer cell, pemetrexed is known to be activated by FPGS, a polyglutamate synthase. I hypothesize that pentaglutamated forms of pemetrexed directly potently inhibit FTCD, in FTCD-overexpressed lung cancer lines, resulting in the apparent cell death and pemetrexed response. This theory has never been

implicated or tested in anti-folate therapeutics, and I hope to determine the answers to these questions in the very near future.

PEMETREXED PERSONALIZED MEDICINE:

RETROSPECTIVE CLINICAL ANALYSIS OF PEMETREXED TREATED PATIENTS, PROPOSED PLANS AND TRANSLATIONAL POTENTIAL

ABSTRACT

In this chapter, I explored the clinical application of our research findings, through retrospective analysis under the IRB protocol #STU 022011-201, in collaboration with Simmons Cancer Center thoracic oncologists, Drs. David Gerber and Joan Schiller, M.D. The purpose of retrospective analysis is to determine whether FTCD is indeed overexpressed in lung cancer patient tissue, and if FTCD expression significantly correlates with patient response to pemetrexed treatment. I describe how initial collection of patient health information was acquired, and how clinical annotations were defined for the final set of 40 patients previously treated with pemetrexed-based chemotherapy. Distribution of stage in this dataset was predominately comprised of Stage IV patients, and there are no Stage I patients in our study. Histology heterogeneity was also observed in our patient dataset, where seven patients' tumors were of squamous cell carcinoma histology. I requested pathology slides from available tissue blocks, and described which methods and markers would be used for retrospective analysis and study of these samples. I determined progression-free and overall survival variables (including censorship) for our retrospective patient population. Finally, I describe the translational potential of this dissertation project with hopes of a prospective clinical trial with FTCD-based biomarker enrollment for pemetrexed treatment.

MATERIALS AND METHODS

Initial Collection of Patients Health Information from UT Southwestern Clinics

Data was collected from the lung cancer repository database provided by UT Southwestern. Access to other patient medical records requires submission and approval of a Human Subjects-Specific clinical protocol to the UT Southwestern Institutional Review Board (IRB). Personnel are required to complete health information certifications such as HIPAA (for Research Subjects) and Good Clinical Practices. Computers where patient health information is accessed must be secured and password protected, and all identifying factors must be removed prior to any public disclosure of results. I used the Social Security Death Index to determine the vital status of each patient, and the date of death if available.

Tissue Availability through Pathology Databases

Patient samples were annotated for available pathology by utilization of two databases through the ERGO electronic records system: vCDR and EPIC. Under EPIC Playground, patient charts can be chronologically reviewed and pathology (path) samples can be visualized under the tab for labs. Tissue samples were annotated by pathology accession number, and collated for all pemetrexed treated patients with available path. I requested tissue from UT Southwestern and Parkland pathology laboratories by the pathology accession numbers provided, and I unable to obtain any tissues that was analyzed by an external company, Veripath, which coincided with path samples starting with the abbreviation, V. Samples provided by Parkland and Neuropath laboratories were

accessible free, whereas UT Southwestern samples required an interdepartmental requisition number for a nominal fee. I requested 10 unstained slides from each sample, and 1 H&E stained slide to confirm histology denoted in the patient's medical records chart.

Clinical Annotations through EPIC of Patients Treated with Pemetrexed

I asked questions regarding each patient, by accessing patient records through EPIC, with the patient's medical record number. I specifically asked the following questions: 1) When did pemetrexed treatment start? 2) When did pemetrexed treatment stop? 3) How many cycles did the patient receive of pemetrexed? 4) What line of treatment was the pemetrexed given? 5) Was pemetrexed given in combination with other drugs? 6) Was pemetrexed given in combination with radiotherapy? 7) What was the best response of the patient after pemetrexed treatment? 8) What degree of response was seen? 9) Was there progression? 10) What was the date of progression? 11) What was the site of progression?

Determination of Progression-Free Survival and Overall Survival

The progression-free survival and overall survival of these patients was divided into two sub-variables: with and without censorship, i.e. removal of patients at the last known follow-up date, due to lack of information. The units of these two calculations are in "days." Progression-free survival was calculated by the subtraction of the date of pemetrexed treatment was begun from the date of progression. Censored progression-free survival was calculated by the subtraction of the date of pemetrexed treatment was begun

from the censored date of progression (date of last follow-up). Overall survival was calculated by the subtraction of the date of diagnosis from the date of death, and censored overall survival was calculated by the subtraction of the date of diagnosis from the censored date of last follow-up.

RESULTS

I wanted to identify patients who had been treated with pemetrexed at UT Southwestern Cancer Clinics. There were 83 patients that fit these criteria with electronic medical records, of which 16 patients are still alive. As a result of verifying both EPIC and vCDR database systems, I was able to identify 40 patients with tissue available at UT Southwestern, Parkland and Neuropath laboratories that were accessible for our study.

Patient Distribution by TNM Staging Classification

There was a diverse distribution of cancer stages among the patient samples, where the most represented group is Stage IV with 20 patients of the 40 (50%) total patients (Figure 1). The least populated group is the early stage patients Stage IIA and IIB with 7.5% of the total number of patients, and there were no patients with Stage I lung cancer in this retrospective clinical dataset.

Stage	Number of Patients
IIA	1
IIB	2
IIIA	6
IIIB	10
IV	20
Unknown	1
Total	**40**

Figure 1. Patient Distribution By Stage Is Diverse In Retrospective Dataset. The table above is a breakdown of the patient dataset by stage as listed in the patient's records. The number of patients in each row corresponds to the actual stage representation.

Histological Representation of Patient Dataset

Within our pemetrexed-treated retrospective patient dataset, seven patients were positive identified to have tumors with squamous cell carcinoma histology, out of the cumulative set of 40 patients.

Progression-Free Survival and Censored Progression-Free Survival Determination

Once I had our list of lung cancer patients with obtainable tissue to study, I wanted to determine variables of progression-free survival for our clinical retrospective analysis. Progression-free survival of our pemetrexed-treated patients ranged from 30 to 715 days with an average PFS of 192 days (Figure 2). Censored progression-free survival ranged from 4 to 1040 days, with an average censored PFS of 390 days.

Overall Survival and Censored Overall Survival Determination

Furthermore, I also defined variables of overall survival for our clinical retrospective analysis. Overall survival of our patient population range was from 4 to 1258 days, with an average OS of 440 days (Figure 2). Censored overall survival ranged from 204 to 1626 days, with an average censored OS of 880 days.

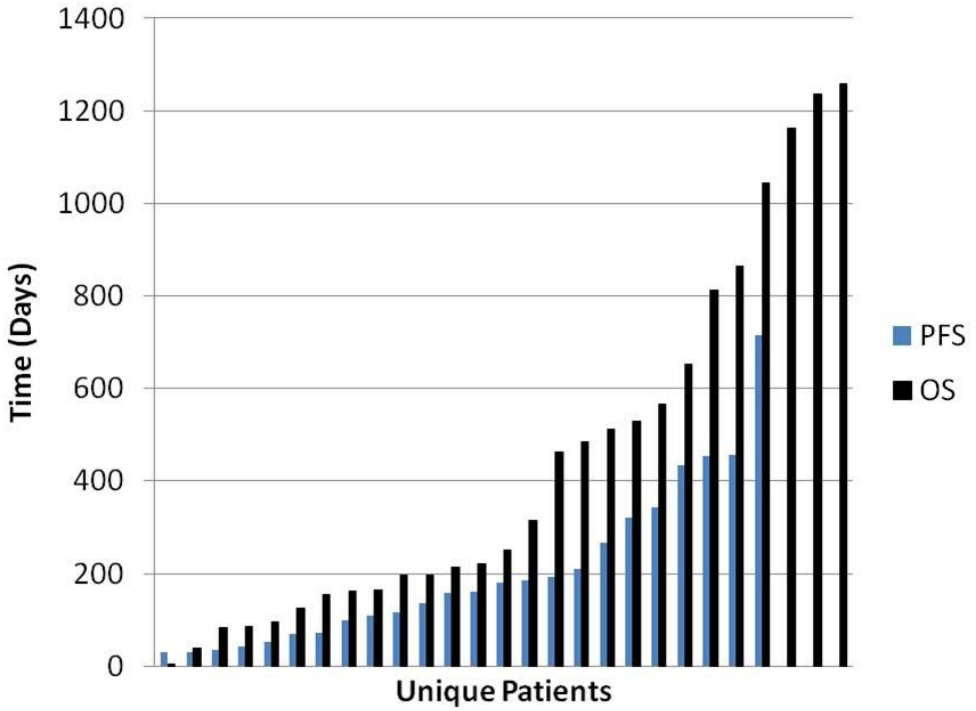

Figure 2. Distribution of Progression-Free Survival and Overall Survival of Unique Patients In Retrospective Dataset. The graphical representation above is a breakdown of the patient dataset by progression-free survival and overall survival as derived from the patient's records. Each bar corresponds to a unique patient case.

DISCUSSION

Under the IRB protocol #STU 022011-201, titled "An Analysis of Genomic and Molecular Profiles of Lung Cancer for the Prediction of Response to Therapy and Clinical Outcomes" with lead Principle Investigator Dr. David Gerber, M.D., I wanted to identify patients that had been treated with pemetrexed-based therapy between the years of 2004-2009 at UT Southwestern.

However, in order to assess any association with FTCD expression and pemetrexed response, I needed to have available pathology tissue slides for further analysis. I reviewed all of the patient's charts for available pathology, and excluded any patients where there was no available sample or sample quality was poor. To know whether patients had path available, I used the electronic records database vCDR. vCDR is pathology specific system, where patient's pathology samples can be reviewed and accessed by the pathology accession number that was assigned to that specific sample by the pathology core. I confirmed our findings by checking if there was truly no available pathology through medical record number, by another medical records database EPIC. EPIC Playground Hyperspace is the core source of electronic medical records for patients seen at the UT Southwestern hospitals.

Stage distribution of our patient dataset for retrospective analysis was split into either Stage IV patients or Stage II and III (Figure 1). I was surprised that Stage IV patients comprised 50% of the total patient population, and also to not see any Stage I

patients in this dataset. There was one patient whose stage was unavailable though our accessible medical records.

Furthermore, our patient dataset appears to be representative of the frequency of histologies which are clinically observed, with a majority of patients' tumor types comprised of adenocarcinoma, and less so with squamous cell carcinoma. Squamous cell carcinoma representation is important for proper resistant controls from previous clinical indications of pemetrexed, in addition to providing histological diversity. Unfortunately, our dataset is not comprised of any patients with large cell carcinoma histologies, another pemetrexed-sensitive, FTCD-overexpressed histotype.

Once I had our list of lung cancer patients with obtainable tissue to study, I wanted to define any clinical data regarding treatment of these patients. So, I asked questions regarding each patient and received our results through EPIC chart access of the patients' medical records (notes, labs, radiological scans, bloodwork). Specifically, I wanted to know when the patient started and ended treatment with pemetrexed, what line of therapy, was it used in combination with other treatments and did the patient progress (when/where). Time of progression was noted once it was confirmed clinically by a radiological scan, such as a CT scan, or a biopsy with malignant cells.

The distribution of progression-free survival and overall survival in our retrospective pemetrexed-treated patient dataset was even and widespread. Progression-free survival ranged from as little as 1 month to nearly two years. Overall survival

spanned from 4 days to nearly 3.5 years for our dataset. I believe the intrinsic variation within our dataset hopefully elucidates drastic differences in pemetrexed response, and therefore, contains patients who were exquisitely sensitive to pemetrexed treatment, who may have tumors that overexpress FTCD.

PROPOSED PLANS AND TRANSLATIONAL POTENTIAL

FTCD-Specific Antibody for Immunohistochemistry

Once I have collected the available pathology tissues for all patients in our retrospective dataset, I will begin immunohistochemical (IHC) staining on the formalin-fixed paraffin-embedded (FFPE) tissue slides for *FTCD* and other key genes I have elucidated in this study for pemetrexed response. I am currently undergoing optimization of a FTCD-specific antibody that can be CLIA-certified for testing of patient samples, therefore, the antibody must be specific for FTCD, work for FFPE tissue samples, and have low background signal/noise. The first two rounds of FTCD antibody optimization were executed with the Santa Cruz goat polyclonal antibody sc-47885; however, preliminary results suggest FTCD-specificity with this polyclonal antibody may be problematic. I am continuing to test other FTCD-specific antibodies, including mouse monoclonal antibodies, in hopes of identifying the best antibody for IHC.

In the circumstance that there are no available FTCD-specific antibodies for IHC, there are other methods to test *FTCD* expression, such as High Throughput Genomics (HTG) by HTG Molecular Diagnostics (Tucson, AZ). Quantitative nuclease protection assay (qNPA) technology can detect RNA extracted from FFPE patient samples (5 μn slides, through addition of gene-specific DNA oligonucleotides during sample lysis, and S1 nuclease digestion of unhybridized RNA and DNA transcripts. The remaining DNA:RNA paired transcripts are RNA-digested, and remaining DNA oligonucleotides are read and quantified.

Examination of Other Genetic Markers in Patient Dataset

When I inquired about available tissue slides for each patient in our dataset, I preliminarily requested 10 unstained slides per patient sample, for FTCD staining, proper controls, and for key genes of interest from this study and in lung cancer. The other genetic markers I hope to soon examine are oncogenes *EGFR*, *KRAS*, and *ALK*, tumor suppressor *TP53*, and pemetrexed-related genes *TYMS*, *DHFR*, *GARFT*, *RFC1*, and *FPGS*. I will use the results of these genetic markers, other clinical annotations, and FTCD or canonical pemetrexed-related genes to determine whether there are any significant associations with pemetrexed response in this retrospective dataset. As levels of these pemetrexed-related genes have been implicated previously as mechanisms of tumor response, I also wish to try correlation analyses with patient response in our tissue bank panel to rule in or out any significant relationships. Because our retrospective panel is small (n=40), I may be unable to achieve any statistical significance, even if there is an apparent trend. Therefore, I am also looking into collaborations with other hospitals with large lung cancer centers, such as Massachusetts General Hospital, or with Eli Lilly Pharmaceuticals.

Translational Potential: Enrollment for Prospective Clinical Trial

Once the retrospective dataset analysis is completed, I will assess whether there is potential to move forward to a prospective biomarker-based clinical trial for pemetrexed-based therapy. There are many factors that will need to be considered prior to launching a prospective enrollment trial, including source of funding, IRB protocols, patient consent forms, multi-center participation, enrollment criteria (inclusion and exclusion),

intellectual property registration, and patient randomization. Accrual of lung cancer patients may take up to two years, and patient follow-up for overall survival and progression-free survival could take up to five years. The design of the clinical trial has not yet been decided. The clinical trial design may be first-line pemetrexed/carboplatin or maintenance pemetrexed with randomization by the presence or absence of FTCD overexpression. I am overtly ecstatic about the translational potential of this research project, and eagerly await the results of the retrospective dataset.

PEMETREXED PERSONALIZED MEDICINE:

BIOSTATISTICS

ABSTRACT

In this chapter, I define the rationale of the biostatistic tests applied for the assessment of significance of our scientific results. In this thesis project, I applied the Student's t-test for the significance of log ratio calculations, correlation analyses, and mouse xenograft treatments to determine whether I could accept or reject the null hypothesis that different sample sets were considered similar. Finally, I applied quantile-quantile normalization to the microarray expression profiling data, to standardize across all cell lines for which I was performing our analysis. With the use of these statistical tests, I can confidently state that the results identified in this dissertation project are likely and probable, where they are found to be statistically significant.

MATERIALS AND METHODS

Student's T-Test

Unpaired two-tailed Student's t-test for a normal distribution was applied to determine statistical significance of small sample sizes, for two-sample sets (i.e. sensitive, resistant; sample sets A and B) with equal variance. The average of the sample, sample size, and standard deviations of each sample set were determined, and p-values < 0.05 were considered statistically significant.

Correlation Analysis

R^2 values or correlation coefficient was defined by

$$Correl(X,Y) = \frac{\sum (x-\bar{x})(y-\bar{y})}{\sqrt{\sum (x-\bar{x})^2 \sum (y-\bar{y})^2}}$$

where x is sample A1, and x bar is mean of sample set A, likewise y is sample B1, and y bar is mean of sample set B, and Σ is the sum of the equation.

Log Ratio

First, the $\log_2$ values were defined for each sample within the sample set, averaged, and then the average $\log_2$ values of two sample sets were subtracted from each other for a final log ratio value.

Quantile-Quantile Normalization

Quantile-quantile normalization can be calculated by taking the lowest number of each sample in a sample set, averaging the sample values and replacing each of those lowest numbers with the averaged lowest number calculated. This set is repeated for each number within each sample for the entire sample set, until all numbers have been quantile normalized.

DISCUSSION

Application of Student's T-Test

Unpaired two-tailed Student's t-test with equal variance for a normal distribution was applied to determine statistical significance of many experimental results I interpreted. Two standard deviations from the mean of the normal distribution were used for a 95% confidence interval, therefore p-values < 0.05 were considered statistically significant.

Correlation Statistics

R^2 values or correlation coefficients were used to determine relationship between the ranges of two sample sets (i.e. sample sets A and B). Correlation coefficients can range between -1 and +1, where 0 is defined by no correlation, +1 is a perfect positive correlation and -1 is a perfect negative correlation. Student's t-test was applied to reject or accept the null hypothesis that the sample sets were identical.

Definition of Log Ratio

The log ratio is a calculation to determine the differences of average $\log_2$ values from two sample sets (i.e. sample set A and B) for comparison. Student's t-test was applied to reject or accept the null hypothesis that the sample sets were identical.

Analysis of Microarray Expression Data by Quantile-Quantile Normalization

Quantile-quantile normalization is the standardization of many samples within a set of samples to account for sample-to-sample noise and variation. Quantile-quantile normalization of microarrays is generally followed by log ratio calculation for hits with large differences between two groups, and Student's t-test for statistical significance, where a p-value < 0.05 is significant.

BIBLIOGRAPHY

REFERENCES

Bareford, M. D., Park, M. A., Yacoub, A., Hamed, H. A., Tang, Y., Cruickshanks, N., Eulitt, P., Hubbard, N., Tye, G., Burow, M. E., *et al.* (2011). Sorafenib Enhances Pemetrexed Cytotoxicity through an Autophagy-Dependent Mechanism in Cancer Cells. Cancer Res *71*, 4955-4967.

Bashour, A. M., and Bloom, G. S. (1998). 58K, a microtubule-binding Golgi protein, is a formiminotransferase cyclodeaminase. J Biol Chem *273*, 19612-19617.

Braakhuis, B. J., Ruiz van Haperen, V. W., Welters, M. J., and Peters, G. J. (1995). Schedule-dependent therapeutic efficacy of the combination of gemcitabine and cisplatin in head and neck cancer xenografts. Eur J Cancer *31A*, 2335-2340.

Britten, C. D., Izbicka, E., Hilsenbeck, S., Lawrence, R., Davidson, K., Cerna, C., Gomez, L., Rowinsky, E. K., Weitman, S., and Von Hoff, D. D. (1999). Activity of the multitargeted antifolate LY231514 in the human tumor cloning assay. Cancer Chemother Pharmacol *44*, 105-110.

Byers, L. A., Sen, B., Saigal, B., Diao, L., Wang, J., Nanjundan, M., Cascone, T., Mills, G. B., Heymach, J. V., and Johnson, F. M. (2009). Reciprocal regulation of c-Src and STAT3 in non-small cell lung cancer. Clin Cancer Res *15*, 6852-6861.

Camidge, D. R., Kono, S. A., Lu, X., Okuyama, S., Baron, A. E., Oton, A. B., Davies, A. M., Varella-Garcia, M., Franklin, W., and Doebele, R. C. (2011). Anaplastic lymphoma kinase gene rearrangements in non-small cell lung cancer are associated with prolonged progression-free survival on pemetrexed. J Thorac Oncol *6*, 774-780.

Ceppi, P., Volante, M., Saviozzi, S., Rapa, I., Novello, S., Cambieri, A., Lo Iacono, M., Cappia, S., Papotti, M., and Scagliotti, G. V. (2006). Squamous cell carcinoma of the lung compared with other histotypes shows higher messenger RNA and protein levels for thymidylate synthase. Cancer *107*, 1589-1596.

Ding, L., Getz, G., Wheeler, D. A., Mardis, E. R., McLellan, M. D., Cibulskis, K., Sougnez, C., Greulich, H., Muzny, D. M., Morgan, M. B., *et al.* (2008). Somatic mutations affect key pathways in lung adenocarcinoma. Nature *455*, 1069-1075.

Fisher, M. D., and D'Orazio, A. (2000). Phase II and III trials: comparison of four chemotherapy regimens in advanced non small-cell lung cancer (ECOG 1594). Clin Lung Cancer *2*, 21-22.

Gao, Y., and Sztul, E. (2001). A novel interaction of the Golgi complex with the vimentin intermediate filament cytoskeleton. J Cell Biol *152*, 877-894.

Gerber, D. E., and Minna, J. D. (2010). ALK inhibition for non-small cell lung cancer: from discovery to therapy in record time. Cancer Cell *18*, 548-551.

Giovannetti, E., Mey, V., Danesi, R., Mosca, I., and Del Tacca, M. (2004). Synergistic cytotoxicity and pharmacogenetics of gemcitabine and pemetrexed combination in pancreatic cancer cell lines. Clin Cancer Res *10*, 2936-2943.

Gridelli, C., Rossi, A., Morgillo, F., Bareschino, M. A., Maione, P., Di Maio, M., and Ciardiello, F. (2007). A randomized phase II study of pemetrexed or RAD001 as second-line treatment of advanced non-small-cell lung cancer in elderly patients: treatment rationale and protocol dynamics. Clin Lung Cancer *8*, 568-571.

Hanauske, A. R., Chen, V., Paoletti, P., and Niyikiza, C. (2001). Pemetrexed disodium: a novel antifolate clinically active against multiple solid tumors. Oncologist *6*, 363-373.

Hanauske, A. R., Eismann, U., Oberschmidt, O., Pospisil, H., Hoffmann, S., Hanauske-Abel, H., Ma, D., Chen, V., Paoletti, P., and Niyikiza, C. (2007). In vitro chemosensitivity of freshly explanted tumor cells to pemetrexed is correlated with target gene expression. Invest New Drugs *25*, 417-423.

Hanna, N., Shepherd, F. A., Fossella, F. V., Pereira, J. R., De Marinis, F., von Pawel, J., Gatzemeier, U., Tsao, T. C., Pless, M., Muller, T., *et al.* (2004). Randomized phase III trial of pemetrexed versus docetaxel in patients with non-small-cell lung cancer previously treated with chemotherapy. J Clin Oncol *22*, 1589-1597.

Izbicka, E., Diaz, A., Streeper, R., Wick, M., Campos, D., Steffen, R., and Saunders, M. (2009). Distinct mechanistic activity profile of pralatrexate in comparison to other antifolates in in vitro and in vivo models of human cancers. Cancer Chemother Pharmacol *64*, 993-999.

Jackman, A. L., and Calvert, A. H. (1995). Folate-based thymidylate synthase inhibitors as anticancer drugs. Ann Oncol *6*, 871-881.

Judde, J. G., Rebucci, M., Vogt, N., de Cremoux, P., Livartowski, A., Chapelier, A., Tran-Perennou, C., Boye, K., Defrance, R., Poupon, M. F., and Bras-Goncalves, R. A. (2007). Gefitinib and chemotherapy combination studies in five novel human non small cell lung cancer xenografts. Evidence linking EGFR signaling to gefitinib antitumor response. Int J Cancer *120*, 1579-1590.

Kim, H. R., Shim, H. S., Chung, J. H., Lee, Y. J., Hong, Y. K., Rha, S. Y., Kim, S. H., Ha, S. J., Kim, S. K., Chung, K. Y., *et al.* (2011). Distinct clinical features and outcomes in never-smokers with nonsmall cell lung cancer who harbor EGFR or KRAS mutations or ALK rearrangement. Cancer.

Koivunen, J. P., Mermel, C., Zejnullahu, K., Murphy, C., Lifshits, E., Holmes, A. J., Choi, H. G., Kim, J., Chiang, D., Thomas, R., *et al.* (2008). EML4-ALK fusion gene and efficacy of an ALK kinase inhibitor in lung cancer. Clin Cancer Res *14*, 4275-4283.

Kondo, H., Kanzawa, F., Nishio, K., Saito, S., and Saijo, N. (1994). In vitro and in vivo effects of cisplatin and etoposide in combination on small cell lung cancer cell lines. Jpn J Cancer Res *85*, 1050-1056.

Kubota, K., Niho, S., Enatsu, S., Nambu, Y., Nishiwaki, Y., Saijo, N., and Fukuoka, M. (2009). Efficacy differences of pemetrexed by histology in pretreated patients with stage IIIB/IV non-small cell lung cancer: review of results from an open-label randomized phase II study. J Thorac Oncol *4*, 1530-1536.

Lee, J. O., Kim, T. M., Lee, S. H., Kim, D. W., Kim, S., Jeon, Y. K., Chung, D. H., Kim, W. H., Kim, Y. T., Yang, S. C., *et al.* (2011). Anaplastic Lymphoma Kinase Translocation: A Predictive Biomarker of Pemetrexed in Patients with Non-small Cell Lung Cancer. J Thorac Oncol.

Lu, X., Errington, J., Curtin, N. J., Lunec, J., and Newell, D. R. (2001). The impact of p53 status on cellular sensitivity to antifolate drugs. Clin Cancer Res *7*, 2114-2123.

Mascaux, C., Iannino, N., Martin, B., Paesmans, M., Berghmans, T., Dusart, M., Haller, A., Lothaire, P., Meert, A. P., Noel, S., *et al.* (2005). The role of RAS oncogene in survival of patients with lung cancer: a systematic review of the literature with meta-analysis. Br J Cancer *92*, 131-139.

Mercalli, A., Sordi, V., Formicola, R., Dandrea, M., Beghelli, S., Scarpa, A., Di Carlo, V., Reni, M., and Piemonti, L. (2007). A preclinical evaluation of pemetrexed and irinotecan combination as second-line chemotherapy in pancreatic cancer. Br J Cancer *96*, 1358-1367.

Morris, S. W., Kirstein, M. N., Valentine, M. B., Dittmer, K. G., Shapiro, D. N., Saltman, D. L., and Look, A. T. (1994). Fusion of a kinase gene, ALK, to a nucleolar protein gene, NPM, in non-Hodgkin's lymphoma. Science *263*, 1281-1284.

Nemati, F., Livartowski, A., De Cremoux, P., Bourgeois, Y., Arvelo, F., Pouillart, P., and Poupon, M. F. (2000). Distinctive potentiating effects of cisplatin and/or ifosfamide combined with etoposide in human small cell lung carcinoma xenografts. Clin Cancer Res *6*, 2075-2086.

Ricciardi, S., Tomao, S., and de Marinis, F. (2009). Pemetrexed as first-line therapy for non-squamous non-small cell lung cancer. Ther Clin Risk Manag *5*, 781-787.

Riely, G. J., Kris, M. G., Rosenbaum, D., Marks, J., Li, A., Chitale, D. A., Nafa, K., Riedel, E. R., Hsu, M., Pao, W., *et al.* (2008). Frequency and distinctive spectrum of KRAS mutations in never smokers with lung adenocarcinoma. Clin Cancer Res *14*, 5731-5734.

Rinaldi, D. A., Kuhn, J. G., Burris, H. A., Dorr, F. A., Rodriguez, G., Eckhardt, S. G., Jones, S., Woodworth, J. R., Baker, S., Langley, C., *et al.* (1999). A phase I

evaluation of multitargeted antifolate (MTA, LY231514), administered every 21 days, utilizing the modified continual reassessment method for dose escalation. Cancer Chemother Pharmacol *44*, 372-380.

Rothbart, S. B., Racanelli, A. C., and Moran, R. G. (2010). Pemetrexed indirectly activates the metabolic kinase AMPK in human carcinomas. Cancer Res *70*, 10299-10309.

Scagliotti, G. V., Parikh, P., von Pawel, J., Biesma, B., Vansteenkiste, J., Manegold, C., Serwatowski, P., Gatzemeier, U., Digumarti, R., Zukin, M., *et al.* (2008). Phase III study comparing cisplatin plus gemcitabine with cisplatin plus pemetrexed in chemotherapy-naive patients with advanced-stage non-small-cell lung cancer. J Clin Oncol *26*, 3543-3551.

Schiller, J. H., von Pawel, J., Schutt, P., Ansari, R. H., Thomas, M., Saleh, M., McCroskey, R. D., Pfeifer, W., Marsland, T. A., Kloecker, G. H., *et al.* (2010). Pemetrexed with or without matuzumab as second-line treatment for patients with stage IIIB/IV non-small cell lung cancer. J Thorac Oncol *5*, 1977-1985.

Schultz, R. M., Patel, V. F., Worzalla, J. F., and Shih, C. (1999). Role of thymidylate synthase in the antitumor activity of the multitargeted antifolate, LY231514. Anticancer Res *19*, 437-443.

Seimiya, M., Tomonaga, T., Matsushita, K., Sunaga, M., Oh-Ishi, M., Kodera, Y., Maeda, T., Takano, S., Togawa, A., Yoshitomi, H., *et al.* (2008). Identification of novel immunohistochemical tumor markers for primary hepatocellular carcinoma; clathrin heavy chain and formiminotransferase cyclodeaminase. Hepatology *48*, 519-530.

Shih, C., Chen, V. J., Gossett, L. S., Gates, S. B., MacKellar, W. C., Habeck, L. L., Shackelford, K. A., Mendelsohn, L. G., Soose, D. J., Patel, V. F., *et al.* (1997). LY231514, a pyrrolo[2,3-d]pyrimidine-based antifolate that inhibits multiple folate-requiring enzymes. Cancer Res *57*, 1116-1123.

Shintani, Y., Ohta, M., Hirabayashi, H., Tanaka, H., Iuchi, K., Nakagawa, K., Maeda, H., Kido, T., Miyoshi, S., and Matsuda, H. (2004). Thymidylate synthase and dihydropyrimidine dehydrogenase mRNA levels in tumor tissues and the efficacy of 5-fluorouracil in patients with non-small-cell lung cancer. Lung Cancer *45*, 189-196.

Smith, P. G., Thomas, H. D., Barlow, H. C., Griffin, R. J., Golding, B. T., Calvert, A. H., Newell, D. R., and Curtin, N. J. (2001). In vitro and in vivo properties of novel nucleoside transport inhibitors with improved pharmacological properties that potentiate antifolate activity. Clin Cancer Res *7*, 2105-2113.

Takezawa, K., Okamoto, I., Okamoto, W., Takeda, M., Sakai, K., Tsukioka, S., Kuwata, K., Yamaguchi, H., Nishio, K., and Nakagawa, K. (2011). Thymidylate synthase as a determinant of pemetrexed sensitivity in non-small cell lung cancer. Br J Cancer *104*, 1594-1601.

Teicher, B. A., Chen, V., Shih, C., Menon, K., Forler, P. A., Phares, V. G., and Amsrud, T. (2000). Treatment regimens including the multitargeted antifolate LY231514 in human tumor xenografts. Clin Cancer Res *6*, 1016-1023.

Thomas, H. D., Saravanan, K., Wang, L. Z., Lin, M. J., Northen, J. S., Barlow, H., Barton, M., Newell, D. R., Griffin, R. J., Golding, B. T., and Curtin, N. J. (2009). Preclinical evaluation of a novel pyrimidopyrimidine for the prevention of

nucleoside and nucleobase reversal of antifolate cytotoxicity. Mol Cancer Ther *8*, 1828-1837.

Tonkinson, J. L., Worzalla, J. F., Teng, C. H., and Mendelsohn, L. G. (1999). Cell cycle modulation by a multitargeted antifolate, LY231514, increases the cytotoxicity and antitumor activity of gemcitabine in HT29 colon carcinoma. Cancer Res *59*, 3671-3676.

Uemura, T., Oguri, T., Ozasa, H., Takakuwa, O., Miyazaki, M., Maeno, K., Sato, S., and Ueda, R. (2010). ABCC11/MRP8 confers pemetrexed resistance in lung cancer. Cancer Sci *101*, 2404-2410.

Vogelzang, N. J., Rusthoven, J. J., Symanowski, J., Denham, C., Kaukel, E., Ruffie, P., Gatzemeier, U., Boyer, M., Emri, S., Manegold, C., *et al.* (2003). Phase III study of pemetrexed in combination with cisplatin versus cisplatin alone in patients with malignant pleural mesothelioma. J Clin Oncol *21*, 2636-2644.

Wang, H., Rayburn, E. R., Wang, W., Kandimalla, E. R., Agrawal, S., and Zhang, R. (2006). Chemotherapy and chemosensitization of non-small cell lung cancer with a novel immunomodulatory oligonucleotide targeting Toll-like receptor 9. Mol Cancer Ther *5*, 1585-1592.

Westerhof, G. R., Schornagel, J. H., Kathmann, I., Jackman, A. L., Rosowsky, A., Forsch, R. A., Hynes, J. B., Boyle, F. T., Peters, G. J., Pinedo, H. M., and et al. (1995). Carrier- and receptor-mediated transport of folate antagonists targeting folate-dependent enzymes: correlates of molecular-structure and biological activity. Mol Pharmacol *48*, 459-471.

Yamori, T., Sato, S., Chikazawa, H., and Kadota, T. (1997). Anti-tumor efficacy of paclitaxel against human lung cancer xenografts. Jpn J Cancer Res *88*, 1205-1210.

Yang, T. Y., Chang, G. C., Chen, K. C., Hung, H. W., Hsu, K. H., Sheu, G. T., and Hsu, S. L. (2011). Sustained activation of ERK and Cdk2/cyclin-A signaling pathway by pemetrexed leading to S-phase arrest and apoptosis in human non-small cell lung cancer A549 cells. Eur J Pharmacol *663*, 17-26.

GEMCITABINE CISPLATIN COMBINATION:

IN VIVO TOXICITY STUDY, MOUSE HOSPITAL TRIALS,

AND TUMORIGENICITY OF NSCLC LINES

ABSTRACT

In this appendix, I define the necessity of a clinically relevant dose schedule for gemcitabine/cisplatin combination treatment *in vivo*. Gemcitabine/cisplatin is a commonly used chemotherapeutic regimen administered as first-line treatment to lung cancer patients. When I performed a peer-review literature search on the use of gemcitabine/cisplatin combination, I was surprised to know that there was not only a lack of dose schedules for mouse models at the clinically relevant ratio of 25/2, but truly, a shortage of lung cancer xenografts treated with the gemcitabine/cisplatin combination. I determined that doses of 75 mg/kg gemcitabine and 6 mg/kg cisplatin are sufficient to significantly reduce tumor burden as single and combination treatments in a H1299 xenograft model. However, the combination treatment results in apparent toxicity and mortality in *NOD/SCID* mice. I further determined the maximum tolerated dose tested of cisplatin single agent to be 4 mg/kg *qwx3*. The maximum tolerated dose tested of gemcitabine/cisplatin combination at a clinically relevant ratio 25/2 was 50 mg/kg gemcitabine and 4 mg/kg cisplatin *qwx3*. Moreover, I determined the tumorigenic potential and rates of tumor formation of 13 NSCLC lines. I identified three distinct groups of tumor formation rates: slow, medium and fast-growing lines, as subcutaneous xenografts in *NOD/SCID* mice. The research findings described in this dissertation will help to hopefully expedite the future study of mechanisms of gemcitabine/cisplatin response in lung cancer.

INTRODUCTION

Lung cancer is a major health problem. The estimated number of new cases and deaths from lung cancer in the United States in 2009 are 219,440 and 159,390, respectively (SEER Cancer Statistics Review, 2010). Upon diagnosis, staging with the TNM malignancy system, and evaluation of current performance status, the physician determines whether the patient's tumor is resectable or non-resectable, otherwise known as is the patient is electable for surgery or not. Chemotherapy is the systemic administration of an anti-tumor agent which is used to effectively shrink, or stabilize the tumor burden of a cancer patient. Chemotherapy is administered to patients either with non-resectable tumors, after resection surgery if there are positive margins, or as a prophylactic for future recurrences. Chemotherapeutic agents are also effective in the management or inhibition of the progression of micro-metastases to other organs, which are unidentifiable using CT/PET scans. Unfortunately, chemotherapy drugs typically are unable to cross the blood/brain barrier and are therefore ineffective in the treatment of brain metastases, in which whole brain radiation or gamma knife treatments can be employed.

Currently, there are FDA-approved chemotherapeutic combinations that are available for first line treatment of lung cancer patients. First line chemotherapy combinations are usually cytotoxic, two-drug cocktails, with one of the drugs being a platinum backbone agent. Depending on the performance status and vitals of the patient, cisplatin or carboplatin may be administered in consideration of the patient's kidney

metabolics. Several of the first line chemotherapeutic combinations are cisplatin or carboplatin combined with paclitaxel, docetaxel, gemcitabine, vinorelbine, or pemetrexed. Clinical trial ECOG 1594 compared the effectiveness of four chemotherapy regimens, and determined that all regimens have the same efficacy, and performance status was the only prognostic factor which associated with patient survival (Fisher and D'Orazio, 2000). The need for personalization of first line administration is great, as current enrollment criteria are not typically based on the patient's molecular makeup or genetic profile, but performance status and tolerability of chemotherapy.

Gemcitabine (Gemzar) is a cytotoxic, intravenous chemotherapeutic designed by Eli Lilly, which was FDA-approved in 1996, and is indicated for advanced stage lung cancer patients in combination with cisplatin. Gemcitabine is a deoxycytidine analog, with two fluorine substitutions at the second carbon of the ribose sugar. Cisplatin is a platinum analog, cytotoxic, intravenous chemotherapy agent approved by FDA in 1978, and has been indicated for the treatment of many cancer types, such as lung, ovarian, bladder, cervical, and testicular cancers. Cisplatin reacts with DNA at the N-7 positions of guanine or adenine, binding in one of two sites, forming either intra- or inter-strand conformations. Both chemotherapeutic reagents interact with the cellular DNA of the cancer, resulting in enhanced drug interactions when used in combination. Gemcitabine and cisplatin cause interference with DNA polymerases, DNA synthesis and repair, resulting in the S-phase specific inhibition of the cell cycle. The maximum tolerated combination dose of gemcitabine/cisplatin is 1,250/100 mg/m², respectively. Interestingly, cisplatin treatment is administered *q3w*, whereas gemcitabine is

administered on days 1 and 8 of each 21 day cycle, thus exhibiting a 25-to-2 gemcitabine/cisplatin drug ratio.

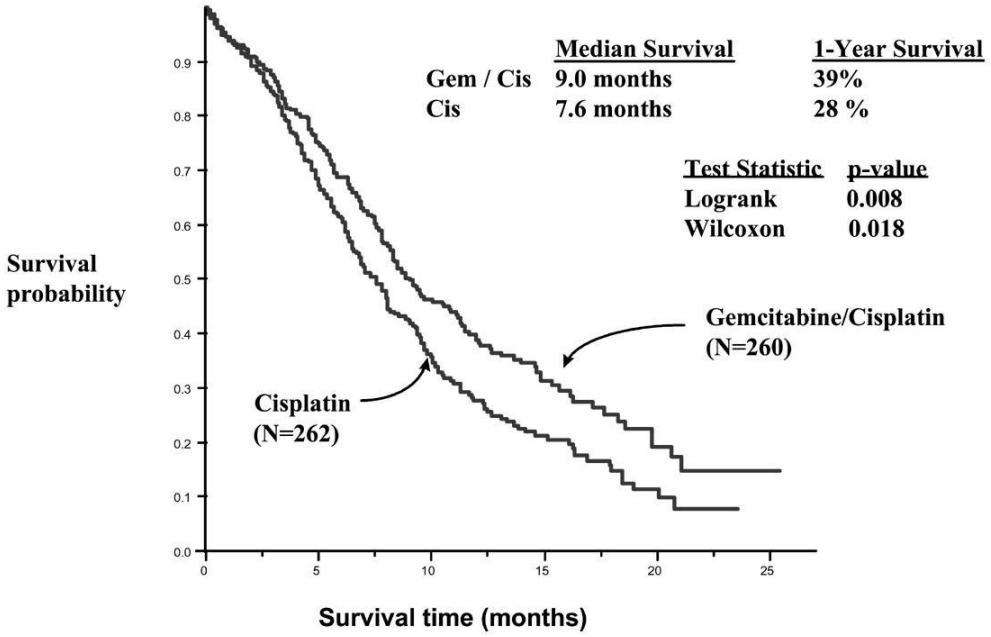

Figure 1. Kaplan-Meier Survival Curve of Patients Treated with Either Gemcitabine/Cisplatin or Cisplatin. NSCLC clinical trial and figure by Eli Lilly Pharmaceuticals. Gemcitabine plus cisplatin versus cisplatin: This study was conducted on patients (n=522) with inoperable Stage IIIA, IIIB, or IV NSCLC who had not received prior chemotherapy. Gemcitabine 1,000 mg/m^2 was administered on days 1, 8, and 15 of a 28-day cycle with cisplatin 100 mg/m^2 administered on day 1 of each cycle. Single-agent cisplatin 100 mg/m^2 was administered on day 1 of each 28-day cycle. The primary endpoint was survival.

When I performed a peer-review literature search on the use of gemcitabine/cisplatin combination, I was surprised to know that there was not only a lack of dose schedules for mouse models at the clinically relevant ratio of 25/2, but truly, a shortage of lung cancer xenografts treated with the gemcitabine/cisplatin combination. Furthermore, available knowledge on the tumorigenicity of lung cancer lines grown as

xenografts and their tumor formation rates would expedite the effectiveness to test chemotherapeutic response *in vivo*.

The necessity for a clinically relevant, safe and well tolerated dose schedule of gemcitabine/cisplatin combination in mouse xenograft models is high, as this combination is administered as first-line treatment to lung cancer patients, to effectively mimic clinical indications and model chemotherapeutic responses.

MATERIALS AND METHODS

Reagents

Drugs used were obtained from the UT Southwestern Campus Pharmacy (Dallas, TX), and handled with aseptic technique. Gemcitabine/Gemzar®, Eli Lilly (Indianapolis, IN) was reconstituted in 0.85% sterile sodium chloride, as per manufacturer's instructions, to make 22 mM solution ($C_9H_{11}F_2N_3O_4$•HCl, MW 299.66). Cisplatin/CDDP, Teva Parenteral Medicines, Inc. (Irvine, CA) is available in 1 mg/mL solution, and kept with minimum exposure to light.

Cell Preparation

With the exception of A549, Calu-1, Calu-3, and Calu-6, which were purchased from the American Type Culture Collection (http://www.atcc.org), all the lung cancer cell lines were obtained from Hamon Center Collection (University of Texas Southwestern Medical Center) (Phelps et al., 1996). All cells were grown in sterile, filtered RPMI 1640 with L-glutamine, Cellgro (Manassas, VA) supplemented with 5% fetal bovine serum, Gemini Biotech (Alachua, FL). The cells were incubated at 37°C in a 5% CO_2, and split with 0.05% trypsin EDTA, Gibco, Invitrogen (Carlsbad, CA) when confluent. All cell lines have been DNA fingerprinted by PowerPlex 1.2 System, Promega (Madison, WI) for identity confirmation, and shown to be free of mycoplasma contamination by e-MycoPCR Mycoplasma Detection Kit, Boca Scientific Inc (Boca Raton, FL).

Mice

Female *NOD/SCID* mice were obtained from Wakeland laboratories, UT Southwestern Mouse Breeding Core (Dallas, TX) at approximately 6-8 weeks of age.

Xenograft Studies

$1x10^6$ cells were injected subcutaneously into the shaved right flank of the mouse, and monitored by calipers ($v = \pi/6*l*w^2$; v, volume; l, length, w, width, where width is the smallest dimension). All mouse procedures are in compliance with UT Southwestern IACUC policies (APN 0575-06-1 and APN 2009-0178).

***In vivo* Toxicity Assays**

Mice received treatments weekly for three weeks and were monitored up to two weeks post-treatment for extensive adverse events or mortalities. Body weight was quantified using a scale, each week after receiving treatment, averaged, and recorded as compared to the average starting control weight. Toxicity was assessed as loss of 10% or more body weight (as denoted by a black line), or mortality.

RESULTS

In Vivo Gemcitabine/Cisplatin Combination Treatment of H1299 Xenografts

NOD/SCID mice (n=40) were injected with large cell carcinoma cell line H1299 ($1x10^6$ cells/mouse) subcutaneously, and randomized at day 25 into four treatment groups: saline control, gemcitabine alone, cisplatin alone, and gemcitabine/cisplatin combination (Figure 2). After the completion of three weekly treatments, the final average tumor volumes at day 45 for each treatment group were 1255.34 (control), 812.89 (gem), 648.76 (cis), and 156.62 mm^3 (gem/cis). Both single agents compared to control treatment were statistically significant (p-values 0.045 (gem) and 0.029 (cis)). The gemcitabine/cisplatin combination was very statistically significantly different from the control treatment group (p-value 0.0017). Unfortunately, there were issues of toxicity in this xenograft treatment study, where three mice in the combination group expired due to significant weight loss as a result of both treatments.

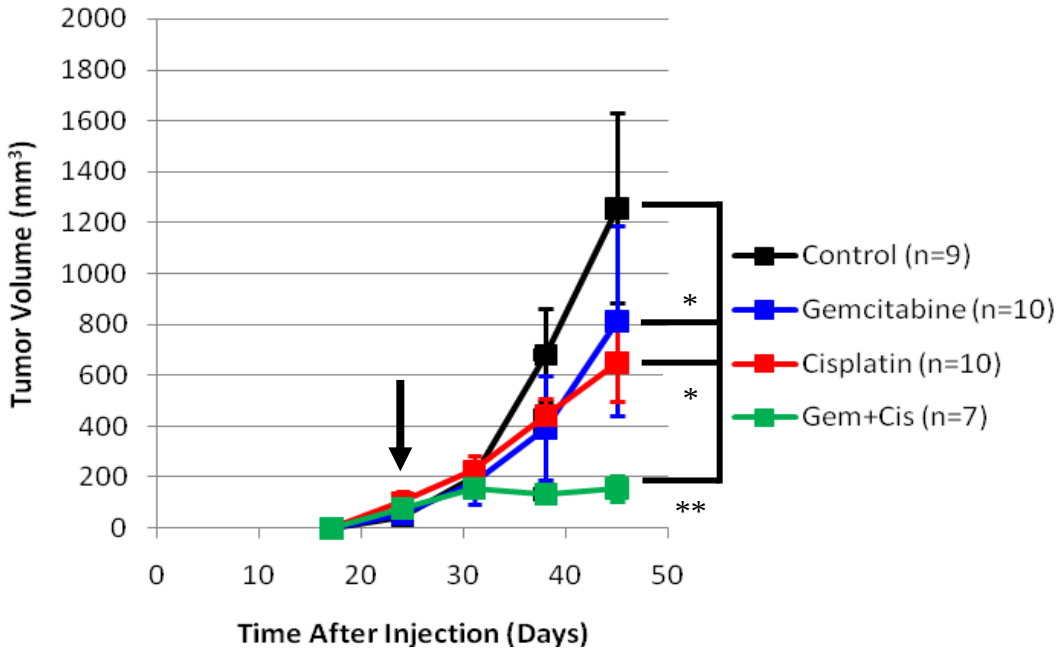

Figure 2. *In Vivo* Mouse Hospital Trial of H1299 with Gemcitabine, Cisplatin and the Combination. Mice were randomized to either gemcitabine 75 mg/kg, cisplatin 6 mg/kg, the combination, or saline control. Treatment was administered *i.p.* to NOD/SCID female mice under a *qwx3* dose schedule. * denotes p-value < 0.05; ** denotes p-value = 0.001.

In Vivo Toxicity Preclinical Model: Single and Combination of Therapeutic Agents

To determine a safe and effective dose schedule for gemcitabine/cisplatin treatments, I decided to establish *in vivo* toxicity models for cisplatin and gemcitabine/cisplatin regimens in *NOD/SCID* mice (Figures 3 and 4). I tested cisplatin 4, 6, 8 mg/kg as a single agent and three combination dose treatments (Gem 50, 62.5, 75 mg/kg + Cis 4, 5, 6 mg/kg, respectively) utilizing a *qwx3* dose schedule.

Toxicity was observed at 6 and 8 mg/kg of cisplatin, and the MTD of cisplatin tested was 4 mg/kg *qwx3* (Figure 3). There were two mortalities at the 8 mg/kg cisplatin dose schedule, and the group was removed from the final treatment. Alternatively, gemcitabine was well tolerated at all doses tested up to 250 mg/kg with no observable toxicities, and no MTD was identified (data not shown).

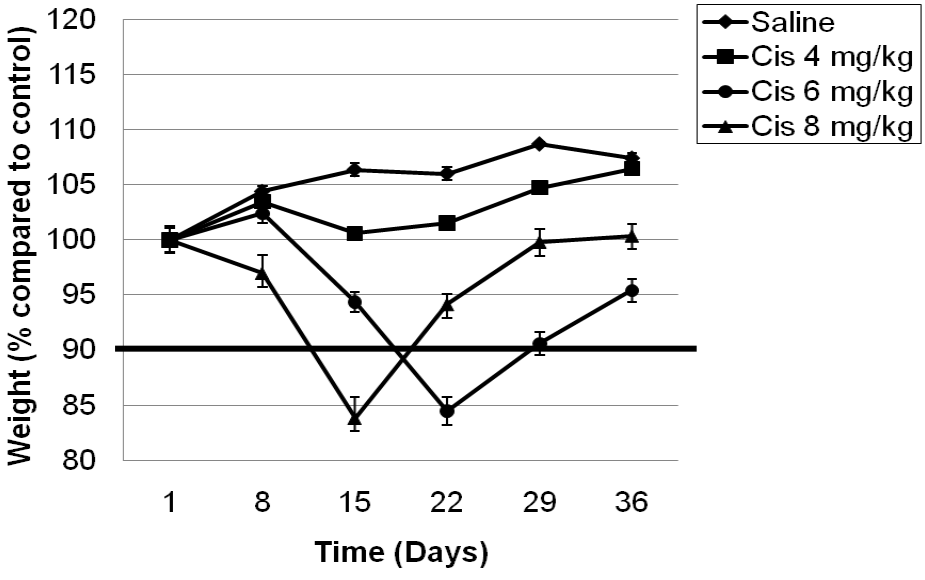

Figure 3. *In Vivo* Toxicity Profile of Cisplatin. Three treatments of cisplatin (4, 6, and 8 mg/kg) or saline control, were administered *i.p.* to *NOD/SCID* female mice (n=5/group) under a *qwx3* dose schedule.

Gemcitabine/cisplatin combination was determined to be safe at Gem 50 + Cis 4 mg/kg *qwx3*, as both Gem 62.5 + Cis 5 mg/kg and Gem 75 + Cis 6 mg/kg *qwx3* dose schedules resulted in greater than 10% body weight loss (Figure 4).

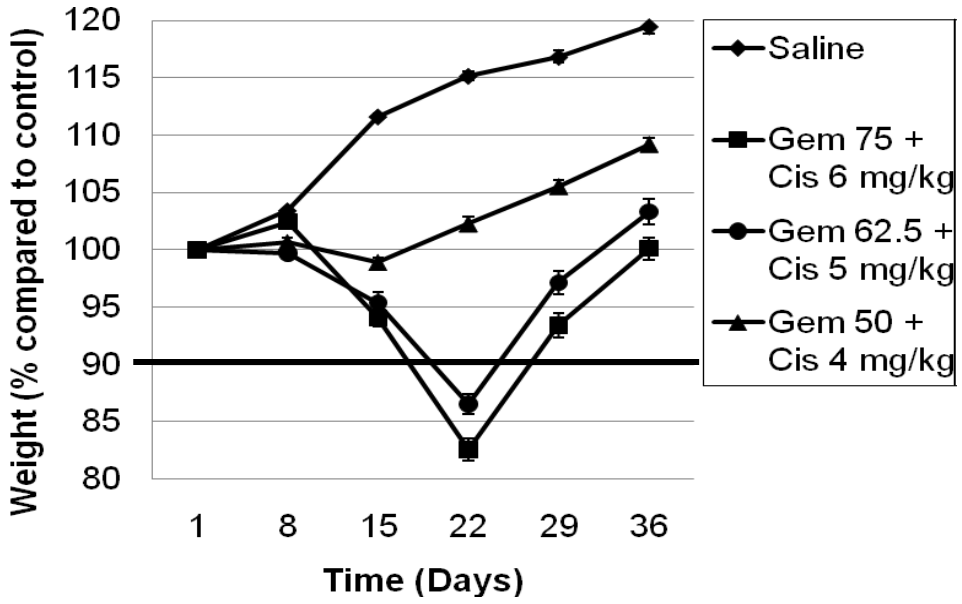

Figure 4. *In Vivo* Toxicity Profile of Gemcitabine/Cisplatin Combination. Three combination dose schedules of Gem (75, 62.5, and 50 mg/kg) and Cis (4, 5, and 6 mg/kg) respectively or saline control, were administered *i.p.* to NOD/SCID female mice (n=5/group) under a *qwx3* dose schedule.

Tumorigenicity of Non-Small Cell Lung Cancer Lines in *NOD/SCID* Mice

I injected 13 different NSCLC cell lines (at $1x10^6$ cells/mouse) subcutaneously into the right flank, and observed tumor formation over time (Figure 5). Two lines (H1693, H661) failed to form sizeable tumors within two months after tumor injection. There were drastic differences in growth rates among our panel of 11 NSCLC lines. To describe these results, I measured the approximate average time-to-1000 mm^3 (TT1000)

for each cell line. Fast growing tumors HCC95, HCC1359, and HCC461 had TT1000 of approximately 30 days. Medium growing tumors HCC515, H2009 and H1299 had approximate TT1000 of 39, 39.5 and 41.5 days respectively. Slow growing tumors H358, Calu-1 and H2882 had an approximate TT1000 of 92, 97 and 105.5 days, respectively.

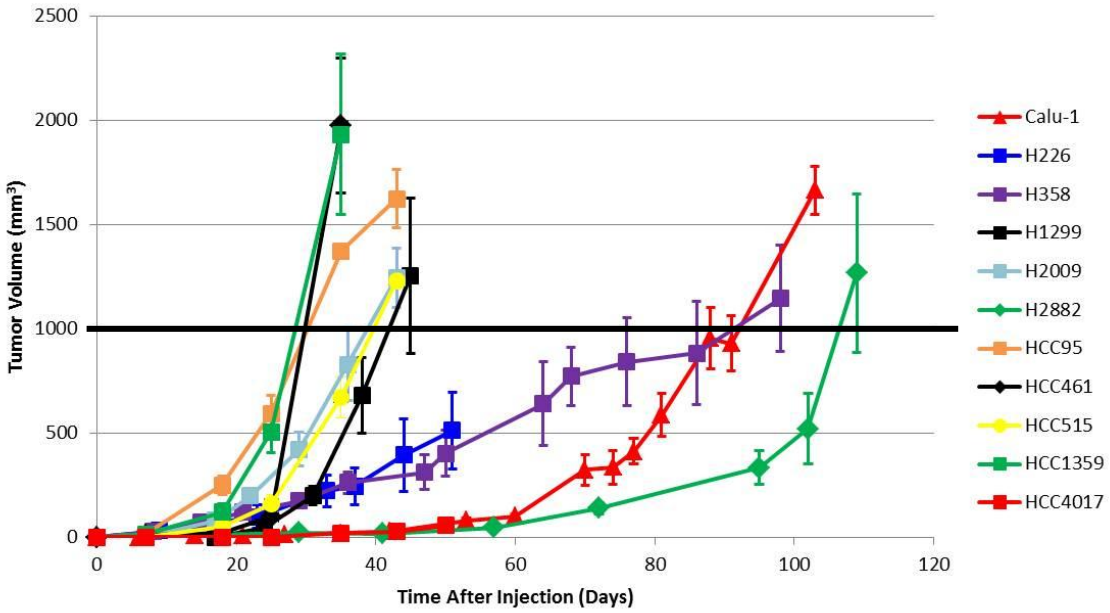

Figure 5. Drastic Differences in Tumorigenic Potential and Rate of Formation Across Panel of Non-Small Cell Lung Cancer Lines. Mice (n=5-10) were injected with $1x10^6$ cells, and monitored by calipers for tumor burden.

DISCUSSION

The purpose of this research proposal was to develop *in vivo* mouse models for gemcitabine/cisplatin combination that were safe, well tolerated and clinically relevant. I wanted to establish these dose schedules, in addition to tumor forming ability of NSCLC cell lines as xenografts, to save time and efforts of future researchers, and to bridge the gap between basic science and the clinic for gemcitabine/cisplatin treatment.

There are only two previous studies of *in vivo* gemcitabine/cisplatin combination treatment in lung cancer (Braakhuis et al., 1995; Judde et al., 2007). Both studies failed to implement the clinically relevant ratio of gemcitabine/cisplatin in their research. The clinically relevant ratio at the MTD of gemcitabine/cisplatin in patients is 25/2, where gemcitabine is administered at 1,250 mg/m^2 and cisplatin at 100 mg/m^2 intravenously. In Braakhuis et al. mice were administered gemcitabine/cisplatin in a 25/1 ratio, however, mice were treated on days 0, 3, 6 and 9 with gemcitabine and days 0 and 5 for cisplatin (Braakhuis et al., 1995). In Judde et al., 2007, mice were treated with an 80/3 (26.6/1) ratio of gemcitabine/cisplatin, where mice were treated every day for 21 days (Judde et al., 2007).

As I was unsure what doses to start with for our study, I pooled together previous studies of cisplatin treatment of xenografts from the peer-reviewed literature. I found 6 mg/kg cisplatin to be a moderately safe dose, between the range of 2 and 9 mg/kg, previous doses tested and published (Kondo et al., 1994; Nemati et al., 2000; Yamori et

al., 1997). I extrapolated the amount of gemcitabine to be used, by applying the 25/2 clinical ratio, and came up with a final dose of 75 mg/kg gemcitabine. I decided to go with a *qwx3* schedule to mimic clinical administration of drug treatments, where cytotoxic agents are administered once every three weeks, not daily.

Therefore, I felt confident in our newly extrapolated dose schedule, and established H1299 xenografts for treatment with each single agent and the combination for study. I was truly surprised to discover apparent toxicity in the combination treatment arm (Figure 2), because our dose schedule was relatively conservative to the other two studies published. Interestingly, both treatments as single agents were fairly well tolerated, and did not result in any other mortality. All dose treatments significantly reduced tumor burden, as compared to control (Figure 2).

After this result, I went back to the drawing board and redesigned our blueprints for the development of the gemcitabine/cisplatin dose schedule. I designed single and combination toxicity studies in naïve *NOD/SCID* mice. I found that cisplatin treatment was very toxic to the mice, and that 4 mg/kg cisplatin was safe and well tolerated in a *qwx3* dose schedule (Figure 3). I did not test 5 mg/kg cisplatin as a single agent, so I cannot definitively state that 4 mg/kg is the MTD of cisplatin for a *qwx3* schedule.

Gemcitabine/cisplatin combination treatments, again, revealed that the 75/6 mg/kg (gem/cis) dose schedule was toxic to mice, and resulted in greater than 10% body weight loss (Figure 4). However, 50/4 mg/kg (gem/cis) was very well tolerated and had

minimal side effects of the body weight of the mice. Interestingly, 62.5/5 mg/kg (gem/cis) was also toxic to the mice, which revealed to us that 5 mg/kg cisplatin is most likely toxic as a single agent, as single agent gemcitabine is well tolerated up to 250 mg/kg, although drug interactions may be playing a key role in toxicity.

Finally, I determined the tumorigenicity of NSCLC cell lines as xenografts in *NOD/SCID* mice. Specifically, I tested 13 different lung cancer lines for their ability to grow subcutaneously in the right flank of mice, at a concentration of 1 million cells per mouse (Figure 5). I identified three different growth rates within our panel, by measuring each line's intrinsic ability to achieve an average tumor burden of 1,000 mm^3. Furthermore, two of the lines I tested were unable to form xenografts within 50 days post injection. I hope that our research will help to expedite the study of NSCLC lines *in vivo* by identifying which lines form xenografts, and at what rates.

ACKNOWLEDGEMENTS

I would like to thank the past and present members of the Minna laboratory, Dr. Yang Xie, and administrators of the Hamon Cancer Center for Therapeutic Oncology for their technical assistance and guidance throughout my thesis research.

I would like to express great gratitude to Helen Yin, the director of the Mechanism of Disease Med into Grad Howard Hughes Initiative and one of my committee members, for taking a risk on me and choosing to enroll me in the inaugural class of the program. I am forever impacted by the experiences as a result of one decision.

I would like to thank my dissertation committee, specifically, my committee chair Dr. Rolf Brekken, Dr. Melanie Cobb, and Dr. Philip Thorpe for their expertise and tremendous support along the path of my graduate career. Their advice and supervision was absolutely instrumental on the decisions and direction of my graduate research.

Finally, I cannot express my gratitude to my heavenly Father, for His gracious mercy and love. I pray His will is always the lighthouse of my life, and to serve Him with each step of every day.